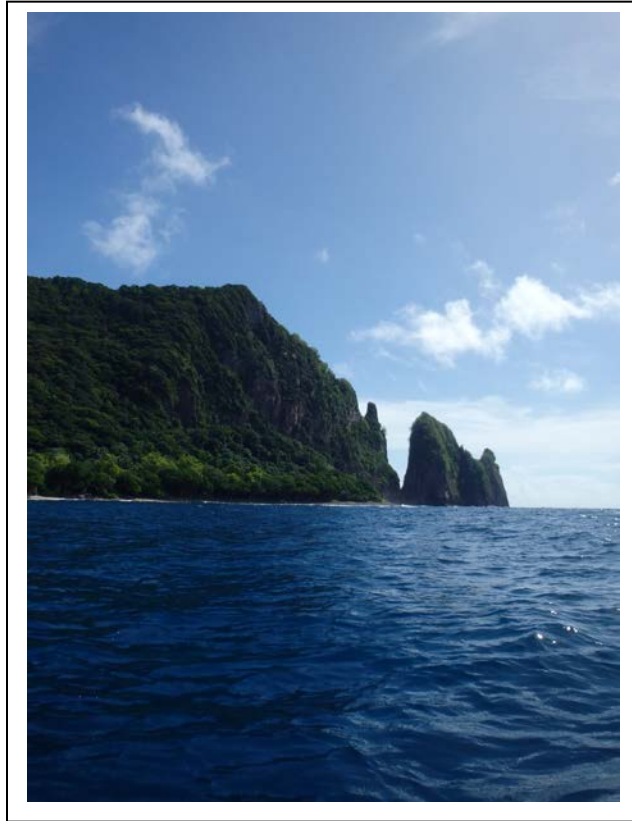


Excess Nutrients in Vatia Bay, American Samoa: Spatiotemporal Variability, Source Identification and Impact on Coral Reef Ecosystems



October 2019

David Whittall

Meagan Curtis

Andrew Mason

Bernardo Vargas-Angel



Acknowledgments

This work would not have been possible without the assistance and logistical support of many individuals. Most notably, Motusaga Vaeoso, Kim McGuire, Trevor Kaituu, Alice Lawrence, Mark MacDonald, Mareike Sudek, Sabrina Woofter, Hideyo Hattori, Jeremy Raynal, Fa'salafa Diana Kitiona and Greg Piniak assisted with field work. Additional staff from NOAA (Beth Lumsden, Noriko Shoji, Paulo Maurin, Rob Warner, Kerry Reardon) and American Samoa



Image 1: Group photo of local partners during field work training in 2015.

Community College (Kelley Tagarino and Francis Leiato) were instrumental in the logistics of sample storage and transport. Local staff from the American Samoa Division of Marine and Wildlife Resources, American Samoa Environmental Protection Agency and the National Park of American Samoa all provided useful input and conversations. This work was supported financially by NOAA's Coral Reef Conservation Program and the National Centers for Coastal Ocean Science. We also thank the following reviewers for their helpful comments that greatly improved the manuscript: Dr. Suzanne Bricker, Dr. Tony Pait and Dr. Greg Piniak.

Citation:

Whitall, D, M Curtis, A Mason, B Vargas-Angel. 2019. Excess Nutrients in Vatia Bay, American Samoa: Spatiotemporal Variability, Source Identification and Impact on Coral Reef Ecosystems. NOAA Technical Memorandum NOS NCCOS 266. Silver Spring. 69 pages. doi:10.25923/j8cp-x570

Mention of trade names or commercial products does not constitute endorsement or recommendation for their use by the United States Government.

Excess Nutrients in Vatia Bay, American Samoa: Spatiotemporal Variability, Source Identification and Impact on Coral Reef Ecosystems

Prepared by the Monitoring and Assessment Branch
Stressor Detection and Impacts (SDI) Division
National Centers for Coastal Ocean Science (NCCOS)
National Ocean Service (NOS)
National Oceanic and Atmospheric Administration (NOAA)
1305 East-West Hwy (SSMC 4, N/SCI 1)
Silver Spring, MD 20910
USA

October 2019

David Whittall

NOAA National Centers for Coastal Ocean Science Stressor Detection and Impacts Division

Andrew Mason

NOAA National Centers for Coastal Ocean Science Stressor Detection and Impacts Division

Meagan Curtis

American Samoa Community College

Bernardo Vargas-Angel

NOAA National Marine Fisheries Service Pacific Islands Fisheries Science Center

NOAA Technical Memorandum NOS NCCOS 266



United States Department of Commerce	National Oceanic and Atmospheric Administration	National Ocean Service
Wilbur Ross Secretary	Neil Jacobs Acting Under Secretary	Nicole LeBoeuf Acting Asst. Administrator

Table of Contents

Acknowledgements	2
Front Material	2
List of Figures	5
List of Tables	7
List of Images	8
Background	9
Study Site Info	9
Objectives	13
Methods	13
Benthic Cover Photo Quadrat Methodology	13
Water Quality Sampling Design	13
Analytical Methods Used for Analysis of Nutrients	15
Analytical Methods Used for Analysis of Tracers	15
Method Detection Limits	16
Statistical Analysis	16
Results and Discussion	17
Spatial Differences in Nutrient Concentrations	17
Temporal Differences in Nutrient Concentrations	18
Tracers	18
Correlations between Analytes	19
Caveats for Interpretation of Tracer Data	19
Putting the Results in Context	19
Comparison with Biological Data	20
Conclusions	24
References	25
Appendix Tables	28
Figures	31

List of Figures

- Figure 1: Location of Vatia Bay.
- Figure 2: Map of sites selected via stratified random sampling design
- Figure 3: Mean concentration of ammonium, nitrate, nitrite, urea and orthophosphate at surface vs bottom across all sites.
- Figure 4: Mean total nitrogen and total phosphorus concentrations at surface vs bottom across all sites.
- Figure 5: Mean silica concentrations at surface vs bottom across all sites.
- Figure 6: Mean surface ammonium concentrations by site.
- Figure 7: Mean surface nitrate concentrations by site.
- Figure 8: Mean surface nitrite concentrations by site.
- Figure 9: Mean surface urea concentrations by site.
- Figure 10: Mean surface total nitrogen concentrations by site.
- Figure 11: Mean surface orthophosphate concentrations by site.
- Figure 12: Mean surface total phosphorus concentrations by site.
- Figure 13: Mean surface silica concentrations by site.
- Figure 14: Mean bottom ammonium concentrations by site.
- Figure 15: Mean bottom nitrate concentrations by site.
- Figure 16: Mean bottom nitrite concentrations by site.
- Figure 17: Mean bottom urea concentrations by site.
- Figure 18: Mean bottom total nitrogen concentrations by site.
- Figure 19: Mean bottom orthophosphate concentrations by site.
- Figure 20: Mean bottom total phosphorus concentrations by site.
- Figure 21: Mean bottom silica concentrations by site.
- Figure 22: Maximum surface ammonium concentrations by site.
- Figure 23: Maximum surface nitrate concentrations by site.
- Figure 24: Maximum surface nitrite concentrations by site.
- Figure 25: Maximum surface urea concentrations by site.
- Figure 26: Maximum surface total nitrogen concentrations by site.
- Figure 27: Maximum surface orthophosphate concentrations by site.
- Figure 28: Maximum surface total phosphorus concentrations by site.
- Figure 29: Maximum surface silica concentrations by site.
- Figure 30: Maximum bottom ammonium concentrations by site.
- Figure 31: Maximum bottom nitrate concentrations by site.
- Figure 32: Maximum bottom nitrite concentrations by site.
- Figure 33: Maximum bottom urea concentrations by site.
- Figure 34: Maximum bottom total nitrogen concentrations by site.
- Figure 35: Maximum bottom orthophosphate concentrations by site.
- Figure 36: Maximum bottom total phosphorus concentrations by site.
- Figure 37: Maximum bottom silica concentrations by site.
- Figure 38: Mean concentration of ammonium, nitrate, nitrite, urea and orthophosphate by strata.
- Figure 39: Mean total nitrogen and total phosphorus concentrations by strata.
- Figure 40: Mean silica concentrations by strata.
- Figure 41: Time series of pressure (in kPa) at the bottom of the stream channel as a proxy for flow volume.

Figure 42: Base flow vs storm flow for ammonium, nitrate, nitrite, urea and orthophosphate.

Figure 43: Base flow vs storm flow total nitrogen and total phosphorus.

Figure 44: Base flow vs storm flow for silica. Units are mg-Si/L. Error bars denote standard error.

Figure 45: Time series of total nitrogen concentration (mg-N/L) for bottom samples at IN1.

Figure 46: Time series of total nitrogen concentration (mg-N/L) for bottom samples at CB25.

Figure 47: Time series of total nitrogen concentration (mg-N/L) for bottom samples at SB9.

Figure 48: Time series of total nitrogen concentration (mg-N/L) for bottom samples at NB18.

Figure 49: Scatterplot of ammonium concentrations (mg-N/L) vs sucralose (ng/L) concentrations in the stream.

Figure 50: Scatterplot of nitrate concentrations (mg-N/L) vs sucralose (ng/L) concentrations in the stream.

Figure 51: Scatterplot of nitrite concentrations (mg-N/L) vs sucralose (ng/L) concentrations in the stream.

Figure 52: Scatterplot of urea concentrations (mg-N/L) vs sucralose (ng/L) concentrations in the stream.

Figure 53: Scatterplot of total nitrogen concentrations (mg-N/L) vs sucralose (ng/L) concentrations in the stream.

Figure 54: Scatterplot of orthophosphate concentrations (mg-P/L) vs sucralose (ng/L) concentrations in the stream.

Figure 55: Scatterplot of total phosphorus concentrations (mg-P/L) vs sucralose (ng/L) concentrations in the stream.

Figure 56: Scatterplot of silica concentrations (mg-Si/L) vs sucralose (ng/L) concentrations in the stream.

Figure 57: Scatterplot of ammonium concentrations (mg-N/L) vs caffeine (ng/L) concentrations in the stream.

Figure 58: Scatterplot of nitrate concentrations (mg-N/L) vs caffeine (ng/L) concentrations in the stream.

Figure 59: Scatterplot of nitrite concentrations (mg-N/L) vs caffeine (ng/L) concentrations in the stream.

Figure 60: Scatterplot of urea concentrations (mg-N/L) vs caffeine (ng/L) concentrations in the stream.

Figure 61: Scatterplot of total nitrogen concentrations (mg-N/L) vs caffeine (ng/L) concentrations in the stream.

Figure 62: Scatterplot of orthophosphate concentrations (mg-P/L) vs caffeine (ng/L) concentrations in the stream.

Figure 63: Scatterplot of total phosphorus concentrations (mg-P/L) vs caffeine (ng/L) concentrations in the stream.

Figure 64: Scatterplot of silica concentrations (mg-P/L) vs caffeine (ng/L) concentrations in the stream.

Figure 65: Zones of coral condition as delineated by Vargas-Angel and Schumacher 2018 based on benthic surveys.

Figure 66: Mean percent cover at photo quadrat sites during 2016.

Figure 67: Bottom water nitrate concentrations (mean of sites IN1, SB9, CB27 and N18, units are mg N/L) over the time period of the photo quadrat benthic assessment.

Figure 68: Bottom water total nitrogen concentrations (mean of sites IN1, SB9, CB27 and N18, units are mg N/L) over the time period of the photo quadrat benthic assessment.

Figure 69: Bottom water ammonium concentrations (mean of sites IN1, SB9, CB27 and N18, units are mg N/L) over the time period of the photo quadrat benthic assessment.

Figure 70: Bottom water nitrite concentrations (mean of sites IN1, SB9, CB27 and N18, units are mg N/L) over the time period of the photo quadrat benthic assessment.

Figure 71: Bottom water urea concentrations (mean of sites IN1, SB9, CB27 and N18, units are mg N/L) over the time period of the photo quadrat benthic assessment.

Figure 72: Bottom water orthophosphate concentrations (mean of sites IN1, SB9, CB27 and N18, units are mg P/L) over the time period of the photo quadrat benthic assessment.

Figure 73: Bottom water total phosphorus concentrations (mean of sites IN1, SB9, CB27 and N18, units are mg P/L) over the time period of the photo quadrat benthic assessment.

Figure 74: Bottom water silicate concentrations (mean of sites IN1, SB9, CB27 and N18, units are mg Si/L) over the time period of the photo quadrat benthic assessment.

List of Appendix Figures

Figure A1: Mean ammonium, nitrate, nitrite, urea and orthophosphate concentrations by strata including stream site.

Figure A2: Mean total nitrogen and total phosphorus concentrations by strata including stream site.

Figure A3: Mean silica concentrations by strata including stream site.

List of Tables

Table 1: Estimated nitrogen budget for Vatia Bay to evaluate potential important sources.

Table 2: Details on each site, including lat/long, depth, strata and site notes.

Table 3: Method detection limits for the analytes measured in this study.

Table 4: Comparison of nitrogen data from this study (denoted with *) and an island wide assessment of water quality (Comeros-Raynall et al. 2017; Island Wide Mean).

Table 5: Median bottom water values for Vatia Bay.

List of Appendix Tables

Table A1: Wilcoxon with post-hoc Dunn's test results for nutrient concentrations by depth.

Table A2: Wilcoxon with post-hoc Dunn's test results for nutrient concentrations by strata.

Table A3: Wilcoxon test results for nutrient concentrations by stream state (base flow vs storm flow).

Table A4: Spearman rank correlations between nutrients.

Table A5: Spearman rank correlations between nutrients and tracers by strata.

List of Images

Image 1: Group photo of local partners during field work training in 2015.

Image 2: Photo of benthos in inner portion of Vatia Bay in 2016.

Image 3: Perennial watershed stream upslope of Vatia Bay.

Image 4: Groundwater seep on beach face at Vatia Bay during low tide.

Image 5: Church and surrounding houses in village of Vatia.

Image 6: Larger than average (approximate 1 hectare) area of agriculture (bananas and taro) in Vatia watershed.

Image 7: Targeted water quality sampling site at bridge by main stream tributary into Vatia Bay.

Image 8: Field personnel preparing to sample Vatia Bay for water quality by sea kayak.

Image 9: View of Vatia Bay from village (north shore).

Image 10: Vetiver grass and biochar nutrient removal system adjacent to piggery in Vatia.

Introduction and Background

Water quality problems, including sedimentation and over enrichment of nutrients, have the potential to adversely impact coral reef ecosystems. Coral reefs evolved in oligotrophic waters, but over the past century have been subjected to increasing levels of nutrients due to human activities. Land based contributions of nutrients to coastal systems originate from a variety of sources. Phosphorus and reactive nitrogen can enter the environment from chemical fertilizers (residential, commercial and agricultural uses), industrial sources, animal waste, and human waste (Galloway et al., 2003). Additionally, nitrogen can be contributed from biological nitrogen fixation and atmospheric nitrogen deposition (originating from fossil fuel combustion and ammonia volatilization from agriculture; Mathews et al., 2002).

Excess nutrient loads can cause increases in macroalgal growth which can have deleterious effects on corals, such as macroalgae outcompeting and overgrowing corals (D'Angelo and Wiedenmann 2014). Macroalgae often become established after a disturbance that causes high coral mortality (Szmant 2002; Fabricius 2005) such as a coral bleaching event, coral disease, a crown of thorns seastar outbreak, or a physical disturbance (storm, tsunami). Once established, macroalgae impedes coral recruitment through a variety of methods (Connell et al. 1997; Hughes and Tanner 2000; Szmant 2002; Fabricius 2005; Kuffner et al. 2006). Furthermore, nitrogen and phosphorus can impact corals directly by lowering fertilization success (Harrison and Ward, 2001), and reducing both photosynthesis and calcification rates (Marubini and Davis, 1996). However, nutrient threshold values, above which coral impacts are likely, have not been well established.

Study Site Description

Vatia Bay is located on the north shore of the island of Tutuila, the largest and most populous island of the U.S. territory of American Samoa (Figure 1). American Samoa's reefs are considered to be among the most pristine in the United States (Birkeland et al. 2008). These reefs host approximately 950 species of fish, 240 species of algae, 330 species of coral and many other species of invertebrates (Birkeland et al. 2008).



Image 2: Photo of benthos in inner portion of Vatia Bay in 2016.

American Samoa exhibits a tropical climate with warm, humid conditions throughout the year. There is a wet season (October to April) and a dry season (May to September), but rainfall is common throughout the year, with annual averages ranging from 320 cm to over 750 cm, depending on topographic location, with mountains receiving more rain (NPS 2015).

The Samoan islands were formed by volcanic activity approximately seven million years ago. On Tutuila, the oldest rocks are from the Masefau dike complexes containing flows cut by basaltic dikes and talus breccias. Younger volcanic rocks include the Alofau and Olomoana volcanic rocks, the Taputapu volcanic rocks, the Pago volcanic series, Leone

volcanic rocks, and the 'Aunu'u tuff. These rocks are from volcanic episodes separated by

periods of erosion. These units typically contain basalt, olivine basalt, picrite- basalt, and hawaiite flows with less common elements including cinder cone and ash deposits (Wingert and Pereira 1981). The youngest map units on Tutuila are the loose calcareous beach sands, slope talus, and fluvial alluvium on the shores and valley floors of the island (Thornberry- Ehrlich 2008).



Image 3: Perennial watershed stream upslope of Vatia Bay.

The Bay is roughly horseshoe shaped, with the opening to the ocean oriented to the north northwest. At its widest point, the Bay is approximately 750 meters wide, and approximately 1 kilometer in length. The benthic habitat of the Bay is a mixture of hard bottom (live coral, coral rubble, pavement), crustose coralline algae (CCA), fleshy macroalgae, and turf algae, with small patches of sand (Vargas-Angel and Schumacher 2018). There have been local concerns about the impacts of land based sources of pollution and water quality on the coral reef ecosystems of Vatia Bay (NOAA CRCP 2012, see Image 2).

There are three perennial streams that bring freshwater inflows from the surrounding watershed into the Bay (Image 3), as well as some additional intermittent streams that may flow during large rainfall events. Additionally, groundwater may play a significant role in the freshwater influxes to the Bay as evidenced by visible beach face seeps at low tide (field observations, see Image 4). The watershed is very steep (Tutuila is a high volcanic island); as a result, the only development in the watershed is very close to the shore, where the topography is flat enough to permit construction. The Bay is ringed by the small village of Vatia (6.5 km² in area), which consists of 116 housing units and 640 residents (US Census, 2010). The land surrounding the village is part of the National Park of American Samoa. The village contains an elementary school and multiple churches, and the shoreline is partially armored with a seawall (Image 5). There is no centralized sewage treatment system for the village.



Image 4: Groundwater seep on beach face at Vatia Bay during low tide.



Image 5: Church and surrounding houses in village of Vatia. Seawall is pictured in the foreground.

Household sewage is treated via septic systems, cesspits, or in some cases, may go untreated. There are some small backyard vegetable gardens, and a slightly larger (approximately one hectare, see Image 6) cleared area in which bananas and taro are grown at a slightly larger scale, but crop agriculture is not prevalent in the watershed. Additionally, there are approximately 10 backyard piggeries, whose standing stock varies. There are on the order of 70 pigs in Vatia at any given time (Diego Ayala, NRCS, personal communication; USDA-NRCS unpublished data from 2015). There is no industry or other businesses in the watershed. As with much of the island, feral or semi-feral dogs are prevalent in the village. An estimate by the island veterinarian places the dog population

between 60 and 150 individuals (Brenda Smith, veterinarian, 2012, personal communication). While fruit bats can play a large role in the biogeochemistry of ecosystems in American Samoa, at the time of this study, there was not a major roost in the Vatia watershed (Adam Miles, biologist, Division of Marine and Wildlife Resources, 2015, personal communication).

Using literature values and site specific census information, a rough estimate of nutrient source apportionment can be calculated (See Table 1). This is not a rigorous mass balance nutrient budget, rather a preliminary estimate to help guide further investigations. This exercise suggests that humans and pigs are the most important contributors of nitrogen to the Bay. Because this (Table 1) is only an estimate, additional field data is required to better understand the relatively role of humans versus pigs. However, it can be difficult to discriminate between two different animal (human vs pig) sources of nutrients. For example, stable nitrogen isotopes can be useful in identifying animal sources versus chemical fertilizers, but are not helpful in identifying specific mammalian sources. Simple microbial analyses (e.g. total coliform or *E. coli*) can detect waste but are not organism specific. More complicated microbial source tracking techniques are not well suited for work in remote areas such as Vatia without access to appropriate laboratory facilities.



Image 6: Larger than average (approximate 1 hectare) area of agriculture (bananas and taro) in Vatia watershed.

Table 1: Estimated nitrogen budget for Vatia Bay to evaluate potential important sources. Note that all rows are anthropogenic in nature except for Forest which is a natural source.

	Number	N/unit/year (kg)	Total N (kg)	%	Reference
People (#)	640	5	3200	43	US Census 2010; Whitall et al. 2004
Pigs (#)	58	52	3016	40	USDA-NRCS 2015; Iowa State 2015
Dogs (#)	150	4	600	8	Brenda Smith, veterinarian, pers. Comm.; Baker et al. 2001
Agriculture (ha)	1	200	200	3	Areal size estimated from satellite images in ArcGIS; Hartemink et al. 2000
Forest (ha)	486	1	486	6	Whitall et al. 2004
Total			6118	100	

In order to better identify potential nutrient sources, two chemicals (caffeine and sucralose) that are unique to the human diet were quantified in the Bay. Caffeine is a common dietary stimulant found in a variety of food and beverages, including coffee, soda, energy drinks, and chocolate, as well as over the counter medications. While natural/plant based sources of caffeine do exist (wild growing coffee or cacao plants), these species are not present in the Vatia watershed (Ian Gurr, horticulturalist, American Samoa Community College, personal communication). Caffeine is excreted in human urine and can persist in the natural environment. Previous studies have quantified caffeine in aquatic systems (Edwards et al. 2015) and found correlations with other indicators of human waste (Knee et al. 2010).

Sucralose (4-chloro-4-deoxy- α ,D-galactopyranosyl-1,6-dichloro-1,6-dideoxy- β ,D-fructofuranoside) is a chlorinated disaccharide derived from sucrose. It is used as an artificial sweetener found in diet beverages, candies and as a stand-alone additive (i.e. under the brand name Splenda). Most ingested sucralose is not metabolized in the human body and is excreted in urine and feces. It is relatively stable in the environment which makes its use as a tracer appealing. It has previously been quantified in freshwater (Spoelstra et al. 2013) and marine (Mead et al. 2009) ecosystems. It has also been shown to outperform other chemical sewage tracers in field assessments (Oppenheimer et al. 2011). Because caffeine is more prevalent in human diets, both sucralose and caffeine were included in the chemical analyses for this study.

Objectives

The goals of this portion of the baseline assessment of Vatia Bay were to:

1. Quantify the magnitude and spatiotemporal variability of surface water nutrients in the Bay;
2. Establish a baseline of nutrient conditions against which to measure changes in the future;
3. Link observed concentrations of nutrients to hydrologic forcing factors and possible nutrient sources;
4. Use human dietary chemical indicators to evaluate if human waste is reaching Vatia Bay;
5. Correlate observed patterns in nutrient dynamics with measured indices of coral ecosystem health.

Methods

Benthic Cover Photo Quadrat Methodology

In order to quantify changes in benthos over time, a subset of five of the eighteen stratified random sites previously surveyed for benthic cover and coral demographics (Vargas-Angel & Schumacher 2018) were monitored for changes in benthic cover, over a period of 12 months with visits in January, June, and December of 2016. The five sites are shown in Figure 2 and were selected from the larger group of sites because they were relatively shallow and easy to access for repeated photography.

At each site, two haphazardly laid, 18-m transects were the focal point of the surveys. Still photographs were taken from a pole mounted camera one meter from the substrate at a frequency of every 1 m along the transect (from 1 meter to 15 meters), for a total 30 photographs per site. The same photoquadrats were re-visited over the course of the 12 months. The photographs documented the benthic community composition, with each still representing approximately 0.75 m² of benthic area. Benthic habitat digital images were quantitatively analyzed using CoralNet (Beijbom et al. 2015), whereby 25 stratified random points were projected on each image and the benthic elements underneath at each point were identified following the classification scheme outlined in Lozada-Misa et al. (2017). In this method, the benthic assemblage was identified to the functional group level, including hard coral, CCA, encrusting macroalgae, fleshy macroalgae, cyanobacteria, *Halimeda*, turf algae, sediment, octocoral, and sessile macroinvertebrates.

Water Quality Sampling Design

Four strata were operationally articulated within the Bay based on proximity to the stream/shore and geography: Inner, Central, North, and South. Within each strata, four sites were randomly selected (using ArcGIS) in order to capture the spatial variability within the Bay (see Figure 2). This stratified random sampling design allows for statistical comparisons among the articulated

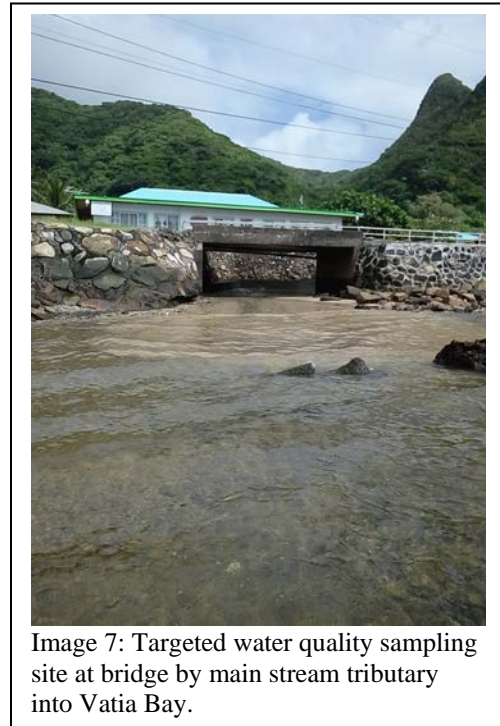


Image 7: Targeted water quality sampling site at bridge by main stream tributary into Vatia Bay.

strata. Additionally, one targeted site was selected at the largest stream channel input to the Bay (just upstream from the largest bridge in the village, see Image 8). Details about each site, including latitude and longitude are shown in Table 2. Sites were accessed by either sea kayak (Image 9) or wading (Image 10). At wading sites, care was taken to sample away from the person's body and on an incoming swell/wave to minimize the potential for contamination. Surface water (0.1 m below surface) and bottom water (via Niskin bottle, just above bottom) were collected for water quality analysis; exceptions to this were very shallow sites (<1 m depth, sites IN3, IN4, SB10, SB11, SB12, NB19, NV20) at which only surface water was sampled, and one site (NB17) which consistently had high wave energy, making deploying the Niskin bottle from the sea kayak unsafe.

Table 2: Details on each site, including lat/long, approximate depth, strata and site notes. Surface and bottom water samples were collected at each site unless otherwise noted.

Site	Depth(m)	Latitude	Longitude	Strata	Notes
CB25	7 m	-14.2479	-170.6724	Central	
CB26	7 m	-14.2462	-170.6717	Central	
CB27	5 m	-14.2481	-170.6703	Central	
CB28	7 m	-14.2459	-170.6701	Central	
IN1	3 m	-14.2494	-170.6732	Inner	
IN2	3 m	-14.2488	-170.6741	Inner	
IN3	<1 m	-14.2507	-170.6737	Inner	surface sample only
IN4	<1 m	-14.2470	-170.6748	Inner	surface sample only
NB17	>10 m	-14.2445	-170.6714	North	surface sample only
NB18	3 m	-14.2462	-170.6726	North	
NB19	<1 m	-14.2460	-170.6733	North	surface sample only
NB20	<1 m	-14.2448	-170.6721	North	surface sample only
SB10	<1 m	-14.2490	-170.6696	South	surface sample only
SB11	<1 m	-14.2504	-170.671	South	surface sample only
SB12	1.5 m	-14.2478	-170.6683	South	
SB9	6 m	-14.2487	-170.6706	South	
Stream	<1 m	-14.2506	-170.6754	Stream	Targeted site at bridge

From 2015 to 2017, each of these sites was visited monthly to collect grab samples. In 2018, sampling efforts focused on capturing precipitation events, so the sampling was conducted at less regular intervals.

High density polyethylene (HDPE) bottles were used for nutrient collections. The bottles were rinsed three times with site water prior to sampling. Nitrile or latex gloves were worn by field personnel to avoid contamination of the samples during handling. Samples were stored on ice, in



Image 8: Field personnel preparing to sample Vatia Bay for water quality by sea kayak.

the dark while in the field, frozen at -20°C upon returning to the lab and not thawed until immediately prior to analysis. Samples were not filtered so that total nutrient levels could be analyzed, rather than only dissolved levels. During some sampling months, extra sample volume was collected (into amber glass vials) for analysis of caffeine and sucralose. These were sampled concurrently with the nutrient samples at the same sites.

Analytical Methods Used for the Analysis of Nutrients

Nutrient laboratory analyses were performed by a NOAA contract lab (Geochemical and Environmental Research Group, Texas A&M University, sub-contract to TDI Brooks). Water samples were analyzed for a standard suite of nutrient analytes: nitrate (NO_3^-), nitrite (NO_2^-), orthophosphate (HPO_4^-), ammonium (NH_4^+), urea ($(\text{NH}_2)_2\text{CO}$), total nitrogen, total phosphorus and silica.

Nitrate and nitrite analyses were based on the methodology of Armstrong et al (1967).

Orthophosphate was measured using the methodology of Bernhardt and Wilhelms (1967) with the modification of hydrazine as reductant. Silicate determination was accomplished using the methods of Armstrong et al. (1967) using stannous chloride. Ammonium analysis was based on the method of Harwood and Kuhn (1970) using dichloro-isocyanurate as the oxidizer. Urea was measured using diacetyl-monoximine and themicarbozide. The total concentrations of nitrogen and phosphorus were determined after an initial decomposition step. This method involves persulfate oxidation while heating the sample in an autoclave (115°C , 20 minutes) (Hansen and Koroleff 1999). After oxidation of the samples, nutrient determination was conducted on the Astoria Pacific analyzer for nitrate and orthophosphate.

Analytical Methods Used for the Analysis of Tracers

Tracers (caffeine and sucralose) were quantified at Florida International University (sub-contract to TDI Brooks) using previously published methods (Wang 2012; Batchu et al 2015). The methodology for sucralose quantification is based on automated online solid-phase extraction (SPE) and high-resolving-power orbitrap mass spectrometer (MS) detection. Operating in full scan (no collision-induced dissociation), detection of the unique isotopic pattern (100:96:31 for $[\text{M}-\text{H}](-)$, $[\text{M}-\text{H}+2](-)$, and $[\text{M}-\text{H}+4](-)$, respectively) was used for ultra-trace quantitation and analyte identification. The method offers fast analysis (14 min per run) and low sample consumption (10 mL per sample) with method detection limits (MDLs) and



Image 9: Field personnel sampling sites on the inner part of Vatia Bay.

method confirmation limits (MCLs) of 1.4 and 5.7 ng/L in seawater, respectively.

The caffeine procedure is based on the combined performance of an Equan MAX Plus online Solid Phase Extraction (SPE) preconcentration system coupled to a high pressure liquid chromatography (LC) system equipped with resolution mass spectrometry detection using a QExactive orbitrap-based mass spectrometer (SPE-LC-HRMS). The analytical separation was carried out using a Hypersil Gold aQ column (100×2.1 mm, 1.9 μm) while the SPE preconcentration column was a Hypersil Gold aQ (0.5×50 mm; Thermo Scientific, West Palm Beach, FL, USA). The automated online SPE clean-up and pre-concentration step was performed using only 10 mL of filtered water samples. The online procedure consists of a diversion valve on the mass spectrometer which is programmed by the data system to control the loading and elution of the two LC columns. In the load position, 10 mL of sample was injected into a 10-mL loop and then loaded onto a SPE column by the loading LC pump, followed by a wash step with 98:2 0.1% formic acid: acetonitrile to remove interferences (flow rate 2 mL/min). The target compounds were retained in the SPE column and the matrix that is not retained during the extraction process was directed to waste while simultaneously the analytical pump equilibrated the analytical column in the starting gradient conditions. After 5 min, when the valve was switched to inject position, the solvent flow through the SPE column was reversed, and the analytes were then backflushed with a gradient of acetonitrile and 0.1% formic acid onto a Hypersil Gold aQ column for separation and quantitation by heated electrospray ionization source (HESI)-MS/MS. After 7 min, the switching valve was returned to the loading position to allow the extraction column to be re-equilibrated with water. The samples were kept at 10 °C in the autosampler. The total run time per sample was 13 min. The analyte was detected on a Q-Exactive Mass spectrometer equipped with an HESI source operated in the positive mode. The capillary temperature was 350 °C with a discharge current of 4 kV and S-lens RF level of 80 %. Sheath gas and auxiliary gas (N₂) were used at a flow rate of 30 and 20 arbitrary units, respectively. The analysis was performed in Parallel Reaction Monitoring (PRM) (with an inclusion list of the exact mass of the target compounds) at a resolution of 35,000. Quantitation is performed by the internal standard approach (concentrations are calculated based on area ratio between the analyte and labeled internal standard) to correct for matrix effects and any losses in the online extraction step. The monitoring ions for caffeine were 195.0877 and 138.0662 and for the labeled caffeine (¹³C₃ caffeine) was 198.0977.

Method Detection Limits

Method detection limits for all compounds are shown in Table 3. Analytical values that were below the MDL were treated with the statistical methods described in Flynn (2010). Briefly, the dataset for each analyte was transformed to near normality (e.g. using a natural log transform) and the below MDL data was then fitted to the curve below the MDL cutoff. The Shapiro Wilk W statistic was maximized using an iterative solving process, which results in an assigned “dummy” value for each value below the detection limit, ranging from zero to the detection limit. This creates a dataset in which the data that are below the MDL have unique values with the same statistical distribution as the data set as a whole and can therefore be analyzed statistically without biasing the data (e.g. without assigning all below MDL data to one half of the MDL value).

Statistical Analysis of Water Quality Data

Because the datasets were not perfectly normal, even with transformation, non-parametric statistics were used to evaluate relationships within the dataset. A Wilcoxon test, with post-hoc Dunn’s analysis was used to examine differences among strata, between depths and between flow regimes. Spearman correlations were used to examine relationships between analytes. Mean and maximum values were also calculated for each site. Relevant statistical findings are discussed in the text below, and presented in tabular form. JMP statistical software was used for all statistical analysis.

Table 3: Method detection limits for the laboratories used in this study.

MDL		<p>Results and Discussion <i>Spatial Differences in Nutrient Concentrations</i> Figures 3 to 5 show mean values of each nutrient concentrations by depth (surface vs bottom). Nitrate, nitrite, orthophosphate</p>
Silicate	0.00196 mg-N/L	
Nitrate	0.00154 mg-N/L	
Nitrate	0.000168 mg-N/L	
Ammonium	0.000798 mg-N/L	
Urea	0.012 mg-N/L	
Orthophosphate	0.00035 mg-P/L	
TN	0.00154 mg-N/L	
TP	0.00035 mg-P/L	
Sucralose	12.1 ng/L	
Caffeine	1.10 ng/L	

and silica all had statistically higher (Wilcoxon test $\alpha=0.05$) concentrations in the surface waters. This indicates that the Bay is not completely mixed and that nutrients associated with freshwater inflows may be staying near the surface with the less dense freshwater. However, this hypothesis is not supported by salinity data collected on site via refractometer, which showed that all sites, surface and bottom had salinities between 38 and 41 psu. The exception to this was the stream site, which had expectedly lower salinity values (which varied depending on tidal state). It is possible that biological processing, rather than solely salinity gradients, are driving the differences between surface and bottom for some nutrients. Nutrient uptake by benthic algae may be one possible explanation of this, given the prevalence of algae (over 60% of benthos is macroalgal/turf cover) throughout a large portion of the Bay (Vargas-Angel and Schumacher 2018).

Figures 6 to 37 show maps of mean and maximum nutrient concentrations at each site for both surface and bottom samples. Mean concentrations represent the chronic nutrient status of the system and maximum values show the acute exposures.

Figures 38 to 40 show mean values of each analyte by strata. These figures are also presented with the stream values in the Appendix (Figures A1 to A3), but the stream values (from a targeted site) should not be statistically compared with stratified random sites in the Bay. There

are significant differences among the strata for nitrate, silica and total phosphorus (Wilcoxon with post-hoc Dunn's test, $\alpha=0.05$), with silica and TP being highest in the Inner and Central strata and nitrate being highest in the South stratum. This suggests that that groundwater, overland flow and the stream all contribute to the nutrient budget of the Bay.

Temporal Differences in Nutrient Concentrations

For a portion of the dataset presented here (July 2015 to December 2016), pressure transducer data were available for the main stream in Vatia as a part of another project. These instream data are a proxy for stream height, and while they do not provide an actual volumetric flow, they can be useful in determining the state of the stream (base flow vs storm flow) in the time leading up to water quality sampling. Figure 41 shows the stream height (as total pressure, i.e. atmospheric pressure, plus pressure due to water height) over time as it relates to when the water quality data were collected. Using these data, water quality sampling time points were binned into "base flow" or "storm flow" and analyzed for differences using a Wilcoxon test. Figure 42 to 44 show base flow versus stormflow mean values. Nitrate, urea, and silica are all higher during storm flows (Wilcoxon, $\alpha=0.05$); ammonium and total nitrogen were higher during base flow. Silica is a useful indicator of runoff/erosion, so this pattern is expected. However, the temporal nitrate pattern is somewhat surprising, because in many watersheds nitrate is primarily transported through groundwater, so base flow concentrations are usually highest, with dilution occurring during storm events. This could mean that groundwater nitrate is relatively unimportant in this system, or that there are strong runoff related sources (e.g. septic, piggeries, small scale crop agriculture) of nitrate reaching the Bay. Urea and ammonium should be tightly linked (i.e. urea is easily converted to ammonium in the environment via enzymatic hydrolysis), so this disconnect is somewhat surprising and suggests that at higher flows this enzymatic process takes some time to occur and higher inorganic nitrogen levels might not be observable until after a storm event.

This temporal variability in nutrient concentrations also has implications for ecosystem effects. Figures 45 to 48 show time series of bottom water total nitrogen concentrations at one site for each stratum (this pattern is consistent across all sites). Note that in each case the bottom water concentration fluctuates by a four to six fold difference; the ecosystem is experiencing both acute and chronic nutrient stress under these conditions.

Tracers

Both tracers of human waste (caffeine and sucralose) were detected in the Bay. Sucralose was detected in 51% of samples analyzed (97 out of 192) and caffeine was detected in 82% of the samples analyzed (157 out of 192). Because human waste is the only potential source of these compounds, this definitively shows that human waste is reaching Vatia Bay. The higher occurrence of caffeine compared to sucralose could be due to higher usage of caffeine by residents of the village, as it is in more food products than sucralose, or may be related to differences in analytical MDL between the two compounds; the MDL for caffeine is an order of magnitude lower than for sucralose.

There were no statistically significant differences (Wilcoxon with post-hoc Dunn's test, $\alpha=0.05$) among strata for sucralose and caffeine concentrations. While not included in the statistical analysis, concentrations of these tracers were generally higher in the stream than in the Bay.

Although dilution is obviously occurring as stream water reaches the Bay, elevated stream concentrations suggests that watershed sources play a role in tracer flux, and therefore indicative of sewage related inputs.

Correlations between Analytes

Nutrient data across all sampling dates were not well correlated with each other (Spearman rank correlation, $\alpha=0.05$). While there were a number of nutrient pairs that had statistically significant correlations, the rho coefficients were relatively low (<0.40). The exception to this was nitrite and urea which had a rho value of 0.65. This could indicate that these nutrients have the same sources in time and space. These relationships were similar if correlations were considered only within strata, or within the same depth.

Tracer concentrations were significantly correlated with multiple nutrient analytes. However, Spearman rho coefficients were generally below 0.40, with the exception of sucralose and urea, which were slightly more strongly correlated in the North and South strata (rho=0.47 and 0.55, respectively). This would be consistent with leaking septic systems (or lack of sewage treatment) contributing a flux of nutrients (as urea, a primary component of human waste) via groundwater or direct overland flow. Unfortunately, there were not enough stream data points to statistically assess the correlations in the stream itself. Scatterplots of the tracers versus individual nutrients (Figures 49-64) suggest that this same relationship with urea may be present in the stream. Interestingly, in the Bay itself, both sucralose and caffeine actually had statistically significant negative relationships with total nitrogen, total phosphorus and nitrate. This could suggest that biological processing (e.g. conversion of urea to ammonium to nitrate, or uptake by benthic algae) effectively decouples the concentration of nutrients in sewage from the tracers. Stream scatter plots may support this hypothesis, as there appear to be relationships between tracers and nutrients (e.g. TN and TP with sucralose) in the stream that are not present in the Bay. This supports that idea that biogeochemical cycling in the Bay may be decoupling the tracer signal from the nutrient signal. Additional tracer and nutrient data from the stream would be useful to better understand this relationship. From a source tracking perspective, urea is the analyte most likely to be associated with both human and animal waste. These correlations demonstrate that human waste is an important, and perhaps the dominant, source of nitrogen to the nutrient budget of Bay.

Caveats for Interpreting Tracer Results

Because caffeine and sucralose are not ubiquitous in the human diet, it is possible that observed spatial differences in tracer concentrations may be attributable to dietary differences between households of the village, rather than differences in sewage flux. However, because no significant differences among strata for tracers were observed, this is probably unlikely.

Putting the Results in Context

In order to put the data from this study into a larger (regional) context, they were compared with water quality data (nitrate, nitrite, ammonium) from a joint study by American Samoa Environmental Protection Agency (ASEPA) and Division of Marine and Wildlife Resources (sites described in Comerros-Raynal et al. 2017; unpublished data) study which quantified water quality on the reef flat in twenty six drainage areas across the island of Tutuila, monthly in 2016 and 2017. These data provide valuable context for what was observed in Vatia. It should be

noted that these twenty-six drainage areas included some more developed areas (e.g. Nu'uuli, Faga'alu) compared to Vatia, which is a relatively small village. The overall means (island wide) of the ASEPA/DMWR studies are similar to what was observed in this study in Vatia (Table 4), with the exception of nitrite which is higher in Vatia.

Table 4: Comparison of mean nitrogen data (SE in parantheses) from this study (denoted with *) and an island wide assessment of water quality (Comeros-Raynall et al. 2017; Island Wide Mean, with SE in parantheses).

Location	Nitrite (mg N/L)	Nitrate (mg N/L)	Ammonia (mg N/L)
Island Wide Mean	0.0013 (0.00007)	0.0408 (0.00269)	0.0158 (0.00159)
Vatia (Bay Wide)*	0.0112 (0.00088)	0.0105 (0.00131)	0.0086 (0.00055)
Vatia Inner*	0.0107 (0.00149)	0.0066 (0.00085)	0.0080 (0.00093)
Vatia Central*	0.0109 (0.00139)	0.0083 (0.00177)	0.0083 (0.00110)
Vatia North*	0.0109 (0.00183)	0.0076 (0.00081)	0.0077 (0.00086)
Vatia South*	0.0105 (0.00166)	0.0108 (0.00315)	0.0087 (0.00107)

Water quality standards for the territory of American Samoa have been enacted by USEPA/ASEPA (USEPA 2013). For embayments such as Vatia Bay, there are nutrient criteria for TP and TN, specifically that the median cannot exceed 0.02 mg/L and 0.15 mg/L respectively. Median values of TP and TN measured in this study (Table 5) indicate that all sites are in exceedance of these water quality standards for TN, and all sites except for SB11 (bottom) exceed the standard for TP. It should be noted that the median for SB11 (bottom) is 0.019, which is just barely below the standard. Based on these water quality standards, in combination with observed benthic prevalence of algae, we can conclude that Vatia Bay is under nutrient stress.

Comparison with Biological Data

Previous work by NOAA's Pacific Islands Fisheries Science Center characterized benthic habitat (cover type and coral species) and metrics of coral health (adult and juvenile coral colony density, colony partial mortality (old and recent), and condition (disease and bleaching) for total scleractinians) at Vatia Bay in 2015 (Vargas-Angel and Schumacher 2018). This study concluded that there were three levels of impact (Figure 65):

- 1) Inner Bay (very poor reef condition) where the benthic community was characterized by very low coral cover, and dominated by fleshy macroalgae;
- 2) Middle Bay (fair to moderate reef condition) where the reef community was dominated by plating/branching corals (*Porites rus*) intermingled with patches of sediment and calcifying macroalgae
- 3) Outer Bay (fair to good condition) where the benthos was characterized by robust coral reef development; community consisted of diverse assemblage of corals with low levels of macroalgae and only minor damage observed.

Qualitatively this biological assessment mirrors the water quality data, i.e. degraded conditions closer to the stream mouth. While it is likely that the corals in Vatia Bay are subjected to multiple stressors, the spatial overlap between water quality issues and degraded habitat strongly suggests that water quality plays a role in reef health.

Table 5: Median bottom water values for Vatia Bay. Territorial water quality standards are 0.15 mg N/L total N and 0.02 mg P/L total P. All sites exceeded the standard for TN and only one site (SB11) did not exceed the standard for TP (highlighted in bold italics).

Site Name	Median TN (mg N/L)	Median TP (mg P/L)
CB25	0.261	0.030
CB26	0.247	0.032
CB27	0.224	0.028
CB28	0.225	0.029
IN1	0.242	0.030
IN2	0.261	0.031
NB18	0.245	0.028
SB11	0.386	<i>0.019</i>
SB9	0.202	0.024

For photo quadrat measurements, site-level and mean benthic cover for the salient functional groups —i.e., hard coral, crustose coralline algae (CCA), encrusting macroalgae, *Halimeda*, and turf algae, are presented in Table 6. Due to the limited sample size (5 sites) of the cover dataset, temporal comparisons of mean functional group cover between the January and December sample periods are presented as 95% confidence intervals (Table 7), whereby if the 95% confidence interval of the difference between means includes zero, the difference between the means is not significant ($P > 0.05$). With the exception of encrusting macroalgae, benthic cover for all other salient functional groups significantly differed between the months of June and December 2016 (Figure 66). The major calcifiers, hard corals and CCA exhibited relative increases of 20% (from 32.2 to 40.4%) and 29% (from 12.3% to 17.4%), respectively (Table 7, Figure 66), while, turf algae and *Halimeda* observed relative decreases in the order of 54.5% and >100%, respectively (Table 7). These significant increases over a relatively short period of time are rather unexpected given the underlying chronic impacts from nutrient enrichment and sediment runoff and turbidity in Vatia. Concomitantly, a significant (>50%) reduction in turf algae cover is also notable. More detailed inspection of the analyzed benthic imagery suggests that coral cover increases were mainly achieved by the expansion and growth of branching and table coral colonies, including *Porites cylindrica* and *Acropora cytherea*. The morphology of these corals allows them to grow vertically and horizontally over shading other low-profile and encrusting taxa; in this case not necessarily overgrowing and displacing the algal taxa, but actually overtopping them.

Table 6: Site-level and mean benthic cover for salient benthic functional groups in Vatia over 3 sample periods in January, June, and December 2016.

Functional group/site	January	June	December
Hard coral			
TUT-2170	40.59	46.93	54.27
TUT-2172	12.85	14.80	18.93
TUT-2174	34.36	50.20	46.67
TUT-2161	33.91	41.18	36.96
TUT-2167	39.33	38.99	44.73
Mean	32.21	38.42	40.31
Coralline algae			
TUT-2170	24.30	20.93	26.93
TUT-2172	13.39	10.40	15.33
TUT-2174	4.41	17.40	13.07
TUT-2161	7.61	9.36	12.75
TUT-2167	11.60	13.89	19.03
Mean	12.26	14.40	17.42
Encrusting macroalgae			
TUT-2170	1.60	2.67	2.27
TUT-2172	1.34	6.13	6.80
TUT-2174	4.01	1.47	4.80
TUT-2161	0.13	1.60	1.15
TUT-2167	0.27	2.27	2.30
Mean	1.47	2.83	3.46
<i>Halimeda</i>			
TUT-2170	2.00	0.13	0.13
TUT-2172	5.62	3.60	3.47
TUT-2174	3.88	0.54	1.33
TUT-2161	0.13	0.13	0.00
TUT-2167	3.47	1.20	2.18
Mean	2.07	1.45	1.45
Turf algae			
TUT-2170	28.70	23.07	10.40
TUT-2172	57.30	51.20	40.67
TUT-2174	50.94	26.37	29.07
TUT-2161	52.34	43.45	41.40
TUT-2167	42.27	38.99	28.36
Mean	46.31	36.61	29.98

Table 7: Statistical temporal comparison of 95% confidence intervals of mean cover of hard corals, CCA, encrusting macroalgae, Halimeda, and turf algae in Vatia Bay surveyed in January and December, 2016. Significant differences are indicated with – or + to represent a significant decrease or increase, respectively.

Functional group	January	December	Relative Percent change	Difference of Means	Confidence interval		Significance $\alpha = 0.05$
					Upper limit	Lower limit	
Hard coral	32.21	40.31	20.10	-8.10	-12.96	-3.24	+
Coralline algae	12.26	17.42	29.62	-5.16	-13.85	-2.35	+
Encrusting macroalgae	1.47	3.46	57.54	-1.99	-4.49	0.51	
Halimeda	3.02	1.42	-112.26	1.60	0.43	2.76	-
Turf algae	46.31	29.98	-54.46	16.33	11.14	21.51	-

These sudden bursts in coral and CCA growth are likely to be driven by the local environmental variability. As such, it is reasonable to hypothesize that the slightly warmer sea temperatures registered during the 2015–2016 ENSO, which did not result in widespread catastrophic bleaching in Vatia, together with below average rainfall (lower runoff), and lower cloud cover during that El Niño year could be implicated in boosting growth rates in the principal calcifiers. Similar observations were recorded during the 1997–98 El Niño in the eastern tropical Pacific where corals linear extension rates were 40–70% greater during the warming event compared to a normal non-ENSO year (Vargas-Ángel et al 2001).

In order to evaluate the potential role of water quality in observed temporal changes in benthic cover, data from the closest water quality site were compared to the photo quadrat data. Note that only sites within 100 meters of the photo quadrat sites were included; as a result, there is no water quality comparison possible at benthic site TU-2167. Bottom water nutrient concentrations were analyzed since this corresponds to the benthic exposure. The time series of nutrient data were analyzed from the inception of the project until the end of the benthic assessment (Dec 2016). By examining water quality data prior to the photo quadrat study, this takes into account that benthic changes, especially as they relate to coral cover do not occur immediately. Because the benthic cover data among the sites were composited, we also composited the water quality data from the relevant sites (IN1, SB9, CB27, NB18).

While there were trends over that time period for individual nutrients, the overall pattern is not clear. Nitrate and total nitrogen had decreasing trends over that time (Figure 67 – 68). All other analytes had increasing trends



Image 10: Vetiver grass and biochar nutrient removal system adjacent to piggery in Vatia (Photo Credit: Paul Sturm, Ridge to Reef)

(Figures 69-73). It should be noted that all temporal patterns (regressions) were relatively weak. It should be noted that relationships between nutrients and benthic changes could be non-linear, but there are not enough data points to adequately address this possibility. It is also possible that the reduction in nitrate and total nitrogen was partially responsible for the changes in benthic cover. Although there are some nutrient management projects that are underway in Vatia (e.g. vetiver grass and biochar treatment of waste from piggeries and the school, see Image 11), these efforts began later than the time period in question. It is likely that the observed nutrient decreases were linked to climate forcing factors (i.e. lower precipitation leading to lower runoff). A decreasing pattern in silica supports this hypothesis, e.g. with lower rainfall and lower runoff/erosion, silica concentrations would be expected to be lower (Figure 74).

Conclusions

This study articulated the spatiotemporal variability in nutrient concentrations in Vatia Bay. Results showed that while the magnitude of nutrient pollution is similar to the island as a whole, it exceeds the territorial water quality standards for embayments (total nitrogen and total phosphorus). Water quality patterns generally mirror the previously observed patterns in coral reef ecosystem condition. While coral reefs in Vatia are almost certainly exposed to multiple stressors (nutrients, sedimentation, temperature, fishing, etc), the data in this paper provide strong evidence that nutrient pollution is a problem in Vatia Bay. Furthermore, the use of sucralose and caffeine and tracers have definitively established that human waste is reaching the Bay. This information is critical to coastal managers in making decisions about remediation activities and best management practices.

Local management agencies selected the Vatia watershed as a priority site for conservation efforts (NOAA CRCP 2012). Proposed strategies to reduce pollution include: improving on-site sewage disposal systems, and preventing future degradation through watershed and land-use planning. Environmental data, such as the dataset presented here, serve as a baseline of current conditions, which are needed to determine the efficacy of management efforts, i.e. measuring change over time. The data presented here can be utilized by coastal managers to best prioritize management strategies in a way to maximize success in decreasing stressors on coral reef ecosystems.

References

- Armstrong, F, Stearns, C. 1967. The measurement of upwelling and subsequent biological processes by means of the Technicon Autoanalyzer and associated equipment. *Deep-Sea Research* 14: 381-389.
- Baker, L, Hope, D, Xu, Y, Edmonds, J, Lauver, L. 2001. Nitrogen Balance for the Central Arizona–Phoenix (CAP) Ecosystem *Ecosystems* 4: 582–602.
- Batchu, S, Ramirez, C, Gardinali, P. 2015. Rapid ultra-trace analysis of sucralose in multiple-origin aqueous samples by online solid-phase extraction coupled to high-resolution mass spectrometry. *Analytical and Bioanalytical Chemistry* 407:3717-25.
- Birkeland C, Craig P, Fenner D, Smith L, Kiene W, Riegl B. 2008. Geologic setting and ecological functioning of coral reefs in American Samoa *Coral Reefs of the USA*. Springer, pp 741-765.
- Beijbom O, Edmunds P, Roelfsema C, Smith J, Kline D, Neal B (2015) Towards Automated Annotation of Benthic Survey Images: Variability of Human Experts and Operational Modes of Automation. *PLoS ONE* 10(7): e0130312. <https://doi.org/10.1371/journal.pone.0130312>
- Bernhardt, H, Wilhelms, A. 1967. The continuous determination of low level iron, soluble phosphate and total phosphate with the AutoAnalyzer. Technicon Symposium.
- Comeros-Raynal, M, Lawrence, A, Sudek, M, Vaeoso, M, McGuire, K, Regis, J, Houk, P. Applying a Ridge to Reef framework to support watershed, water quality, and community-based fisheries management in American Samoa. Final Report to US EPA Wetland Program Development Grant Program.
- Connell J, Hughes T, Wallace C. 1997. A 30-year study of coral abundance, recruitment, and disturbance at several scales in space and time. *Ecological Monographs* 67: 461-488.
- D'Angelo, C, and Wiedenmann, J. 2014. Impacts of nutrient enrichment on coral reefs: New perspectives and implications for coastal management and reef survival. *Current Opinion in Environmental Sustainability* 7:82–93.
- Edwards, Q, Kulikov, S and Garner-O'Neale, L. 2015. Caffeine in surface and wastewaters in Barbados, West Indies.. SpringerPlus (open access journal) DOI 10.1186/s40064-015-0809-x
- Fabricius K. 2005. Effects of terrestrial runoff on the ecology of corals and coral reefs: review and synthesis. *Marine pollution bulletin* 50: 125-146.
- Flynn, Michael R. 2010. Analysis of censored exposure data by constrained maximization of the Shapiro–Wilk W statistic. *Ann. Occup. Hyg.*, Vol. 54, No. 3, pp. 263–271.
- Galloway J, Aber, J, Erisman, J, Seitzinger, S, Howarth, R, Cowling, E, Cosby B. 2003. The nitrogen cascade. *BioScience* 53: 341–356.

Hansen, H, Koroleff, F. 1999. Determination of Nutrients. Methods of Seawater Analysis. K. Grasshoff, K. Kremling and M. Ernhardt. New York, Wiley-VCH.

Harrison, P, Ward, S. 2001. Elevated levels of nitrogen and phosphorus reduce fertilisation success of gametes from scleractinian reef corals. *Marine Biology* 39:1057-1068.

Hartemink, A, Johnston, M, O'Sullivan, J, Poloma, S. 2000. Nitrogen use efficiency of taro and sweet potato in the humid lowlands of Papua New Guinea *Agriculture, Ecosystems and Environment* 79:271–280.

Harwood, J., Kuhn, A. 1970. A colorimetric method for ammonia in natural waters. *Water Research* 4: 805 - 811.

Hughes T, Tanner J. 2000. Recruitment failure, life histories, and long-term decline of Caribbean corals. *Ecology* 81: 2250-2263.

Iowa State University Extension. 2019. Ag Decision Maker – Manure Calculator.
<https://www.extension.iastate.edu/AGDM/livestock/xls/b1-65manurecalculator.xlsx>

Knee, K, Gossett, R, Boehm A, Paytan, A. 2010. Caffeine and agricultural pesticide concentrations in surface water and groundwater on the north shore of Kauai (Hawaii, USA) *Marine Pollution Bulletin* 60:1376–1382.

Kuffner I, Walters L, Becerro M, Paul V, Ritson-Williams R, Beach K. 2006. Inhibition of coral recruitment by macroalgae and cyanobacteria. *Marine Ecology Progress Series* 323: 107-117.

Lozada-Misa P., Schumacher, B, Vargas-Ángel, B. 2017. Analysis of benthic survey images via CoralNet: a summary of standard operating procedures and guidelines. *Pacific Islands Fish. Sci. Cent., Natl. Mar. Fish. Serv., NOAA, Honolulu, HI 96818-5007. Pacific Islands Fish. Sci. Cent. Admin. Rep. H-17-02, 175 p.* <https://doi.org/V5/10.7289/V5/AR-PIFSC-H-17-02>.

Marubini, F, Davies, P. 1996. Nitrate increases zooxanthellae population density and reduces skeletogenesis in corals. *Marine Biology* 127: 319-328.

Mathews, L, Homans, F, Easter, K. 2002. Estimating the benefits of phosphorus pollution reductions: An application in the Minnesota River. *Journal of the American Water Resources Association* 38: 1217-1223.

Mead, R., Morgan, J, Brooks, G, Avery Jr.,R, Kieber,J, Kirk, A, Skrabal, S, Willey, J. 2009. Occurrence of the artificial sweetener sucralose in coastal and marine waters of the United States *Marine Chemistry* 116:13-17.

National Park Service (NSP). 2015. Weather of American Samoa National Park.
<http://www.nps.gov/npsa/planyourvisit/weather.htm>

NOAA CRCP 2012. American Samoa's Coral Reef Management Priorities.
https://www.coris.noaa.gov/activities/management_priorities/amsam_mngmnt.pdf

Oppenheimer, J, Eaton, A, Badruzzaman, M, Haghani, A, Jacangelo, J. 2011. Occurrence and suitability of sucralose as an indicator compound of wastewater loading to surface waters in urbanized regions *Water Res.* 45: 4019– 4027.

Spoelstra J, Schiff S, Brown S. 2013. Artificial Sweeteners in a Large Canadian River Reflect Human Consumption in the Watershed. *PLoS ONE* 8(12): e82706.
<https://doi.org/10.1371/journal.pone.0082706>

Szmant, A. 2002. Nutrient enrichment on coral reefs: is it a major cause of coral reef decline? *Estuaries* 25: 743-766.

Thornberry- Ehrlich, T. 2008. National Park of American Samoa Geologic Resource Evaluation Report. Natural Resource Report NPS/NRPC/GRD/NRR—2008/025. National Park Service, Denver, Colorado.

USEPA. American Samoa Water Quality Standards. 2013 Revision Administrative Rule No. 001-2013.

US Census. 2010. Island Area: American Samoa, Population Counts for Places (Villages).
https://www.census.gov/population/www/cen2010/island_area/as.html

Vargas-Ángel, Bernardo; Zapata, Fernando A.; Hernández, Helena; Jiménez, Juan M. 2001. *Bulletin of Marine Science* 69: 111-132.

Vargas-Angel, B., Schumacher, B. 2018. Baseline Surveys for Coral Reef Community Structure and Demographics in Vatia and Faga'alu Bay, American Samoa NOAA Pacific Islands Fisheries Science Center, PIFSC Special Publication, SP-18-002, 38 pp.

Wang, C. 2012. "Assessment of the Occurrence and Potential Effects of Pharmaceuticals and Personal Care Products in South Florida Waters and Sediments". FIU Electronic Theses and Dissertations. 689. <https://digitalcommons.fiu.edu/etd/689>

Whitall, D, Castro, M, Driscoll, C. 2004. Evaluation of management strategies for reducing nitrogen loadings to four US estuaries. *Science of the Total Environment* 333:25-36.

Wingert, E, Pereira, J. 1981. A coastal zone management atlas of American Samoa. University of Hawaii Cartography Laboratory, GSA Bulletin 55: 13- 17.

Appendix

Table A1: Wilcoxon with post-hoc Dunn's test results for nutrient concentrations by depth. Only statistically significant ($\alpha=0.05$) relationships are shown.

Analyte	Score Mean		Z	p-Value
	Difference	Std Err Dif		
HSIO3-	148.32	15.57	9.53	0.0000
NO3-	101.10	15.55	6.50	0.0000
HPO4=	54.43	15.57	3.50	0.0005
NO2-	37.05	15.57	2.38	0.0173

Table A2: Wilcoxon with post-hoc Dunn's test results for nutrient concentrations by strata. Only statistically significant ($\alpha=0.05$) relationships are shown.

Y	Stratum1	Stratum2	Score Mean		Z	p-Value
			Difference	Std Err Dif		
HSIO3-	Inner	Central	125.39	19.56	6.41	0.0000
HSIO3-	Inner	South	117.74	21.83	5.39	0.0000
HSIO3-	Inner	North	83.63	22.01	3.80	0.0015
NO3-	North	Central	73.78	20.69	3.57	0.0036
TP	Inner	South	69.79	21.83	3.20	0.0139
TP	Inner	North	64.59	22.01	2.93	0.0334

Table A3: Wilcoxon test results for nutrient concentrations by stream state (base flow vs storm flow). Only statistically significant ($\alpha=0.05$) relationships are shown.

Analyte	ChiSquare	DF	Prob>ChiSq
HSIO3-	20.94	1	4.7466E-06
NO3-	17.34	1	3.1259E-05
Urea	17.29	1	3.2047E-05
NH4+	17.23	1	3.3155E-05
TN	7.66	1	0.00564339

Table A4: Spearman rank correlations between nutrients. Only statistically significant ($\alpha=0.05$) relationships are shown.

Variable	by Variable	Spearman ρ	Prob> ρ
NO2-	Urea	0.651	3.42E-78
HSIO3-	HPO4=	0.368	5.99E-22
HPO4=	NO2-	0.348	1.22E-19
HSIO3-	Urea	0.343	5E-19
TP	HPO4=	0.342	5.85E-19
HSIO3-	NO2-	0.328	1.91E-17
HPO4=	Urea	0.291	6.42E-14
TP	NO2-	0.291	6.79E-14
TP	Urea	0.278	8.37E-13
TP	HSIO3-	0.247	2.49E-10
HSIO3-	NO3-	0.204	2.04E-07
TN	NO3-	0.125	0.001553
TN	NH4+	0.099	0.012121
TN	HPO4=	-0.084	0.034155
HSIO3-	NH4+	-0.127	0.001317
TN	NO2-	-0.176	7.33E-06
Urea	NH4+	-0.181	4.4E-06
NO2-	NH4+	-0.192	1.01E-06
NO2-	NO3-	-0.212	6.03E-08
TN	Urea	-0.239	1.04E-09
Urea	NO3-	-0.252	1.08E-10
TP	TN	-0.255	6.11E-11

Table A5: Spearman rank correlations between nutrients and tracers by strata. Only statistically significant ($\alpha=0.05$) relationships are shown. Relationships with a rho value of greater than 0.4 (or < -0.4) are highlighted in bold italics.

Strata	Variable	by Variable	Spearman ρ	Prob> ρ
Central	Caffeine	Urea	0.353712	0.004140681
Central	Caffeine	NH4+	0.28202	0.02396197
Central	Caffeine	NO2-	0.24756	0.048579831
Central	Caffeine	NO3-	-0.33251	0.00726464
Inner	Caffeine	Sucralose	0.342737	0.019716549
Inner	Caffeine	HPO4=	0.293401	0.047819439
<i>North</i>	<i>Caffeine</i>	<i>NO3-</i>	<i>-0.51277</i>	<i>0.001174306</i>
<i>North</i>	<i>Caffeine</i>	<i>TN</i>	<i>-0.6</i>	<i>8.66747E-05</i>
Central	Sucralose	HPO4=	0.382217	0.001828692
Central	Sucralose	Urea	0.263022	0.035743881
<i>Central</i>	<i>Sucralose</i>	<i>TN</i>	<i>-0.51399</i>	<i>1.39822E-05</i>
Inner	Sucralose	HPO4=	0.334825	0.022936719
Inner	Sucralose	Urea	0.326946	0.026570181
Inner	Sucralose	TN	-0.34751	0.01796525
<i>North</i>	<i>Sucralose</i>	<i>Urea</i>	<i>0.470302</i>	<i>0.003310633</i>
North	Sucralose	HSIO3-	0.393338	0.016020934
<i>North</i>	<i>Sucralose</i>	<i>TN</i>	<i>-0.40332</i>	<i>0.013313384</i>
<i>North</i>	<i>Sucralose</i>	<i>NO3-</i>	<i>-0.49242</i>	<i>0.001961726</i>
<i>South</i>	<i>Sucralose</i>	<i>Urea</i>	<i>0.548628</i>	<i>0.000246968</i>
South	Sucralose	TN	-0.39931	0.010694938
<i>South</i>	<i>Sucralose</i>	<i>TP</i>	<i>-0.42865</i>	<i>0.005785734</i>



Figure 1: Location of Vatia Bay. Inset shows location of American Samoa.

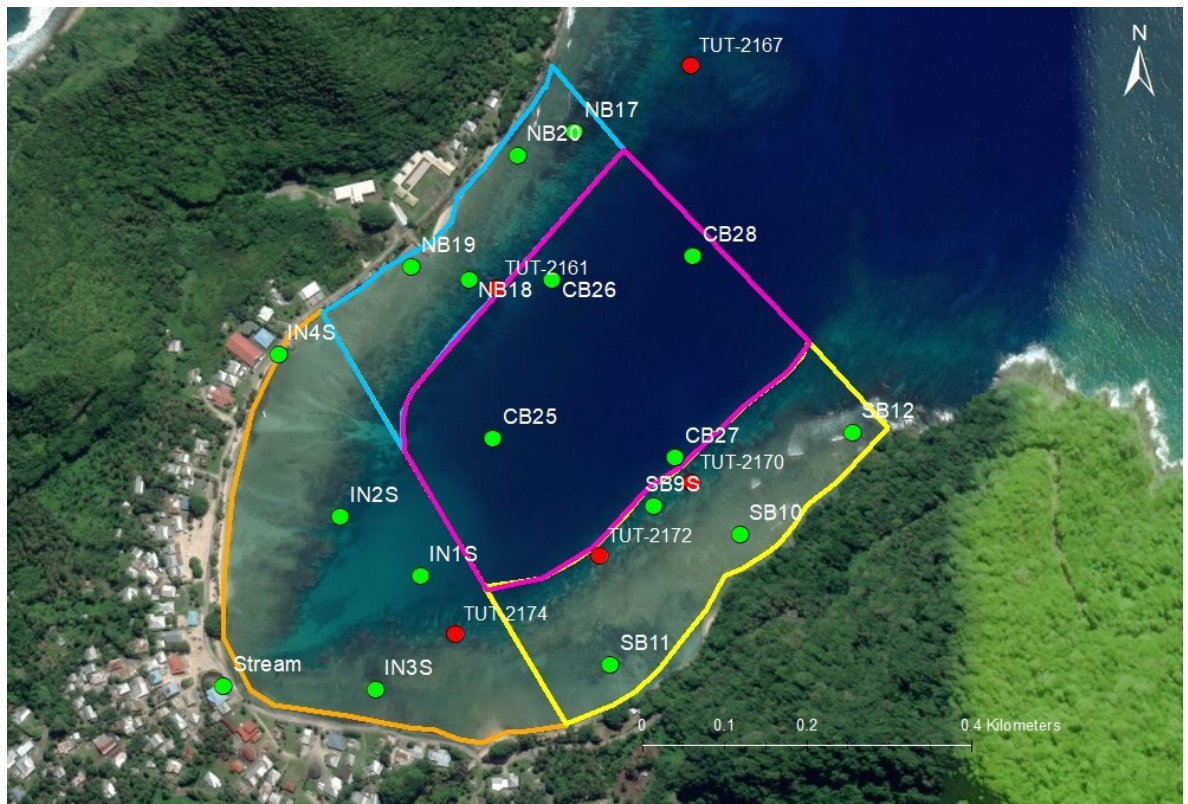
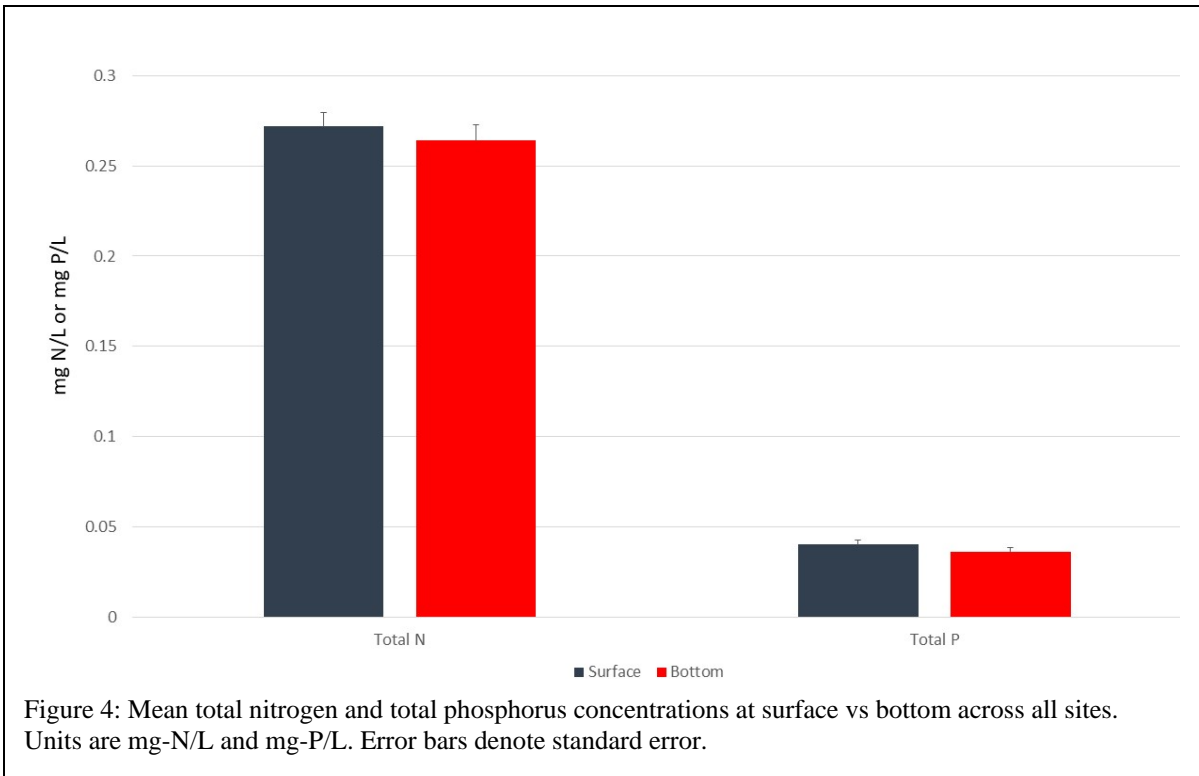
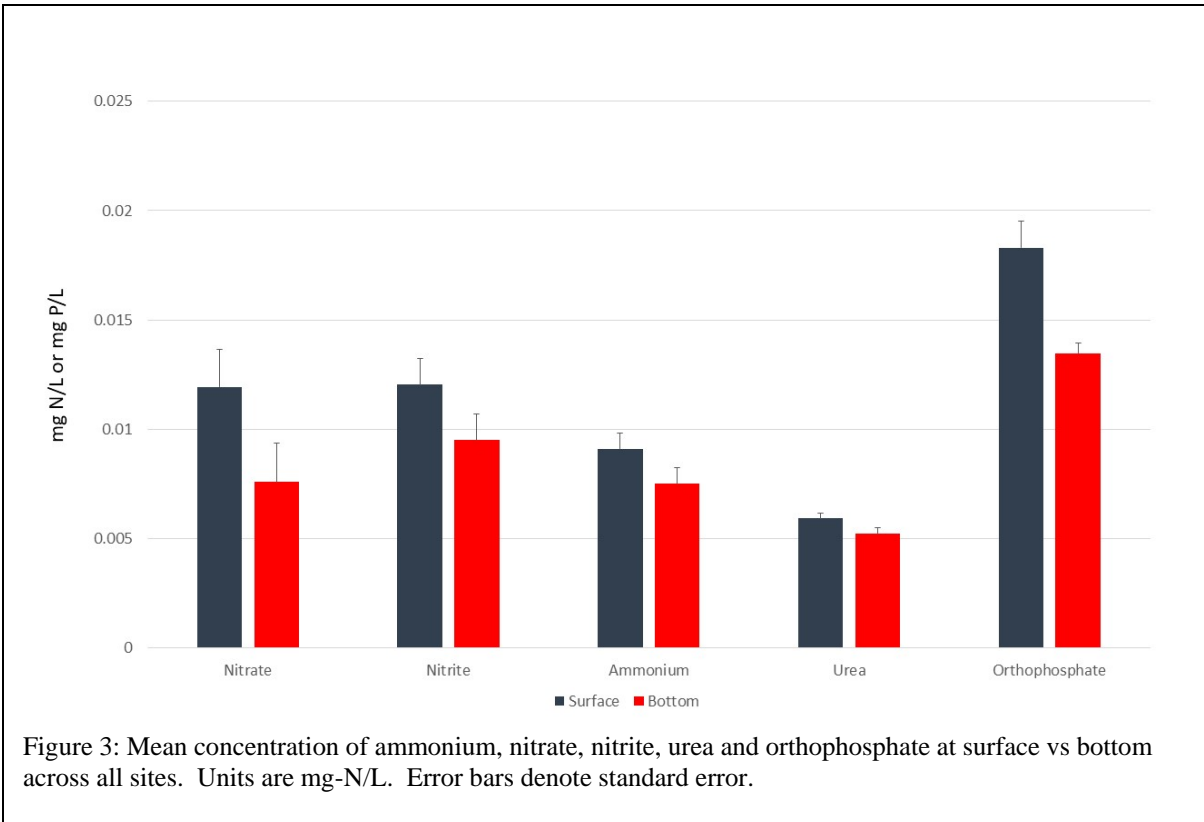
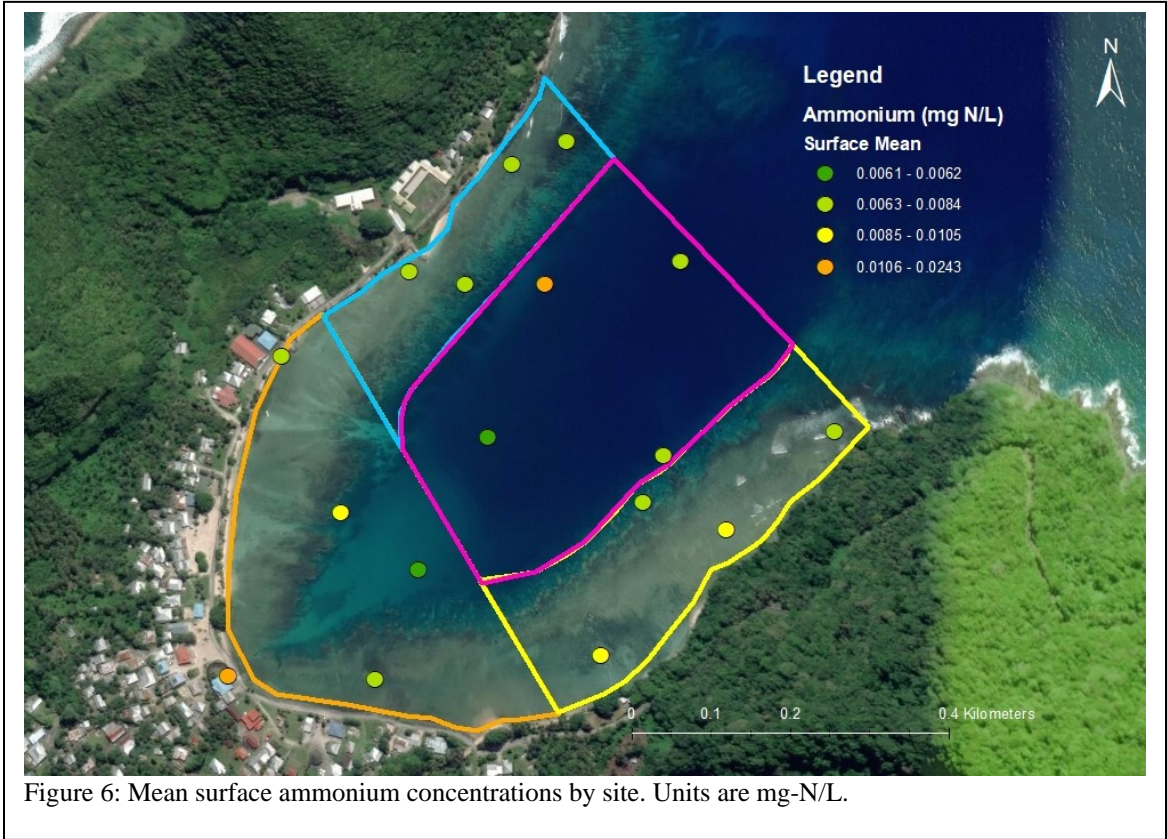
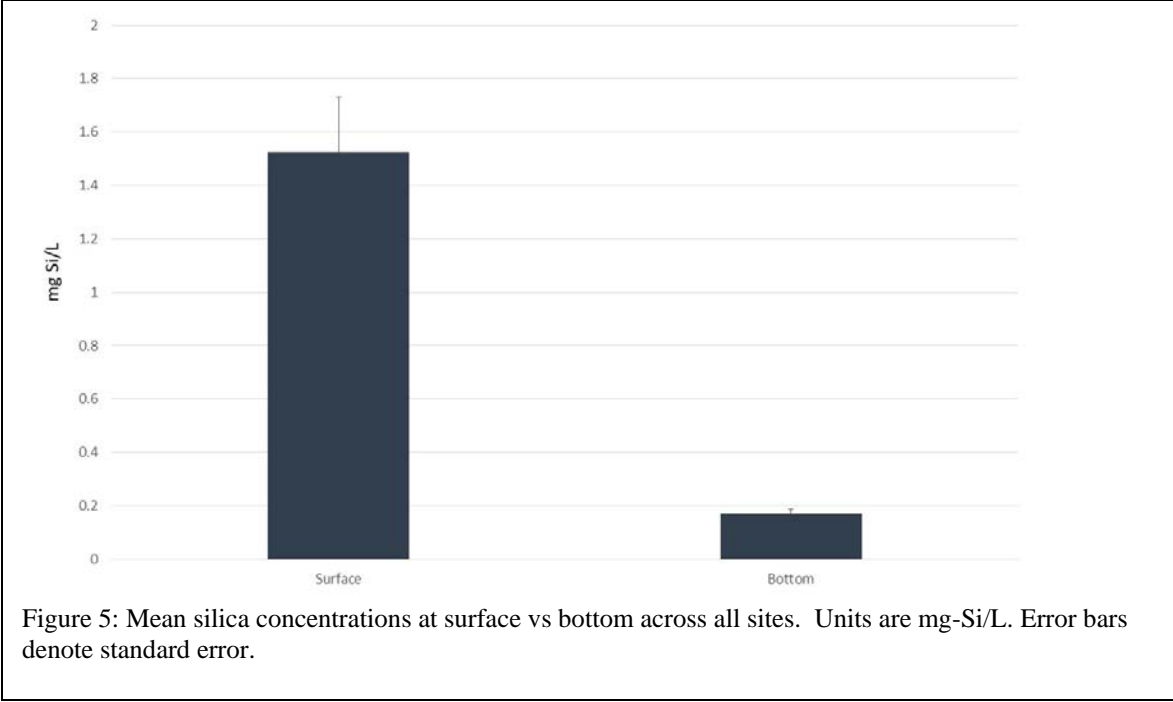


Figure 2: Map of water quality sites (green dots) selected via stratified random sampling design. Colored lines depict strata. Red dots show photo quadrat benthic sites.





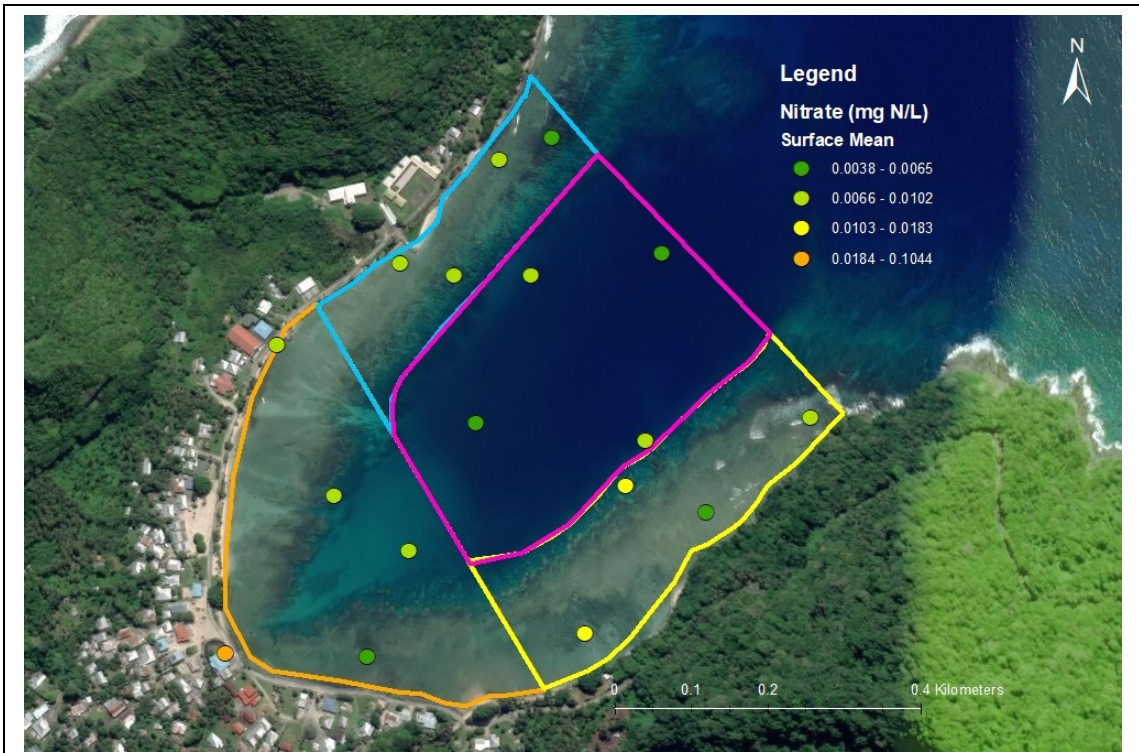


Figure 7: Mean surface nitrate concentrations by site. Units are mg-N/L.

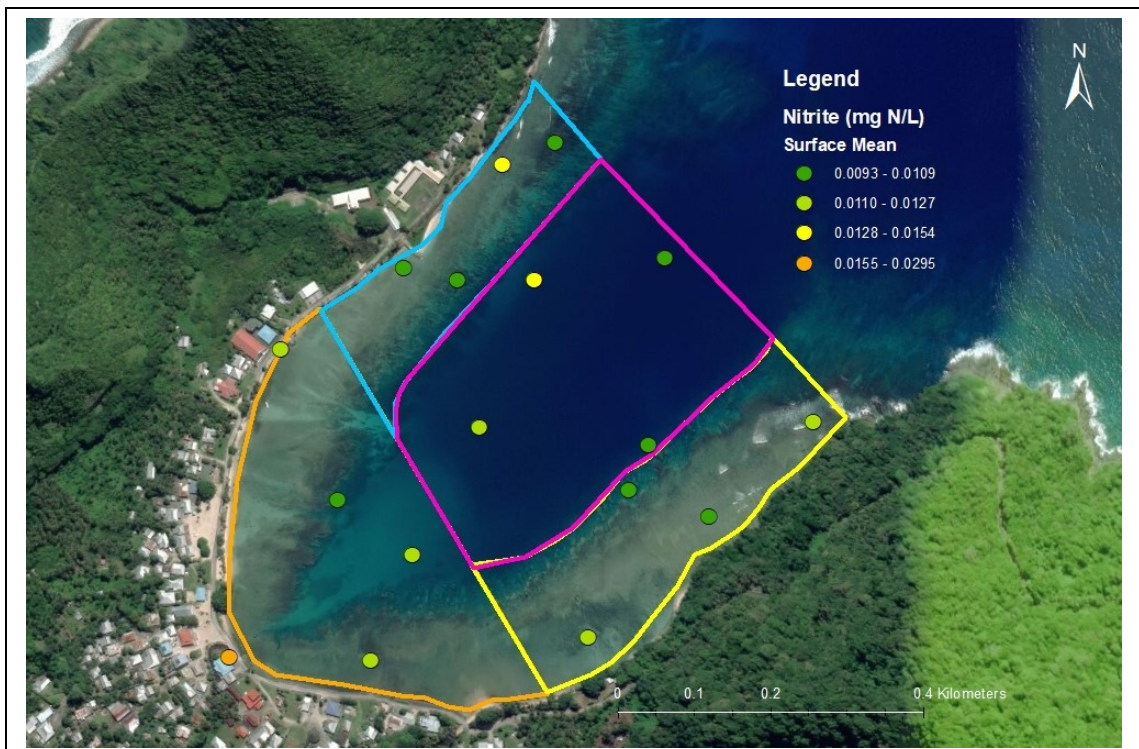


Figure 8: Mean surface nitrite concentrations by site. Units are mg-N/L.

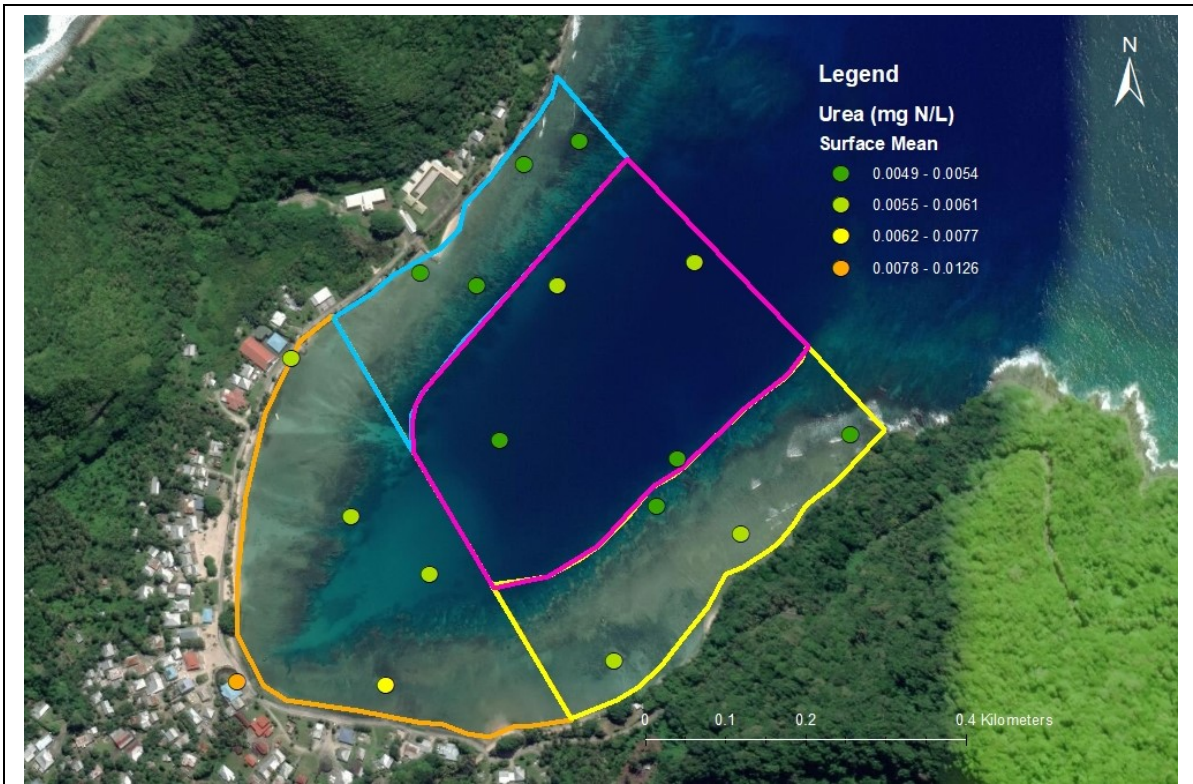


Figure 9: Mean surface urea concentrations by site. Units are mg-N/L

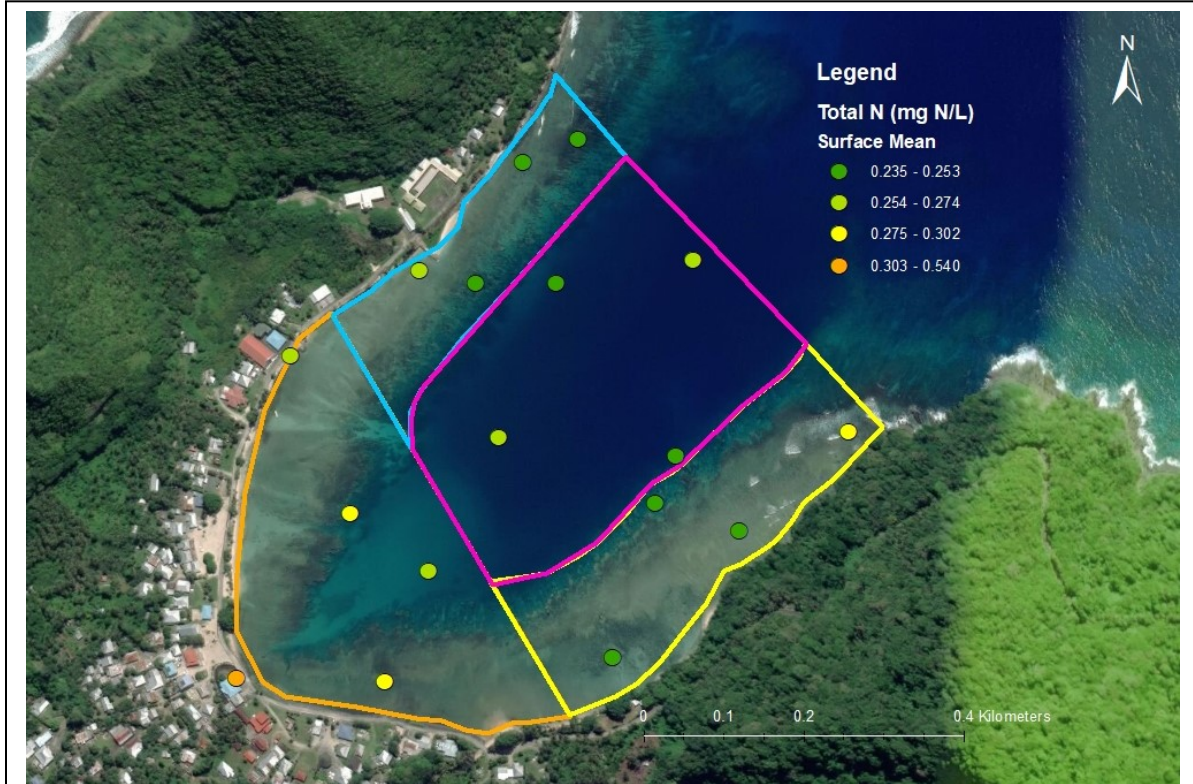


Figure 10: Mean surface total nitrogen concentrations by site. Units are mg-N/L.

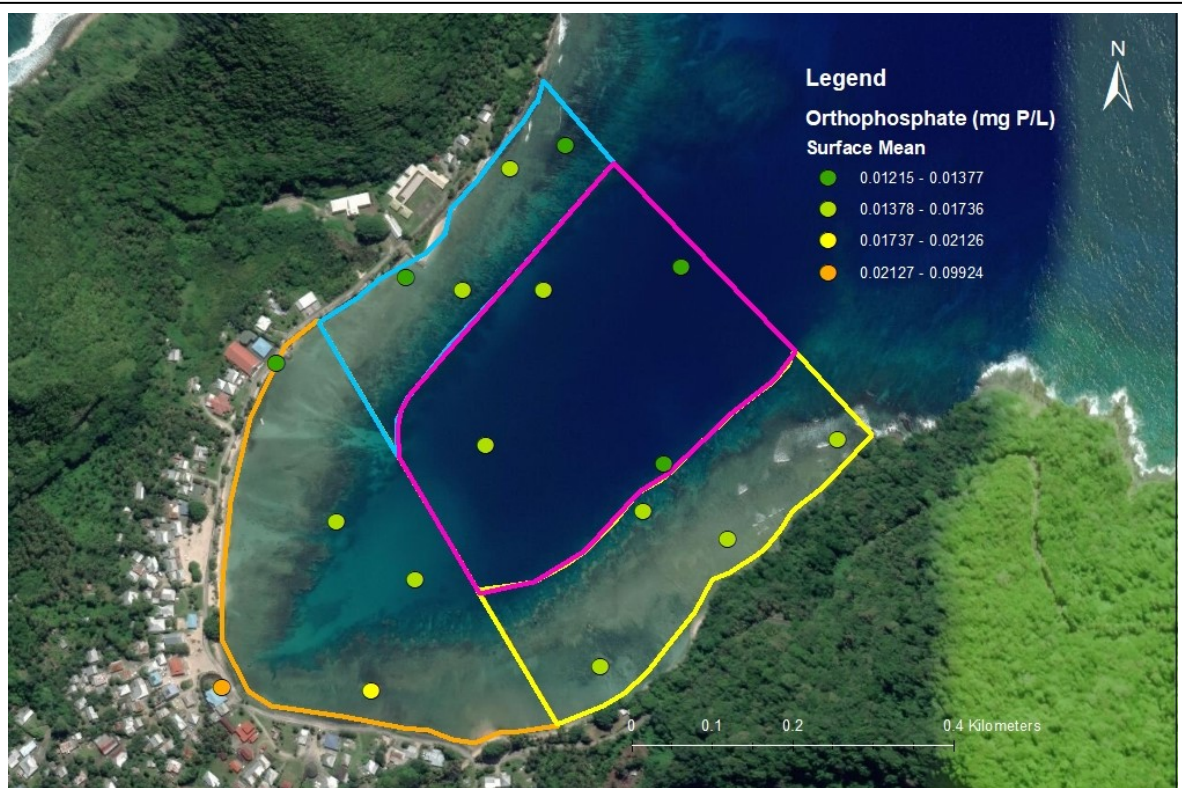


Figure 11: Mean surface orthophosphate concentrations by site. Units are mg-P/L.

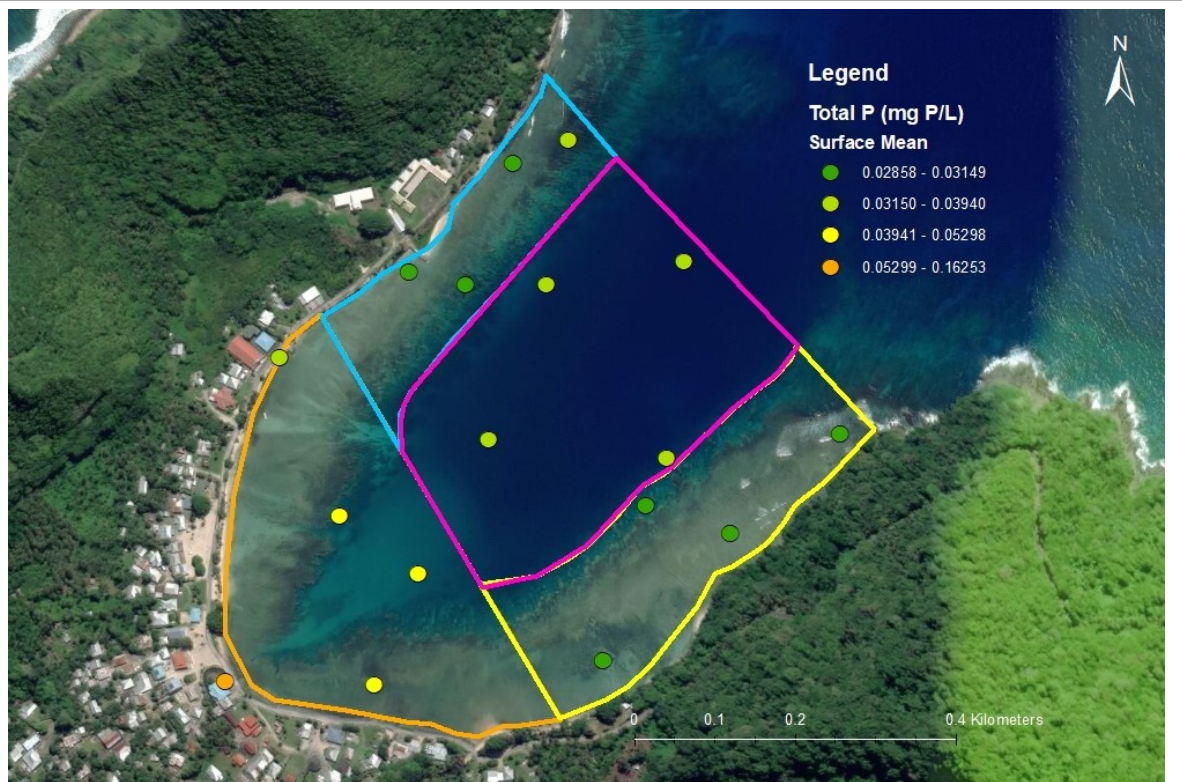


Figure 12: Mean surface total phosphorus concentrations by site. Units are mg-P/L.

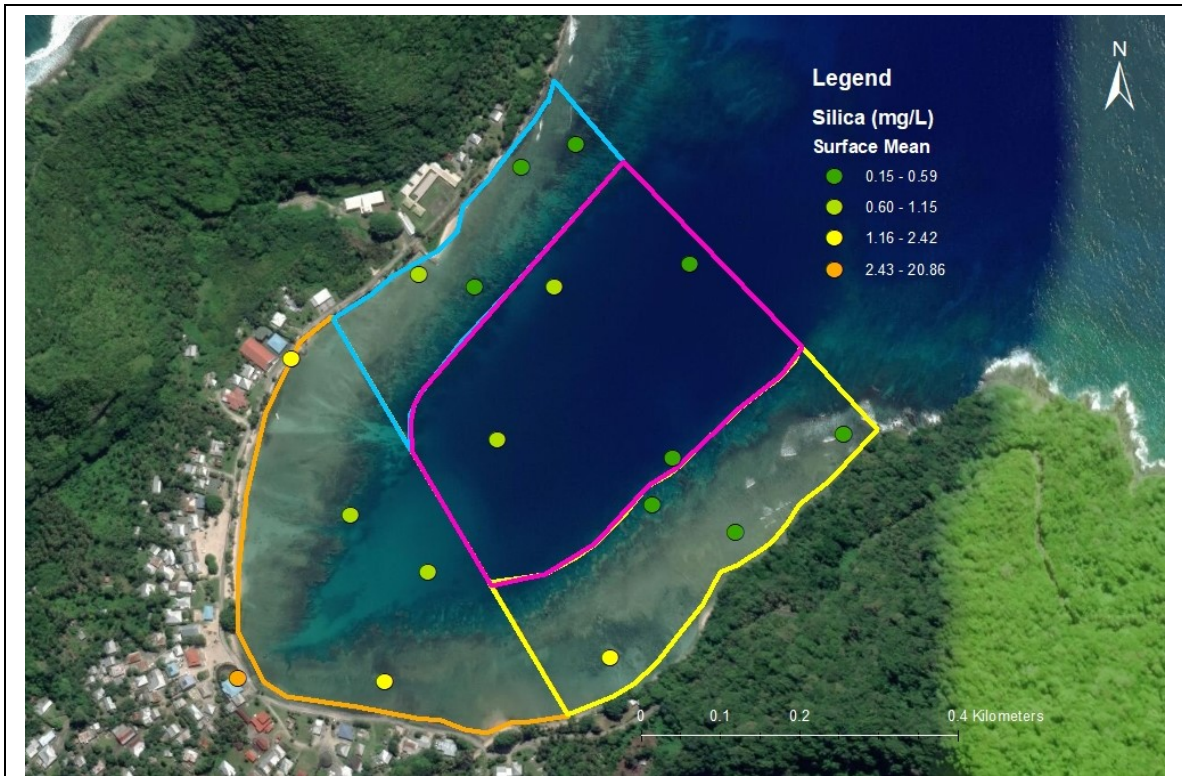


Figure 13: Mean surface silica concentrations by site. Units are mg-Si/L.

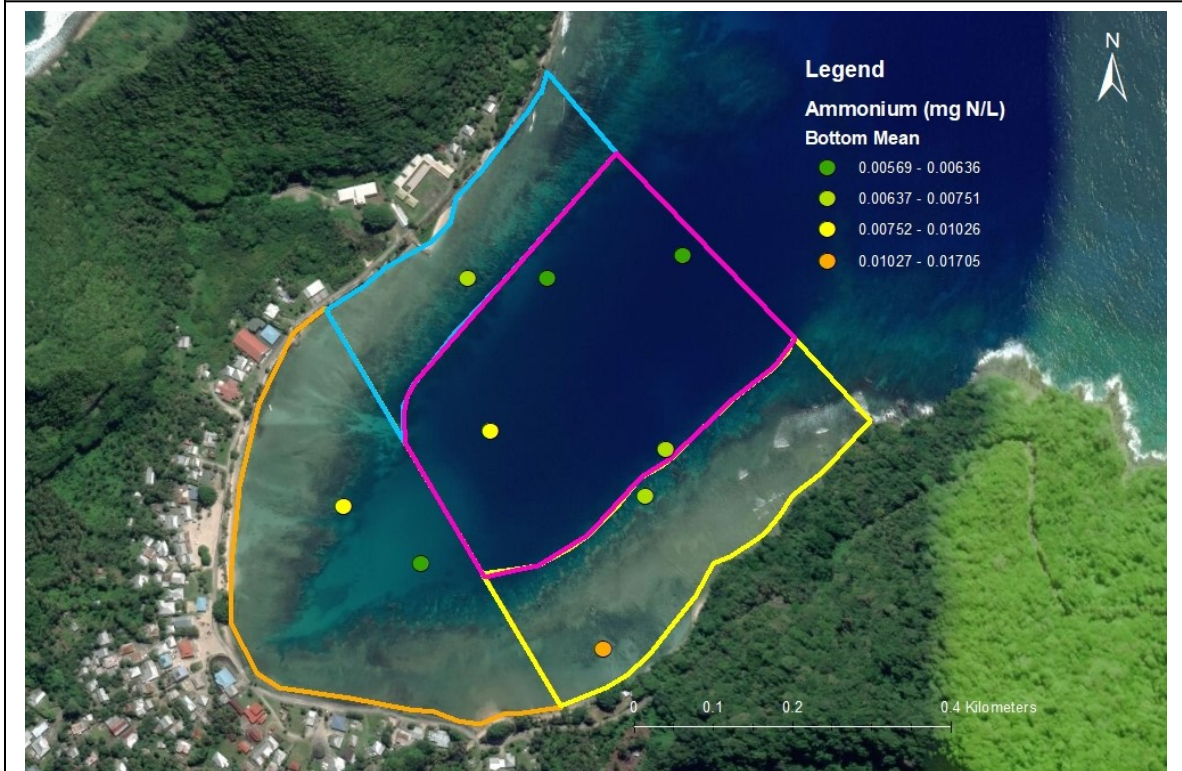


Figure 14: Mean bottom ammonium concentrations by site. Units are mg-N/L.

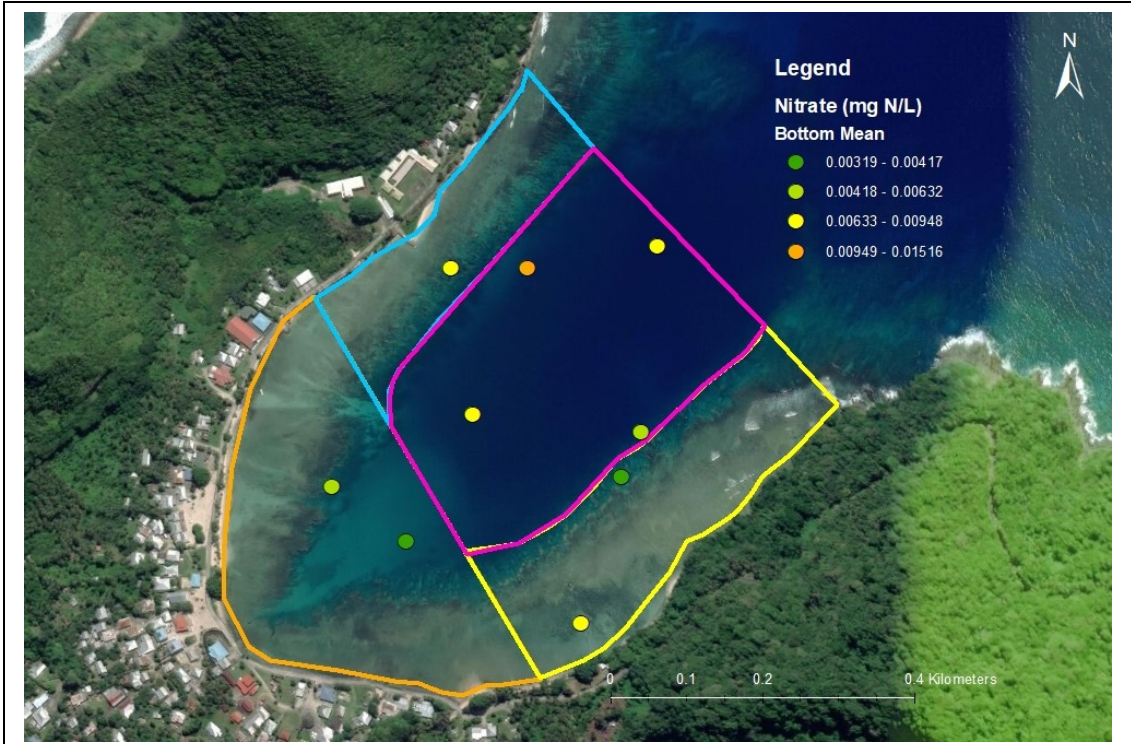


Figure 15: Mean bottom nitrate concentrations by site. Units are mg-N/L.

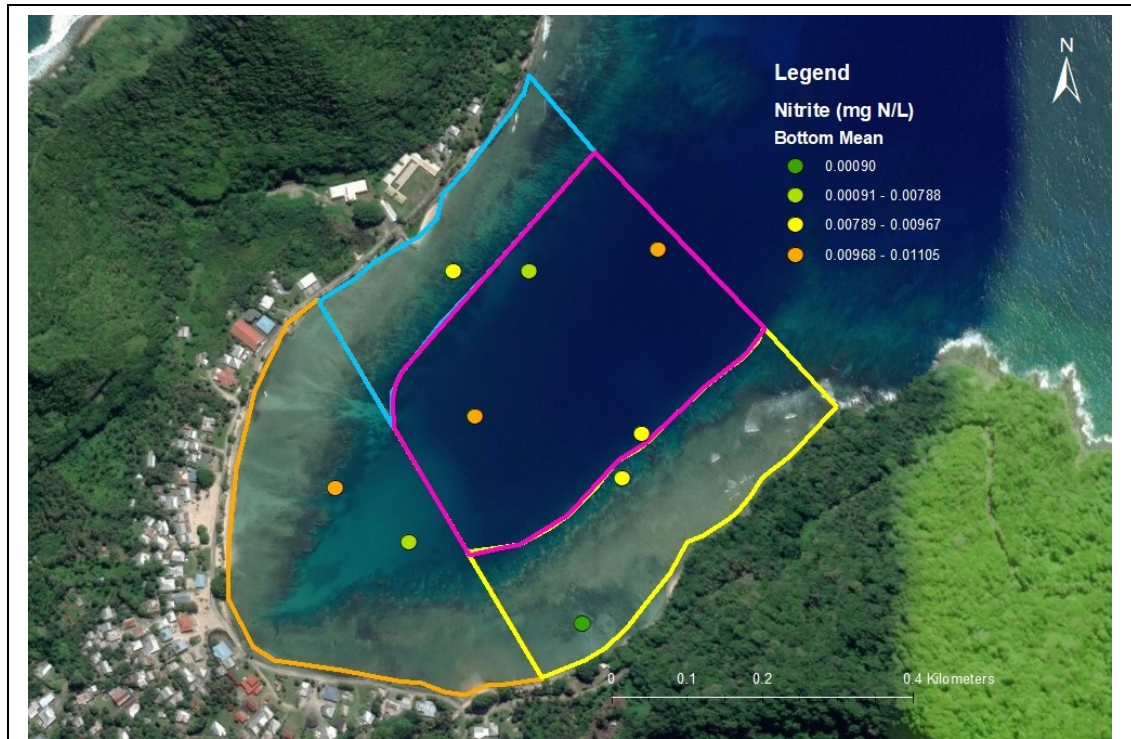


Figure 16: Mean bottom nitrite concentrations by site. Units are mg-N/L.

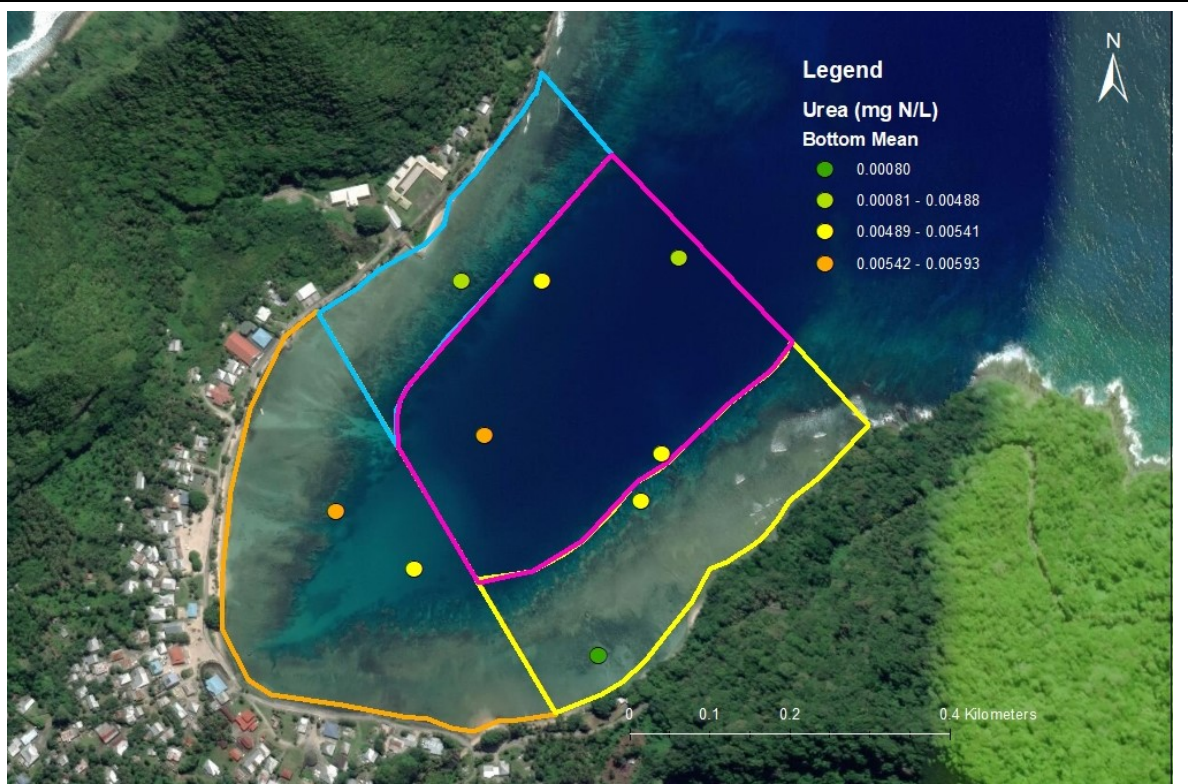


Figure 17: Mean bottom urea concentrations by site. Units are mg-N/L.

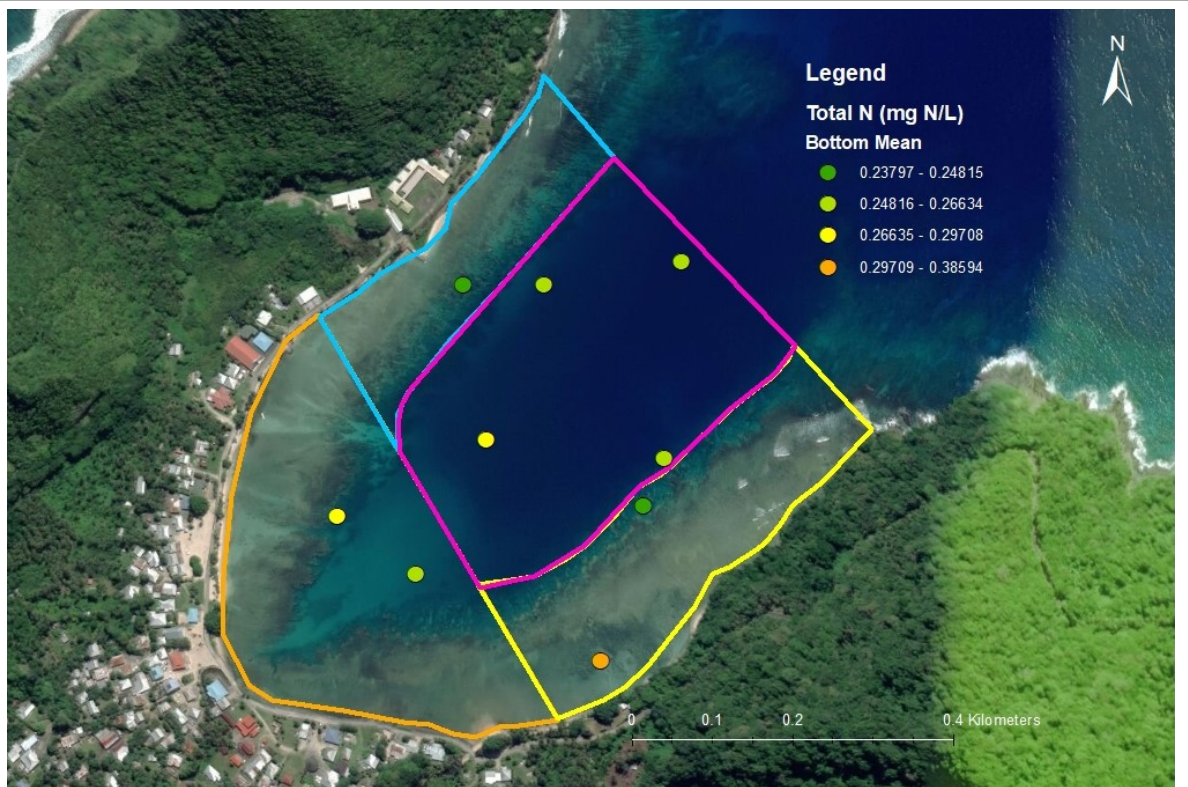


Figure 18: Mean bottom total nitrogen concentrations by site. Units are mg-N/L.

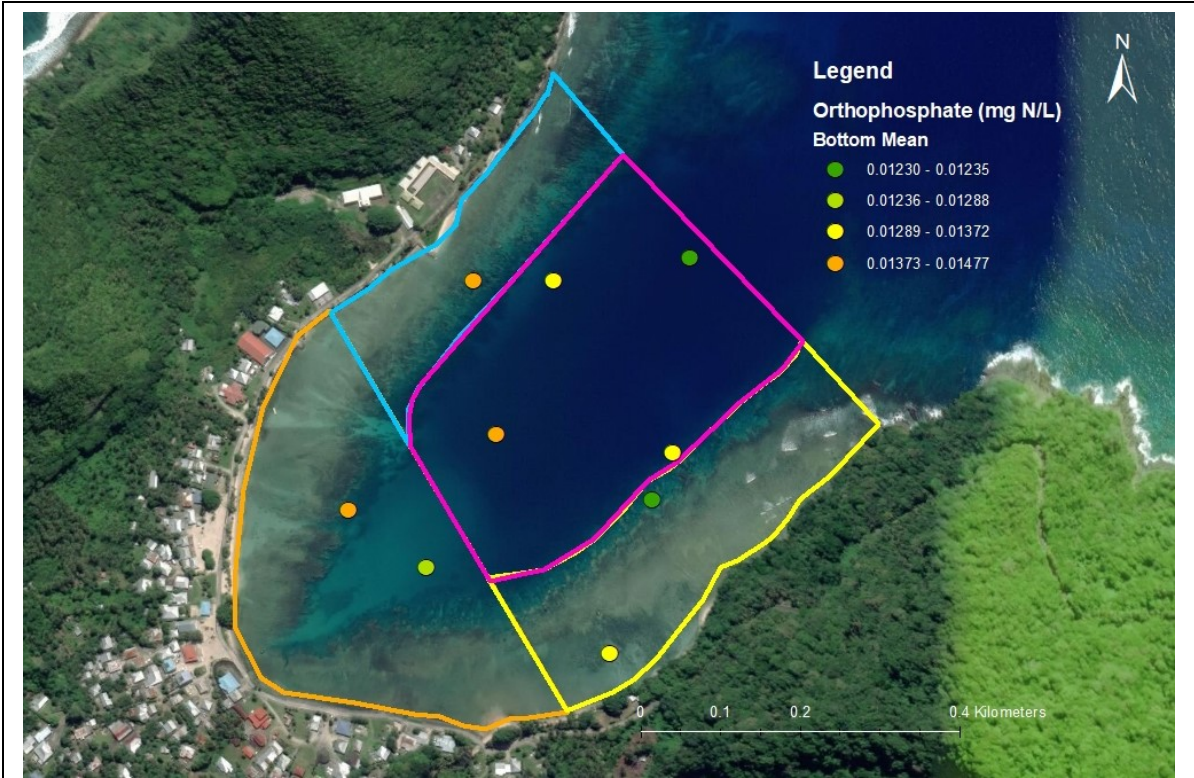


Figure 19: Mean bottom orthophosphate concentrations by site. Units are mg-P/L.

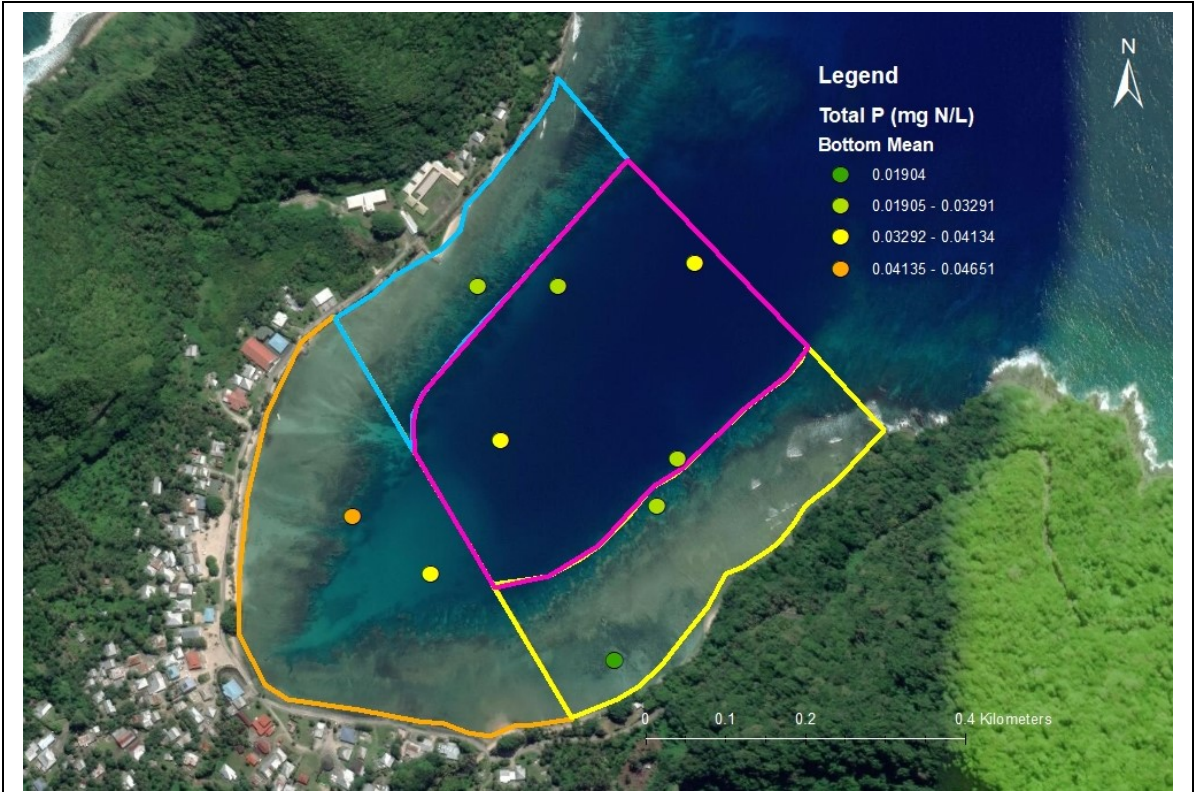


Figure 20: Mean bottom total phosphorus concentrations by site. Units are mg-P/L.

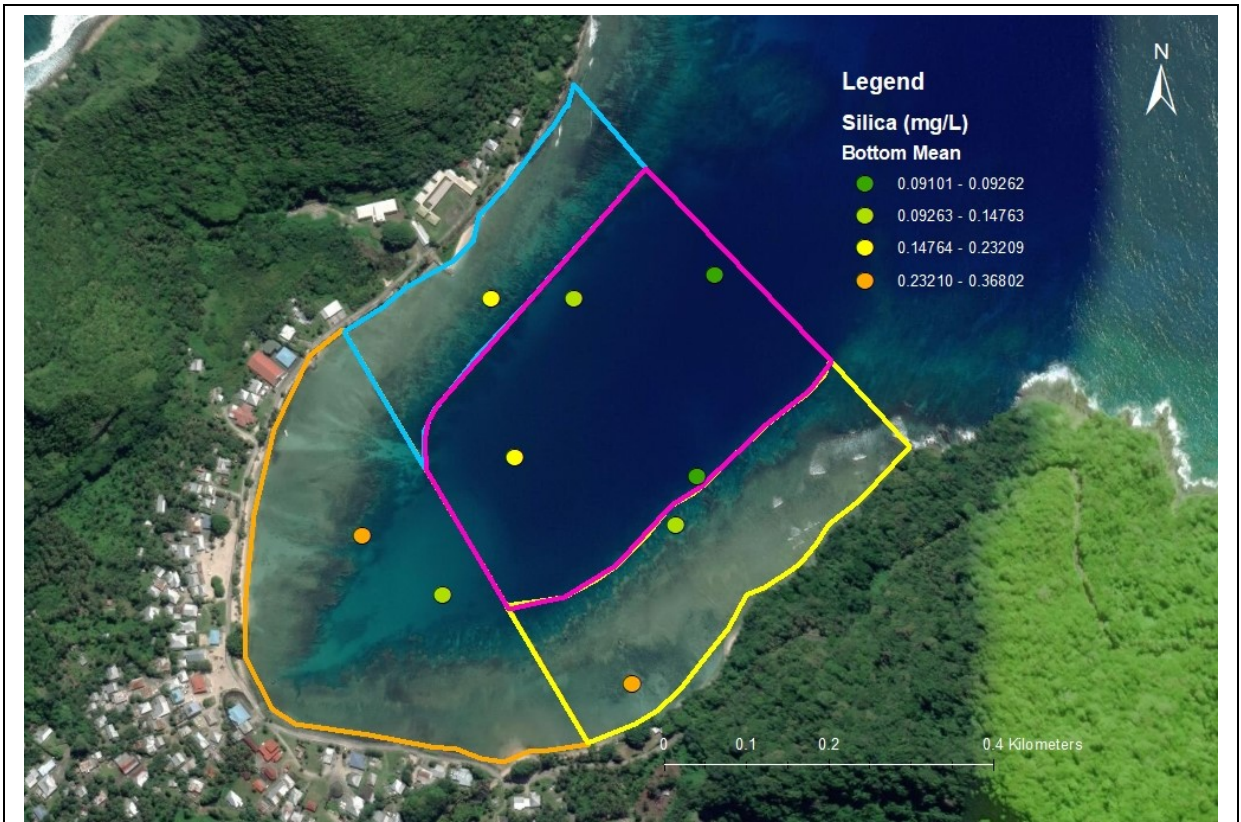


Figure 21: Mean bottom silica concentrations by site. Units are mg-Si/L.

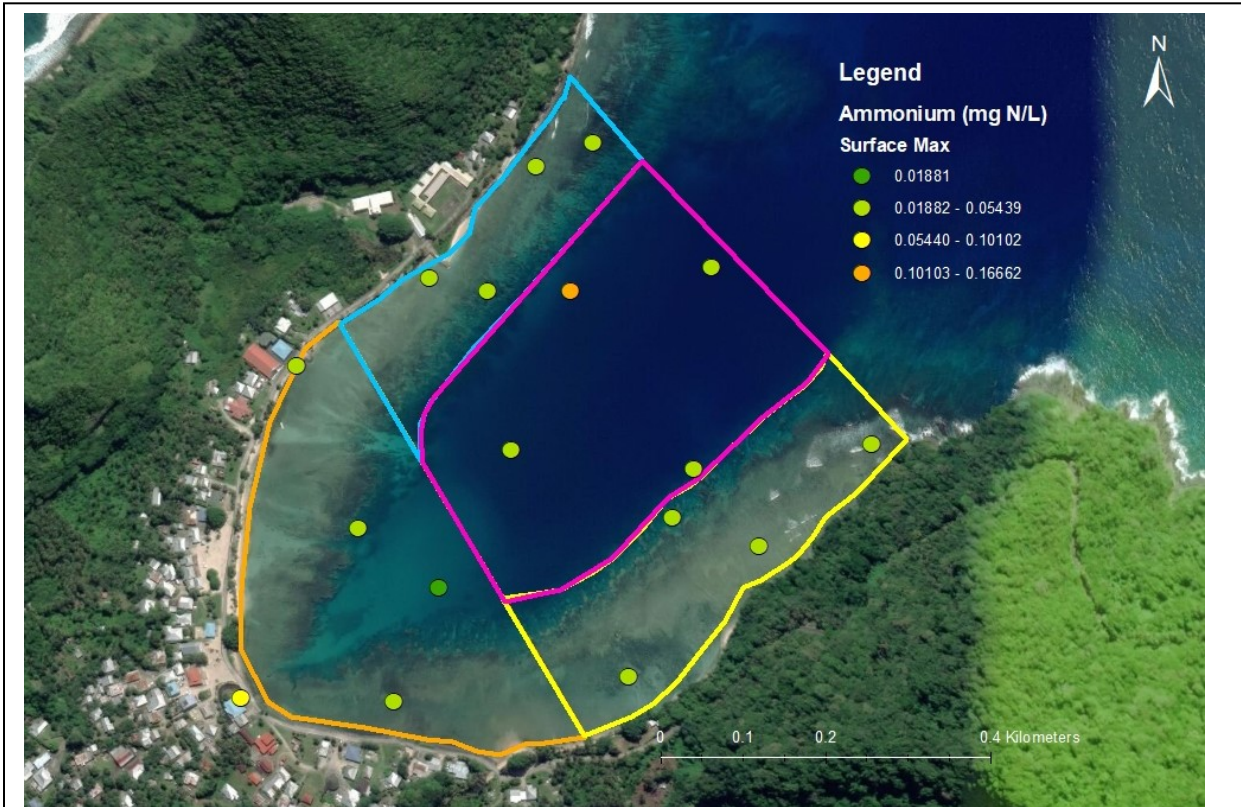


Figure 22: Maximum surface ammonium concentrations by site. Units are mg-N/L.

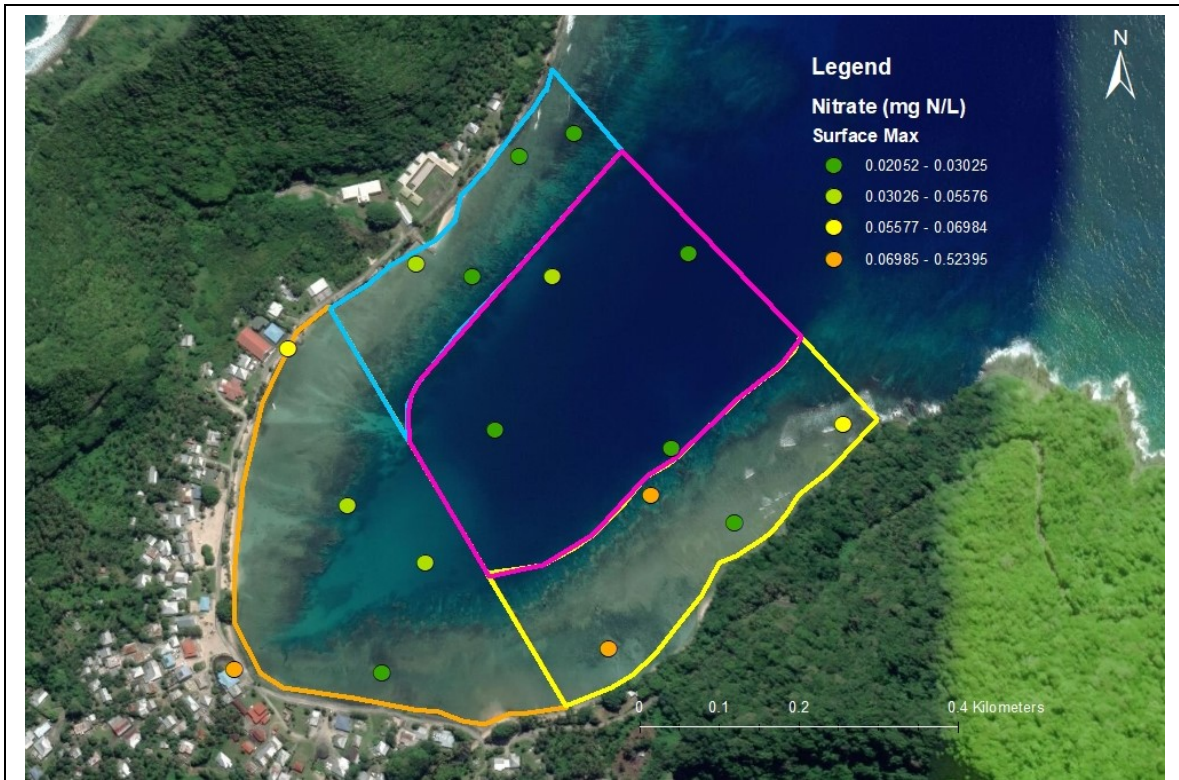


Figure 23: Maximum surface nitrate concentrations by site. Units are mg-N/L.

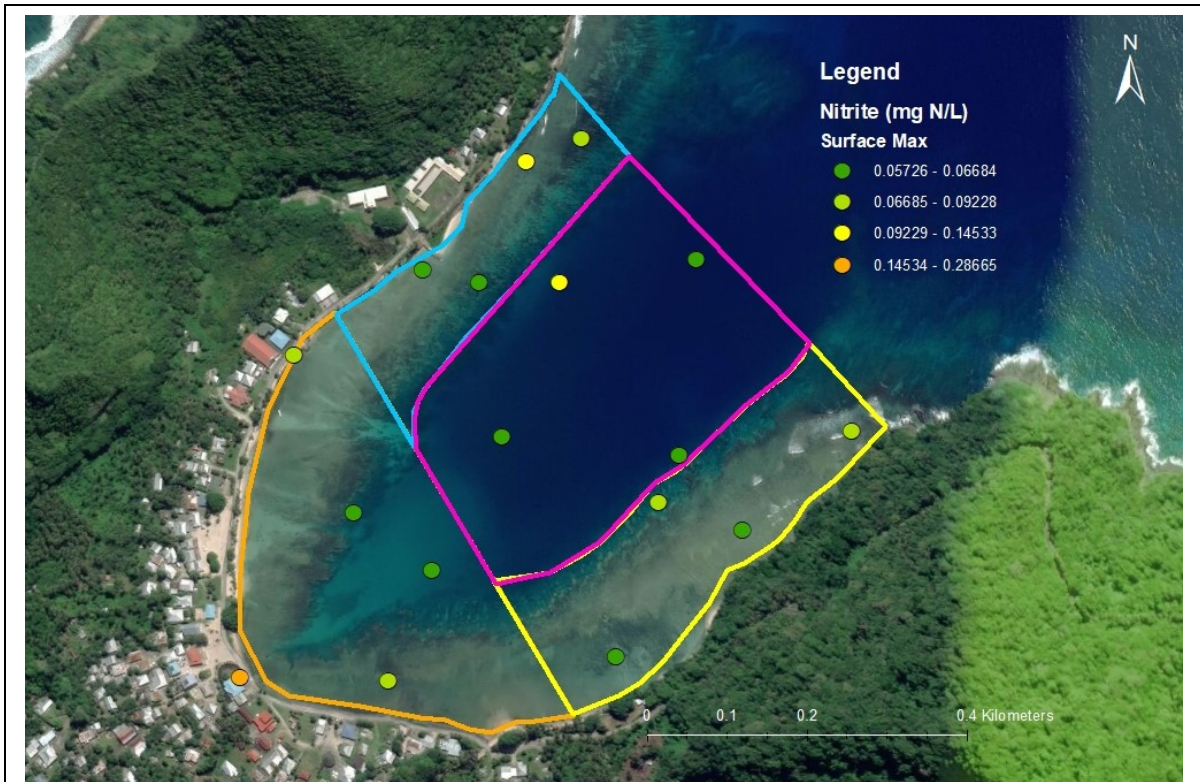


Figure 24: Maximum surface nitrite concentrations by site. Units are mg-N/L.

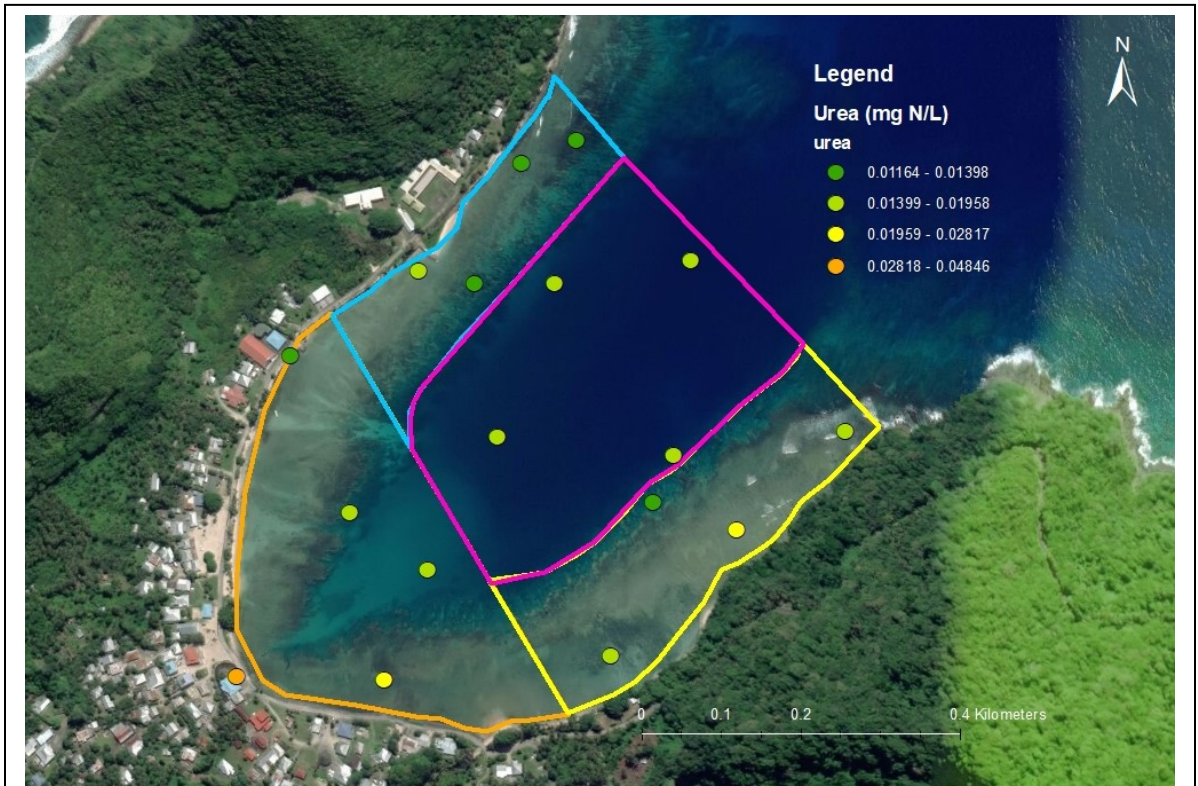


Figure 25: Maximum surface urea concentrations by site. Units are mg-N/L.

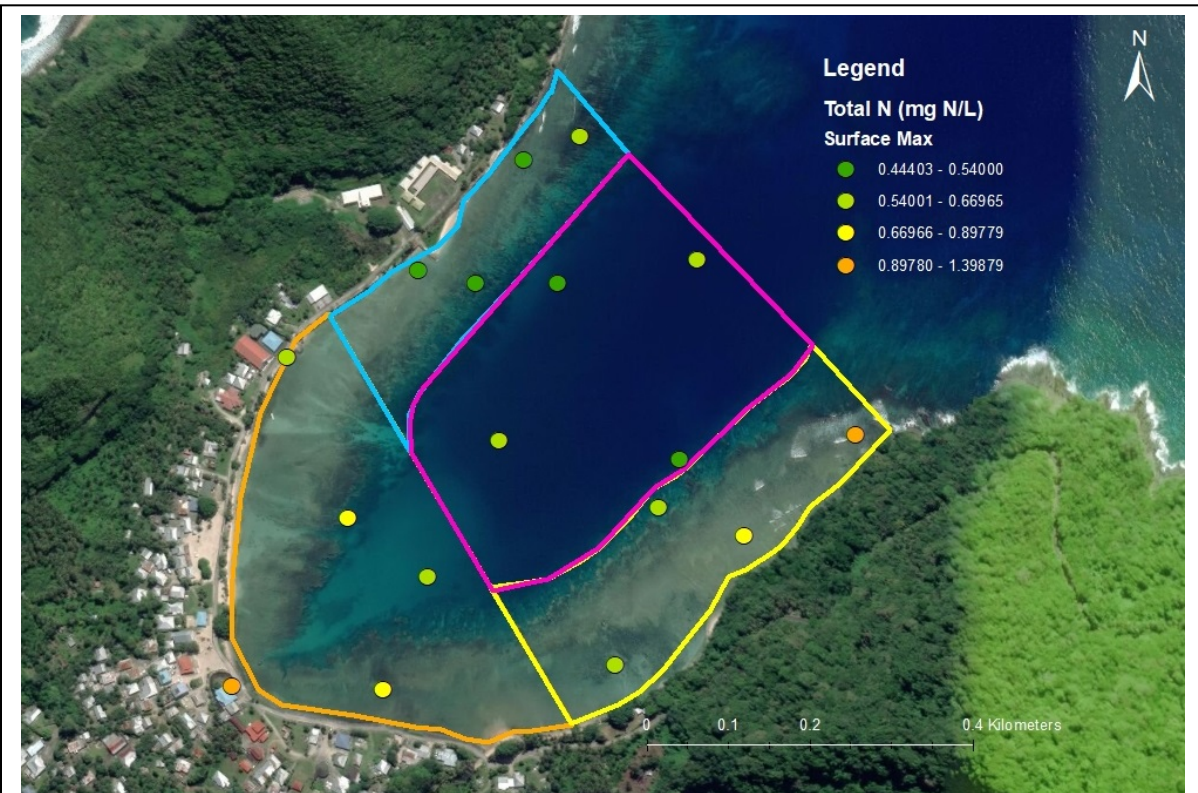


Figure 26: Maximum surface total nitrogen concentrations by site. Units are mg-N/L.

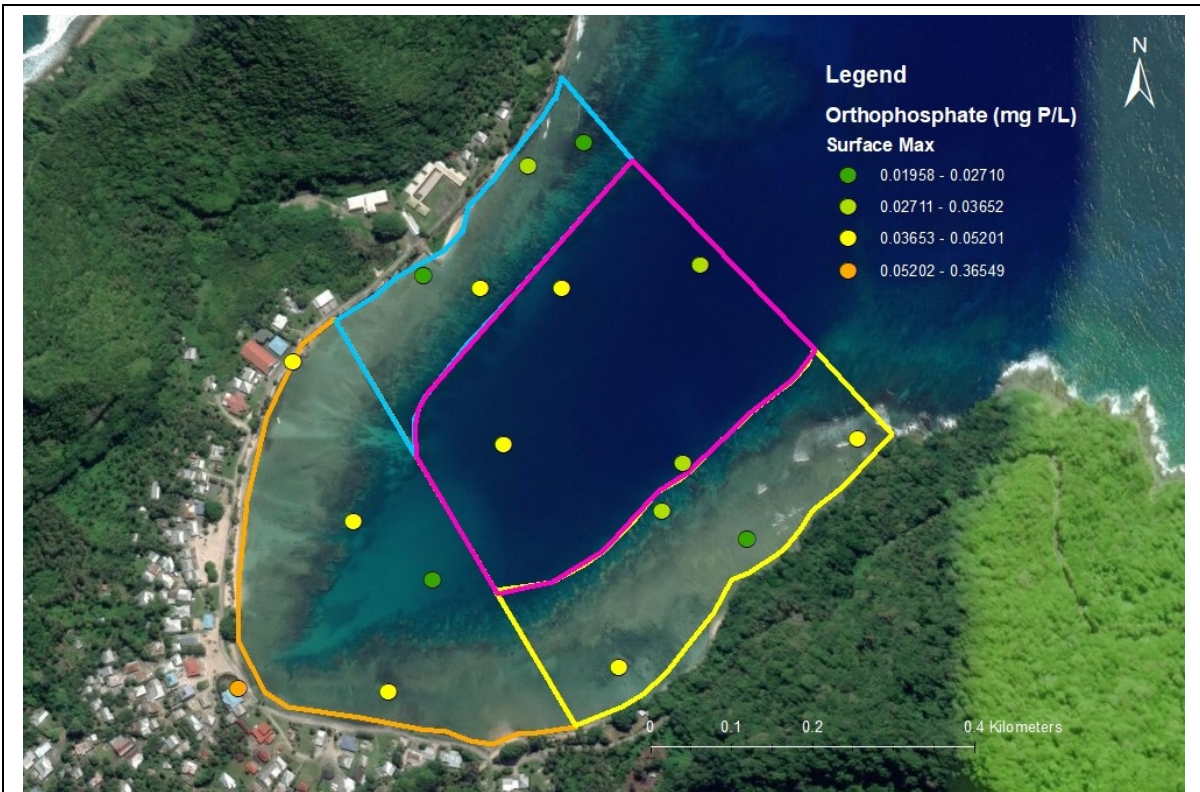


Figure 27: Maximum surface orthophosphate concentrations by site. Units are mg-P/L.

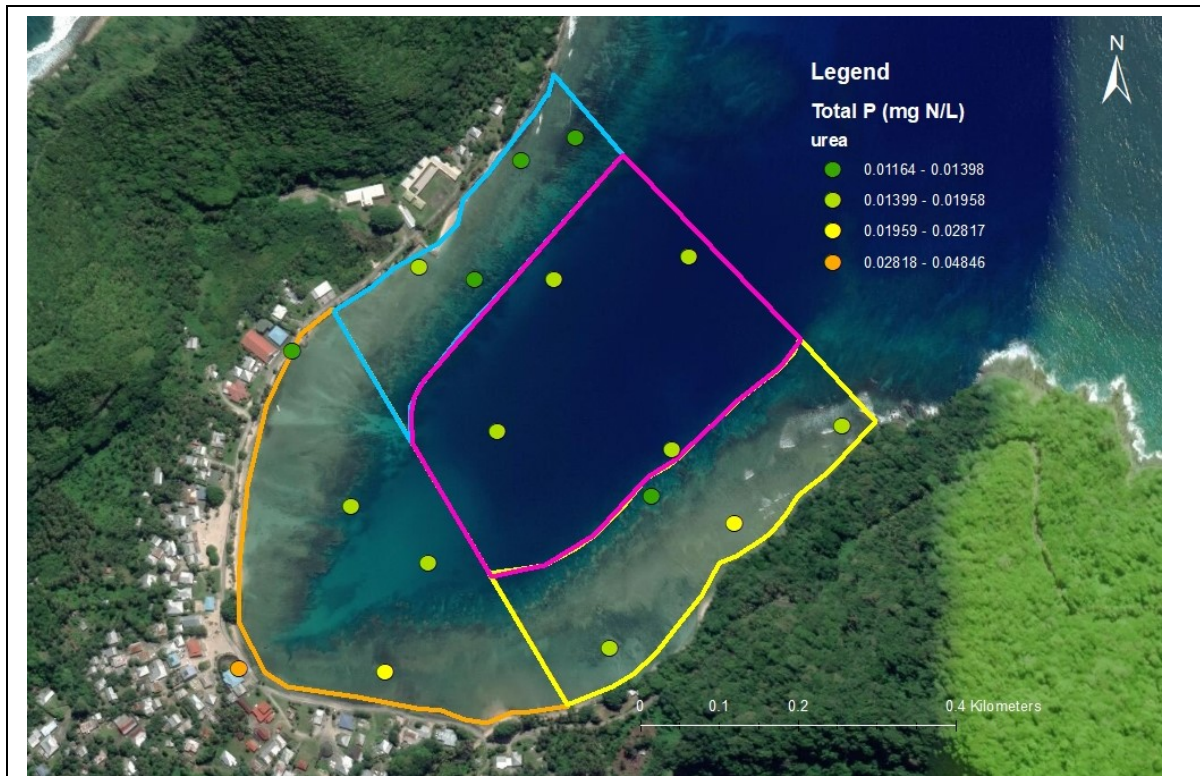


Figure 28: Maximum surface total phosphorus concentrations by site. Units are mg-P/L.

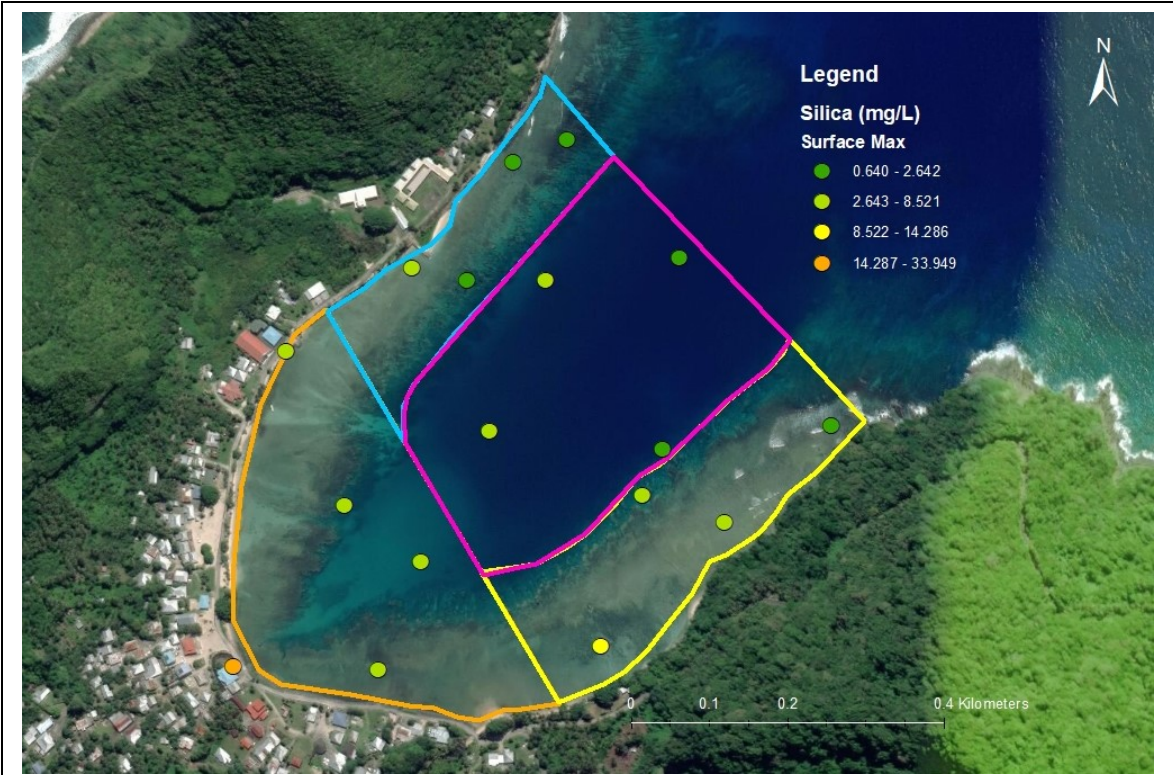


Figure 29: Maximum surface silica concentrations by site. Units are mg-Si/L.

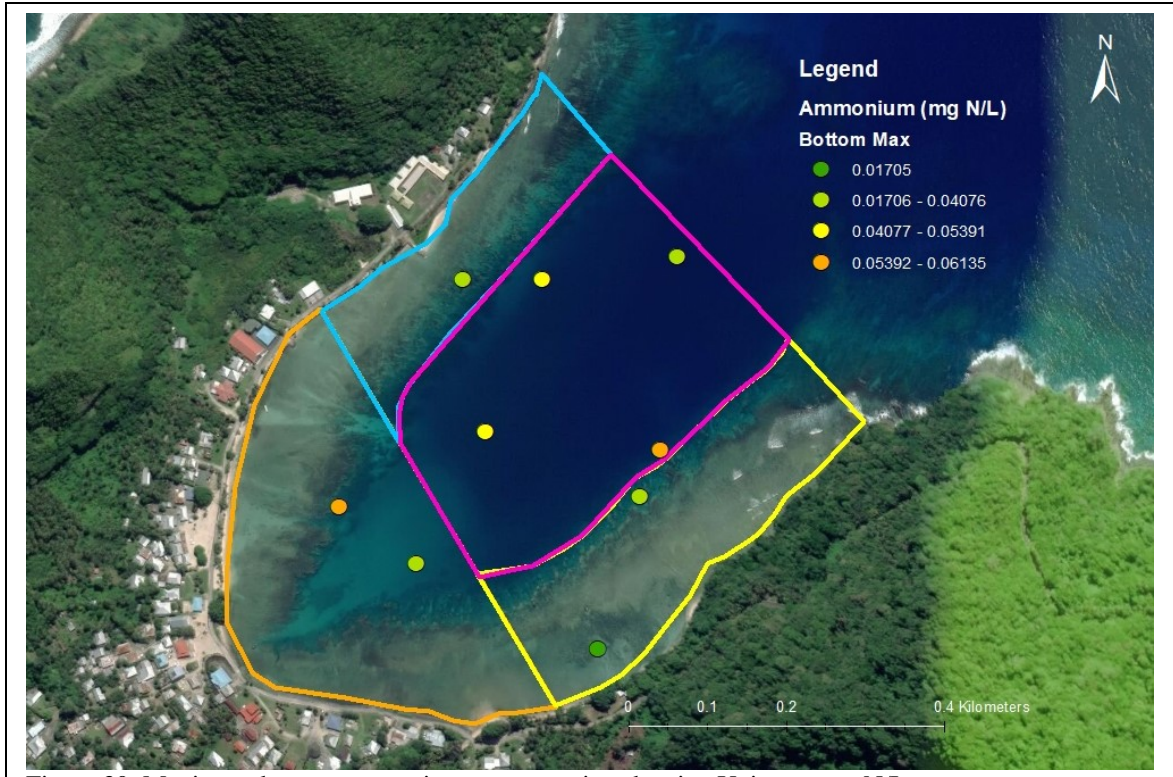


Figure 30: Maximum bottom ammonium concentrations by site. Units are mg-N/L.

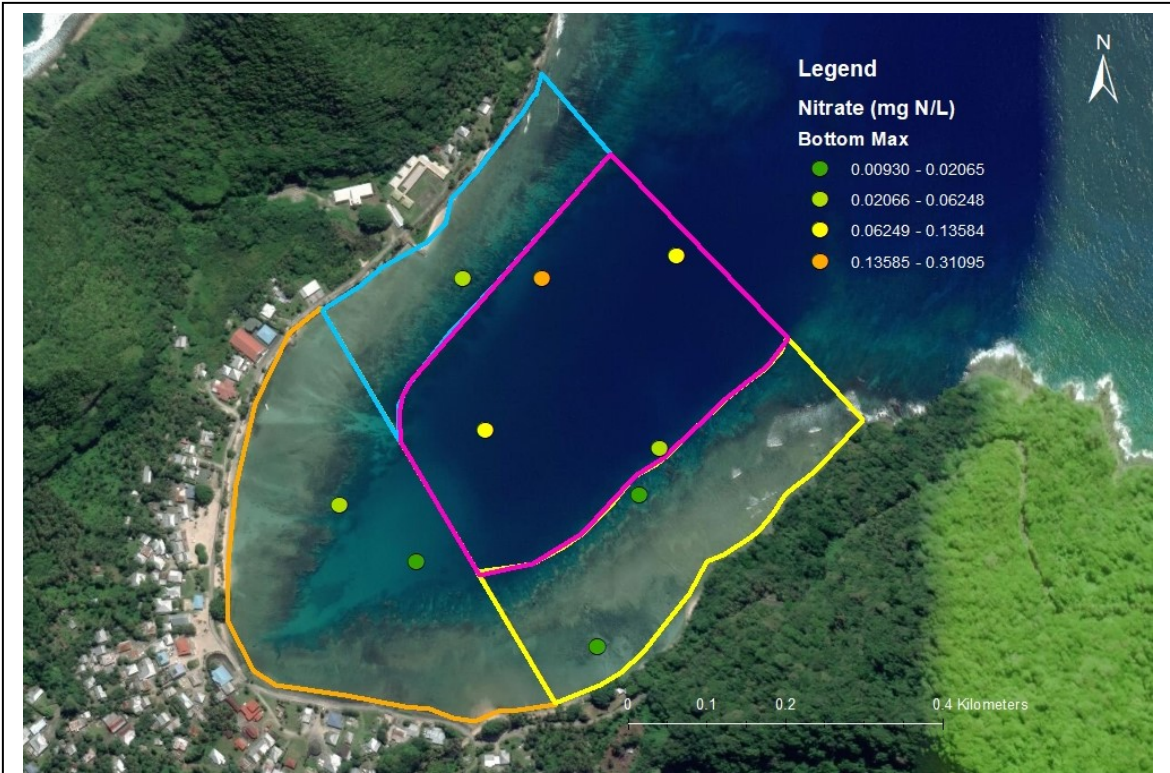


Figure 31: Maximum bottom nitrate concentrations by site. Units are mg-N/L.

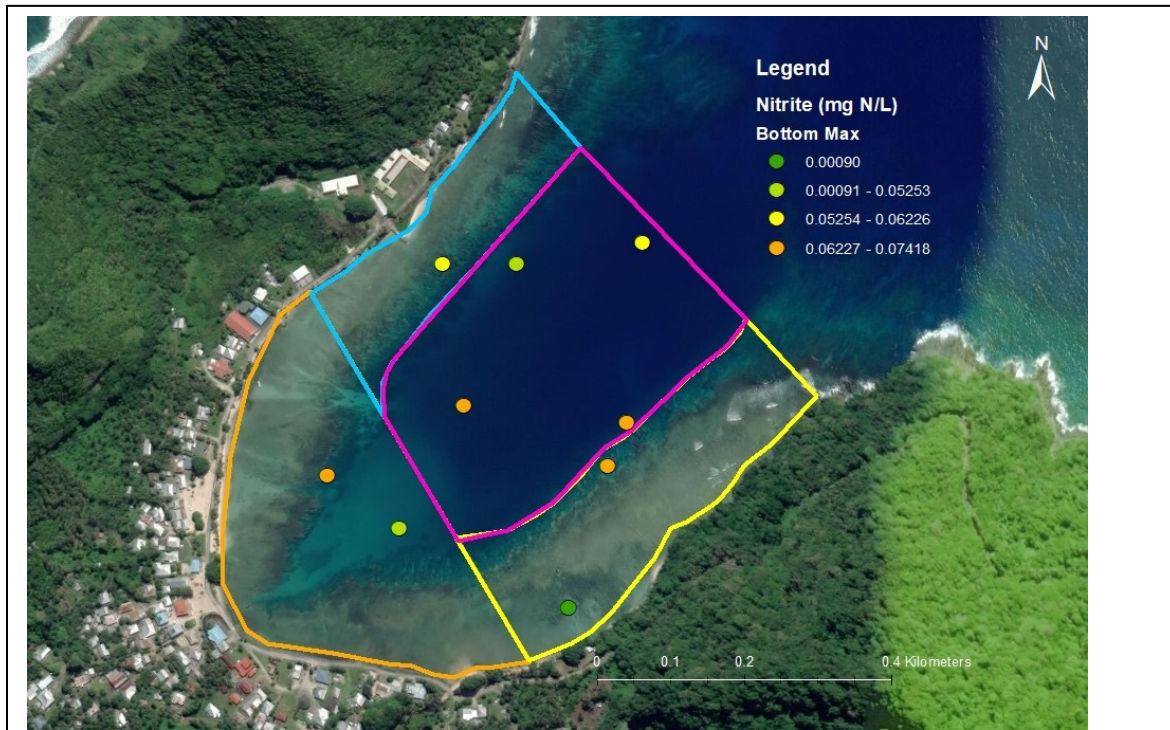


Figure 32: Maximum bottom nitrite concentrations by site. Units are mg-N/L.

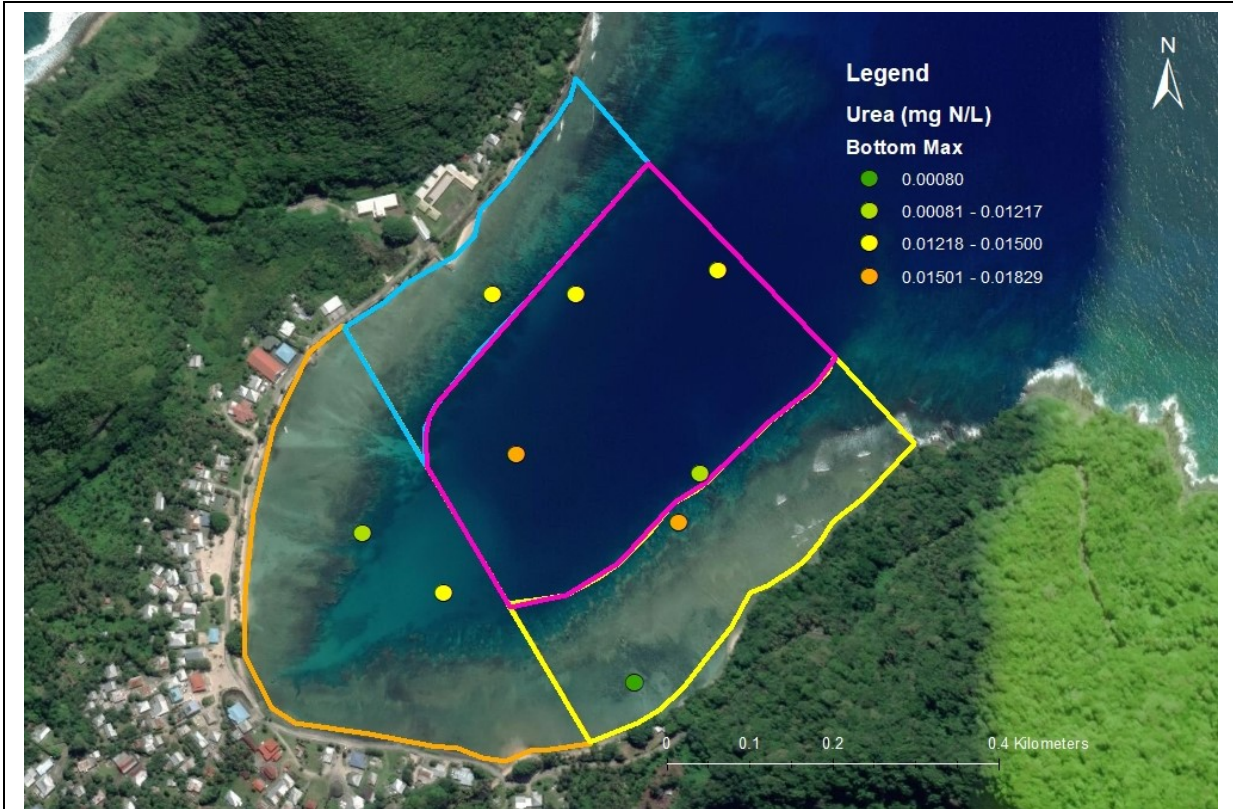


Figure 33: Maximum bottom urea concentrations by site. Units are mg-N/L.

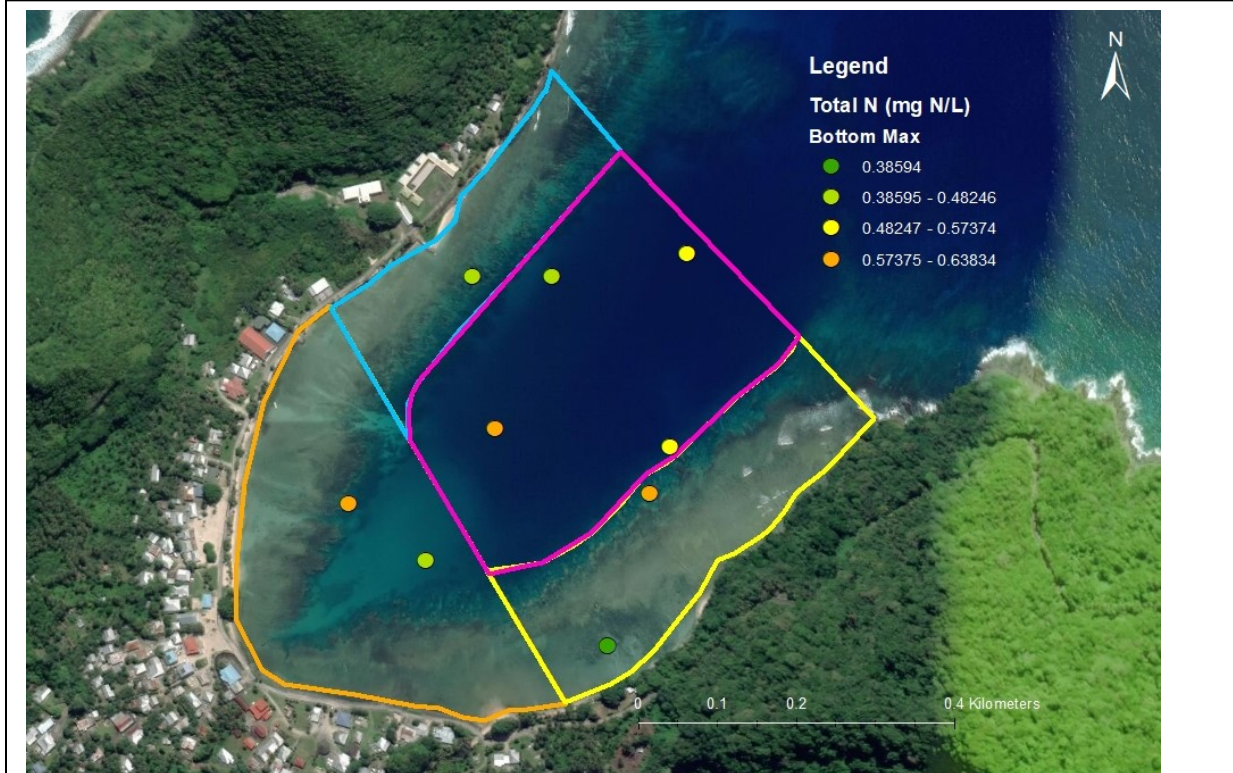


Figure 34: Maximum bottom total nitrogen concentrations by site. Units are mg-N/L.

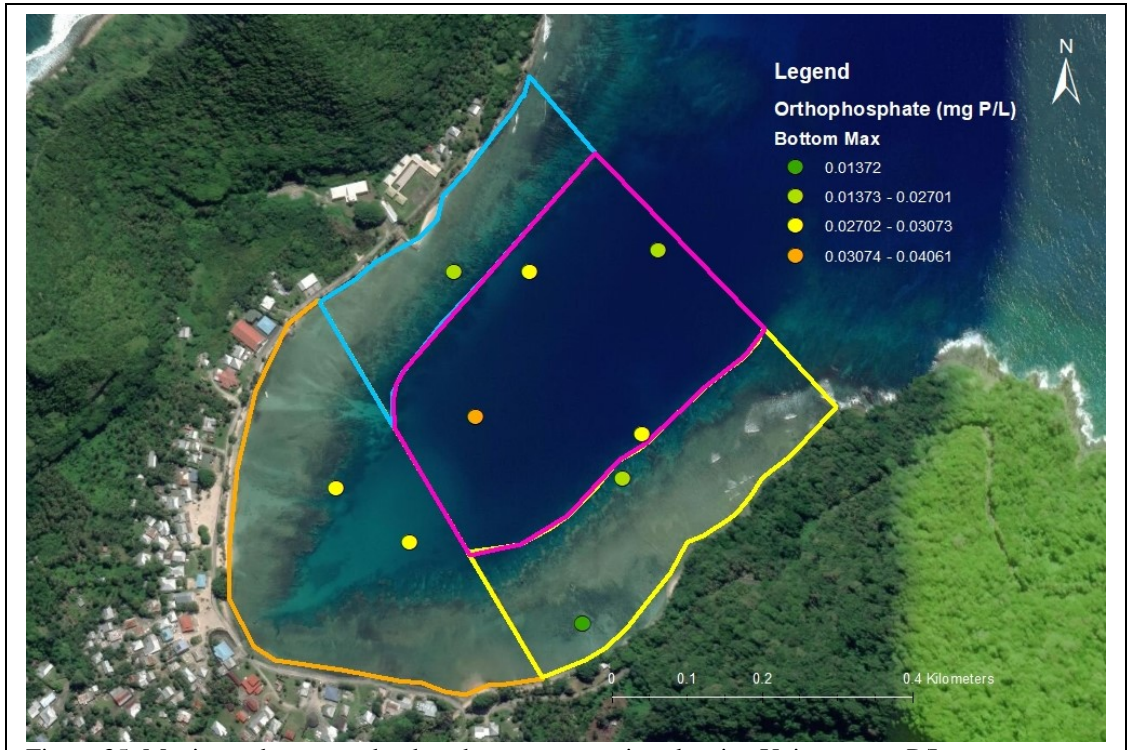


Figure 35: Maximum bottom orthophosphate concentrations by site. Units are mg-P/L.

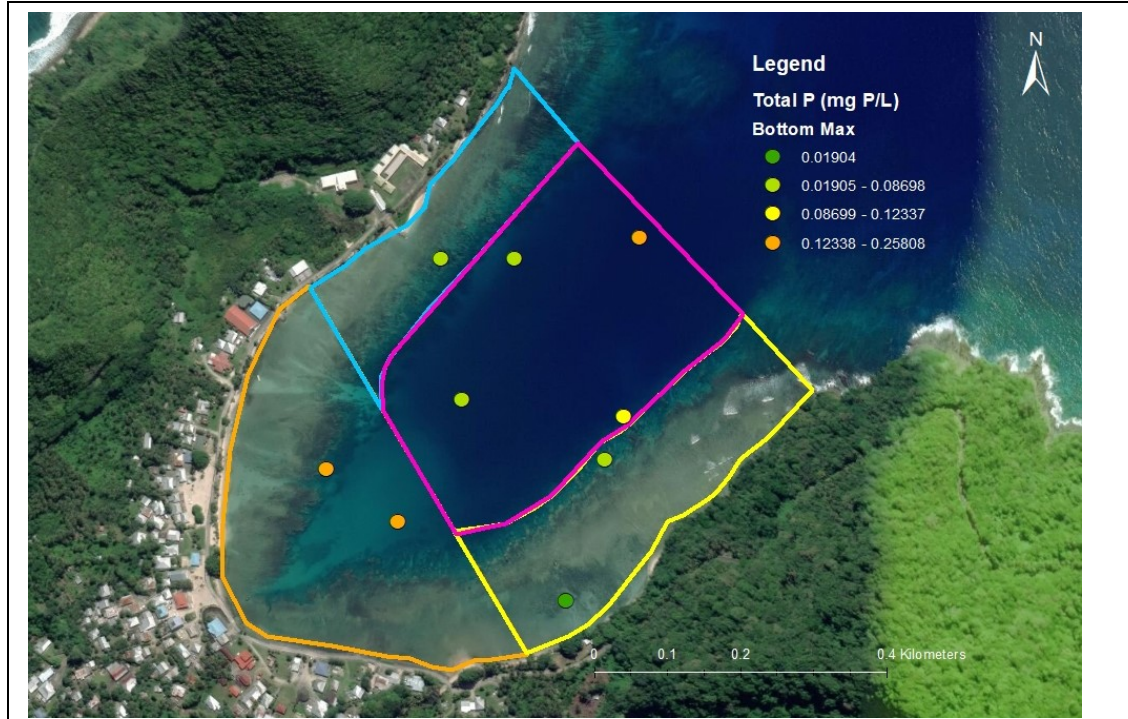


Figure 36: Maximum bottom total phosphorus concentrations by site. Units are mg-P/L.

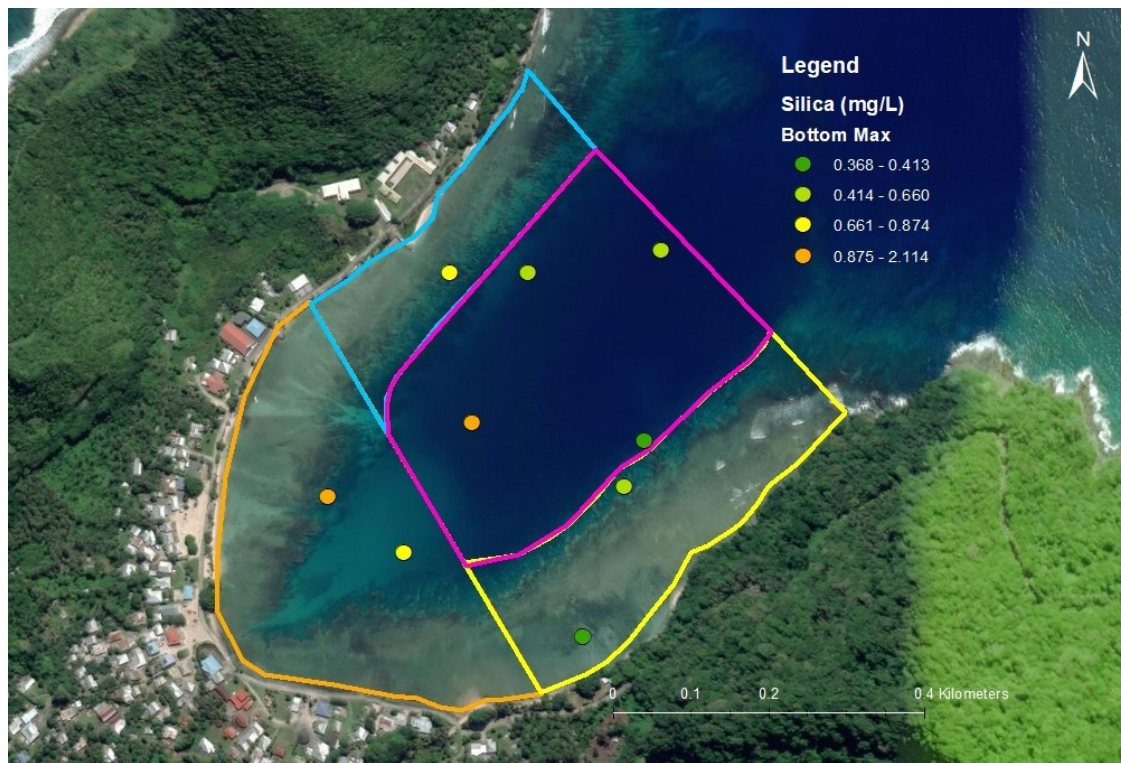


Figure 37: Maximum bottom silica concentrations by site. Units are mg-Si/L.

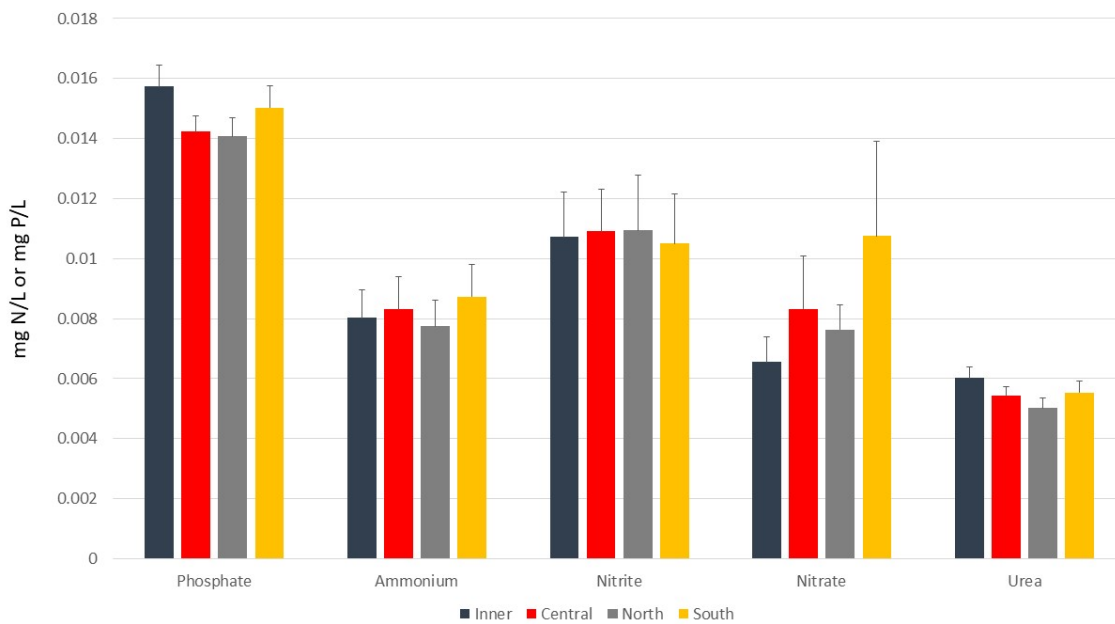
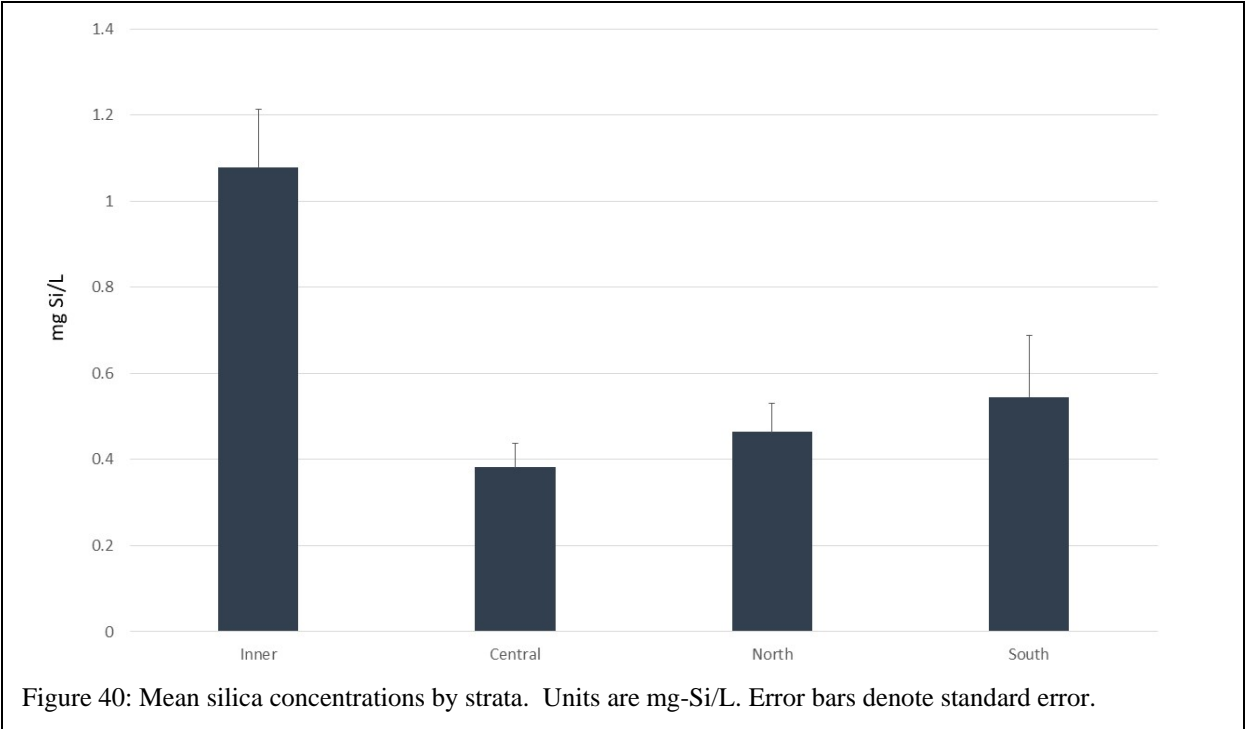
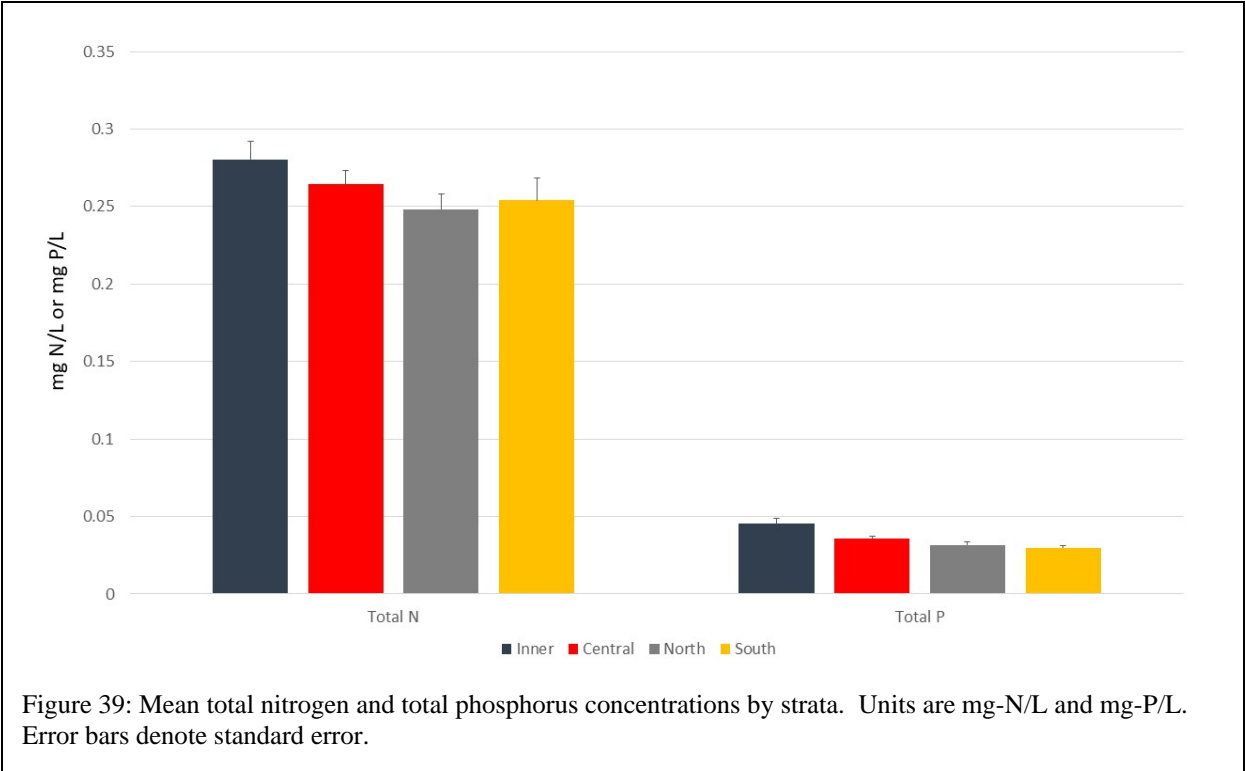


Figure 38: Mean concentration of ammonium, nitrate, nitrite, urea and phosphate by strata. Units are mg-N/L. Error bars denote standard error.



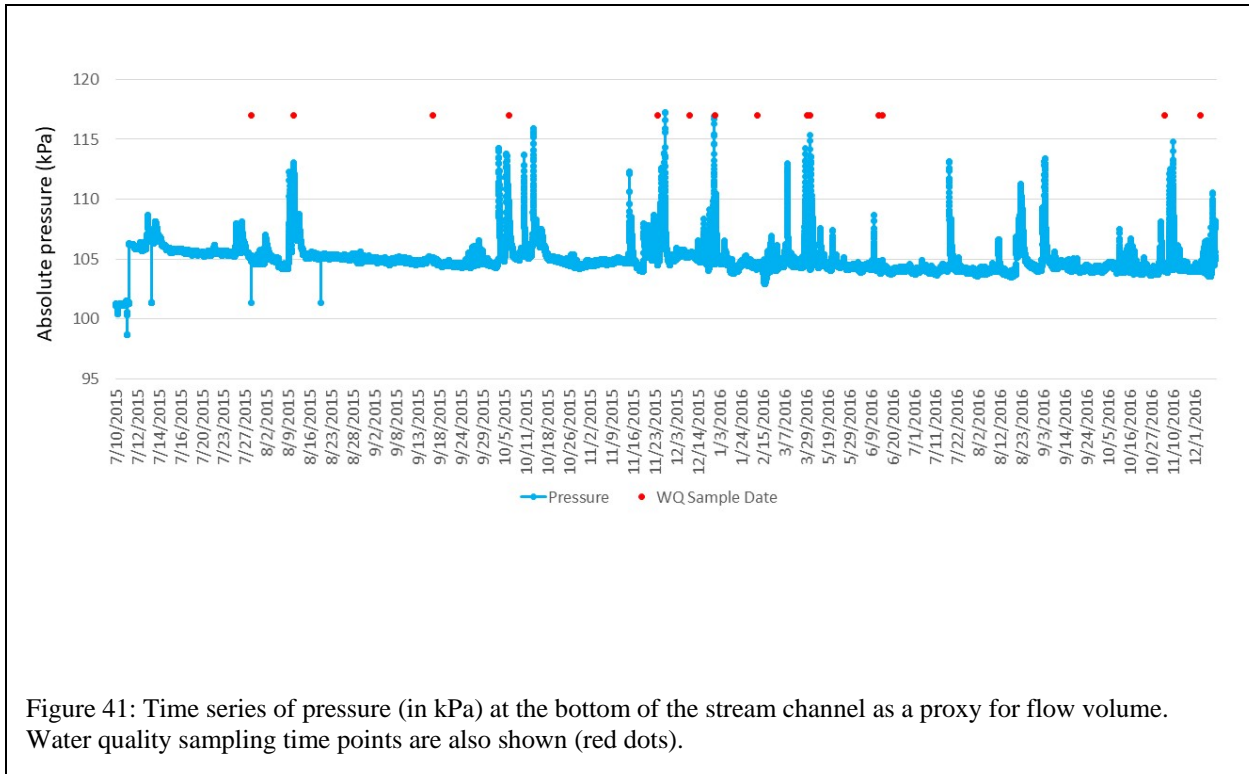


Figure 41: Time series of pressure (in kPa) at the bottom of the stream channel as a proxy for flow volume. Water quality sampling time points are also shown (red dots).

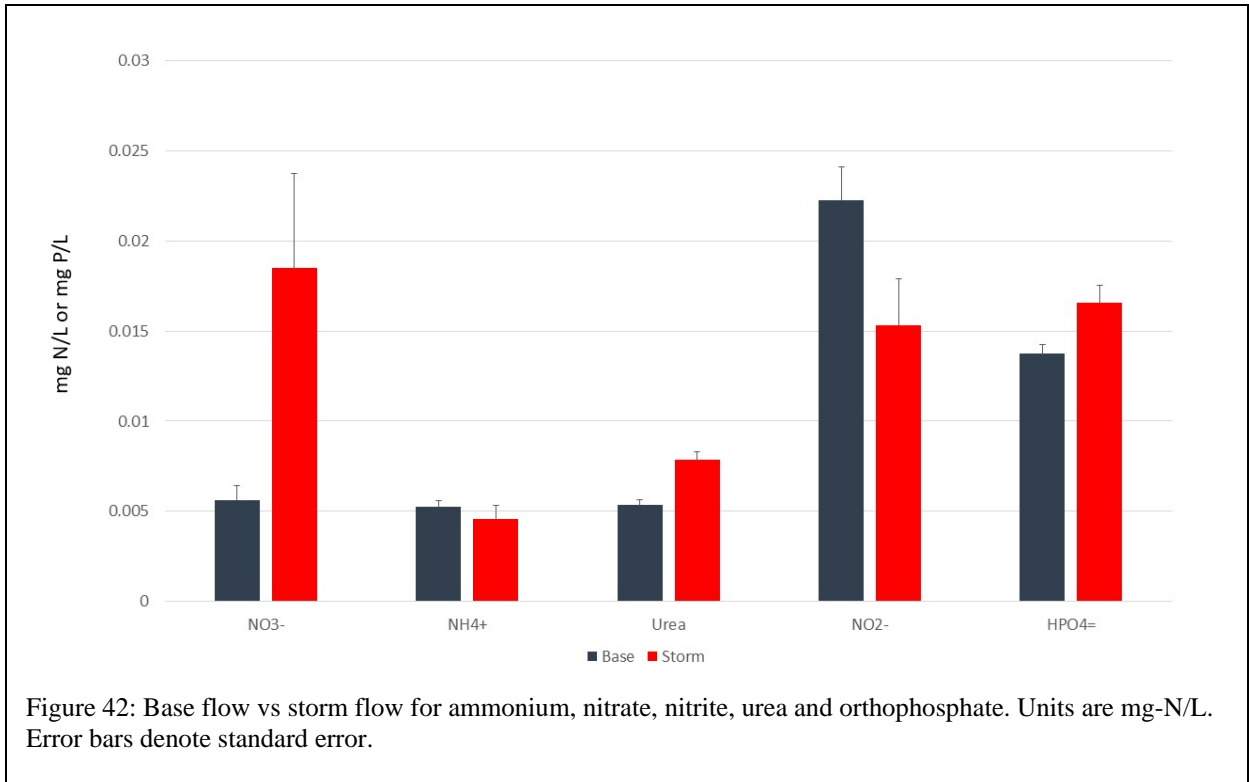


Figure 42: Base flow vs storm flow for ammonium, nitrate, nitrite, urea and orthophosphate. Units are mg-N/L. Error bars denote standard error.

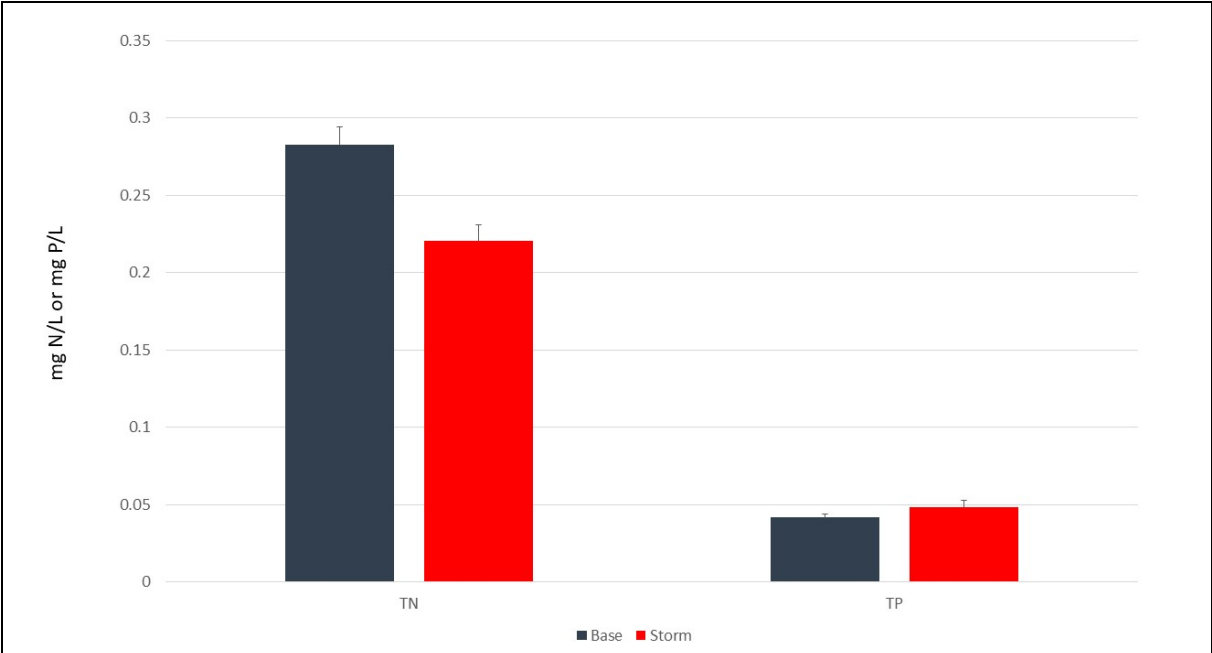


Figure 43: Base flow vs storm flow total nitrogen and total phosphorus. Units are mg-N/L. Error bars denote standard error.

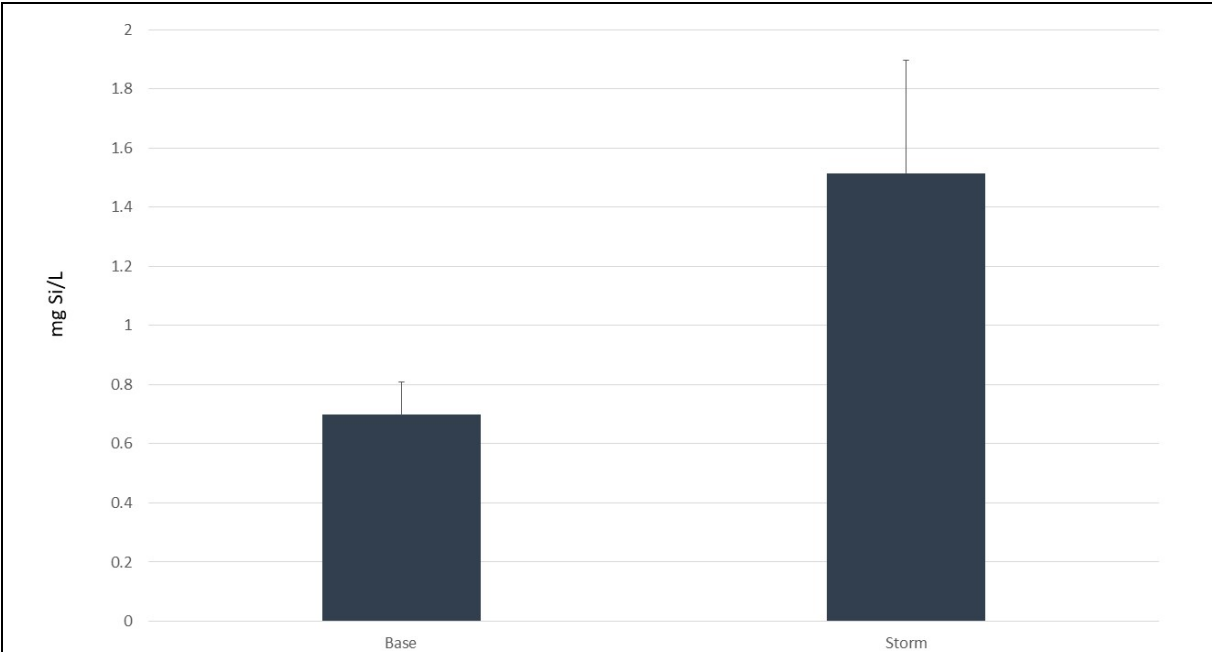


Figure 44: Base flow vs storm flow for silica. Units are mg-N/L. Error bars denote standard error.

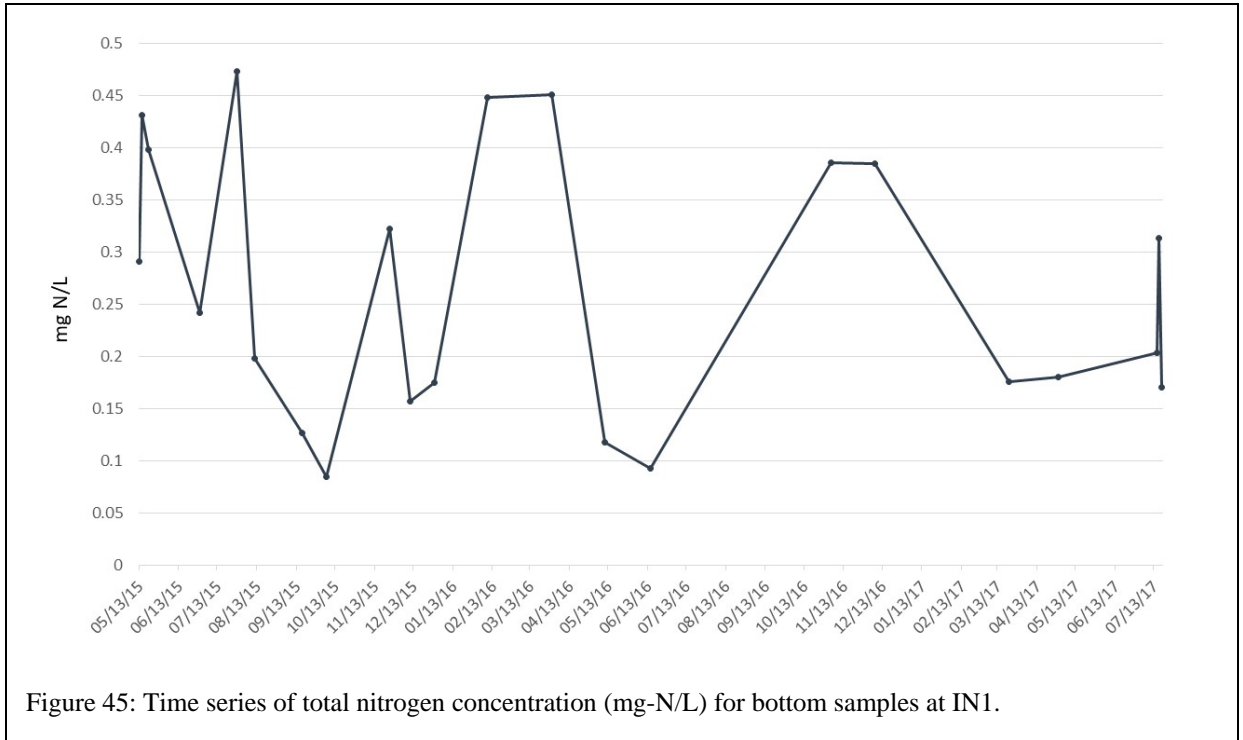


Figure 45: Time series of total nitrogen concentration (mg-N/L) for bottom samples at IN1.

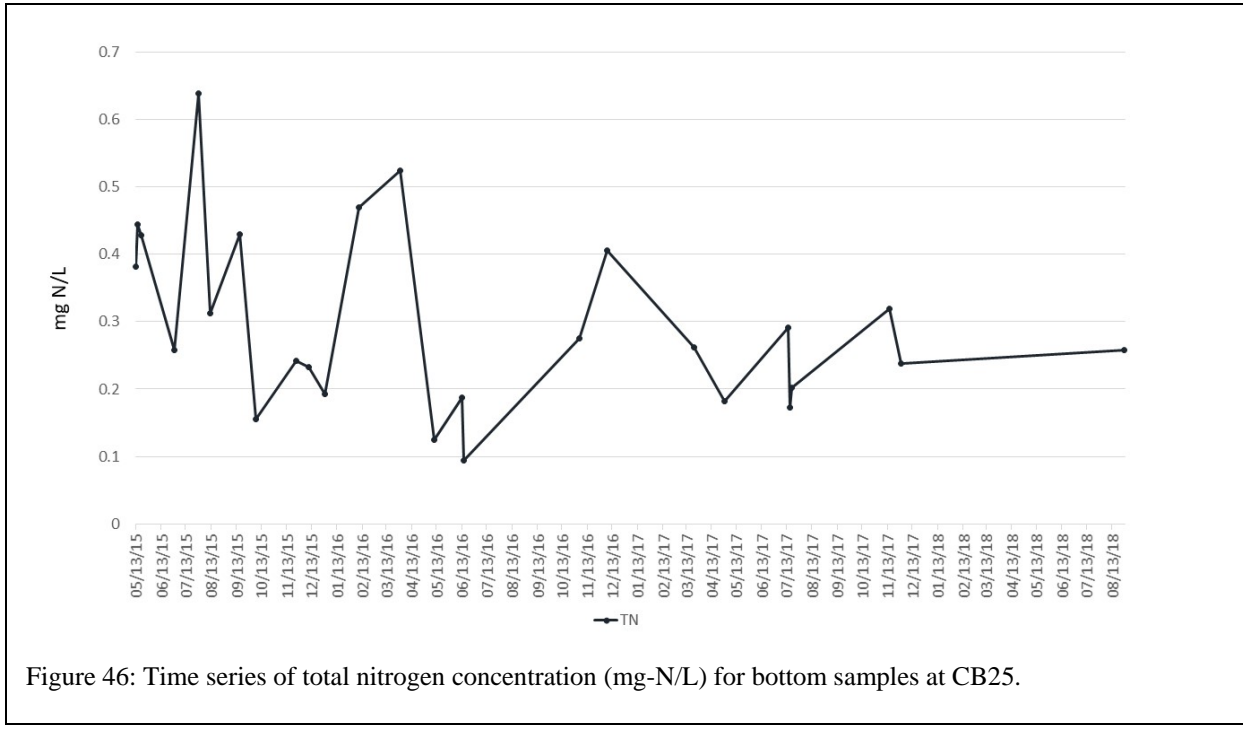


Figure 46: Time series of total nitrogen concentration (mg-N/L) for bottom samples at CB25.

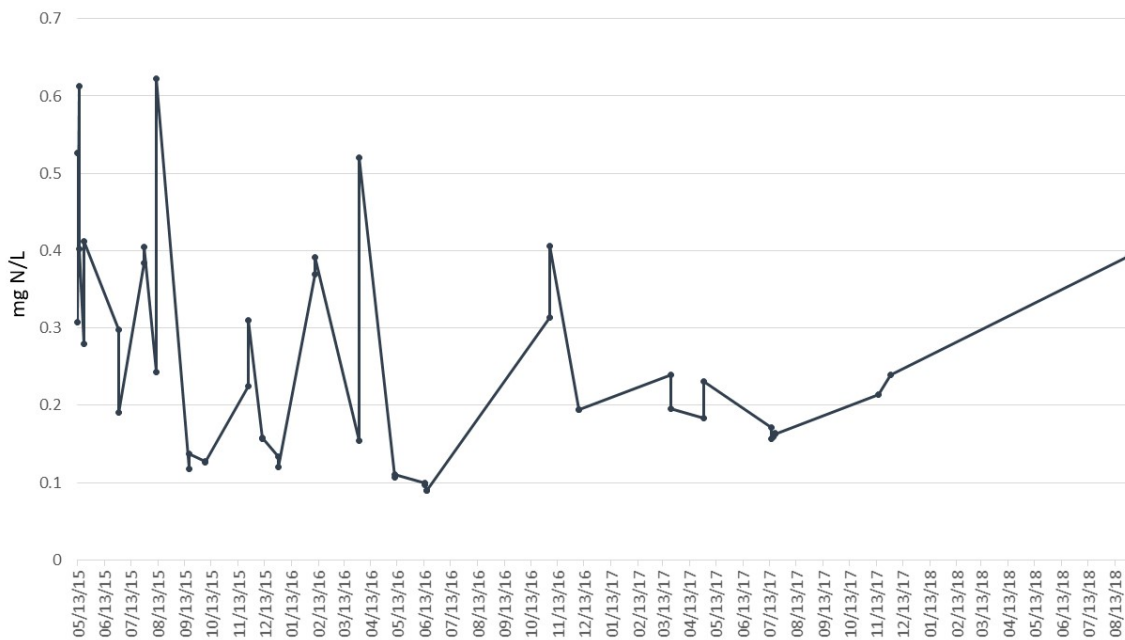


Figure 47: Time series of total nitrogen concentration (mg-N/L) for bottom samples at SB9.

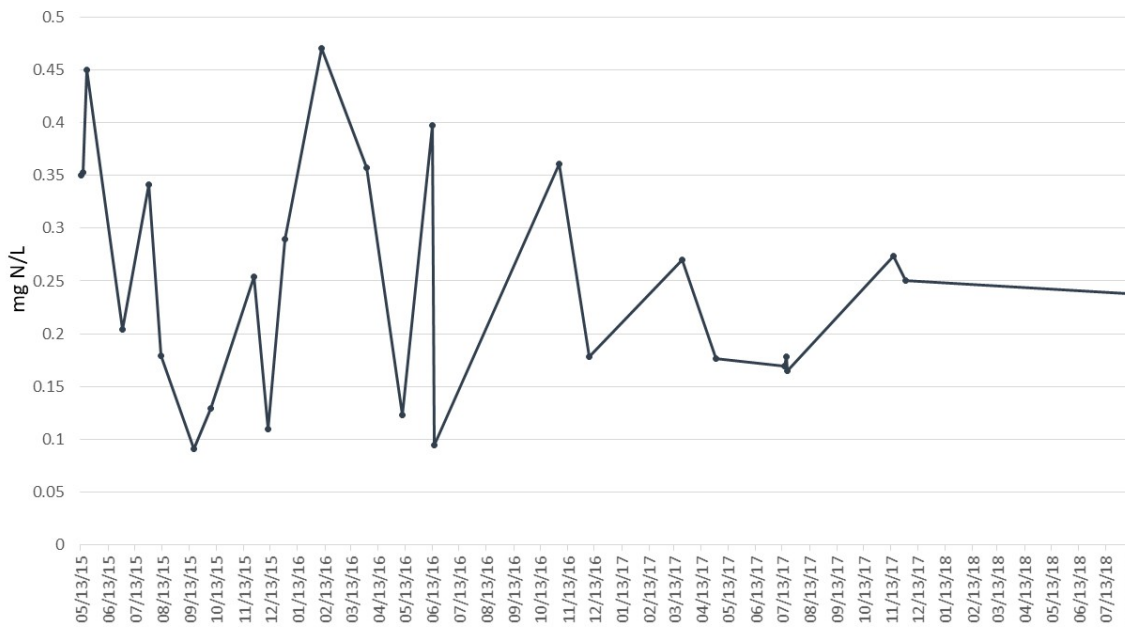
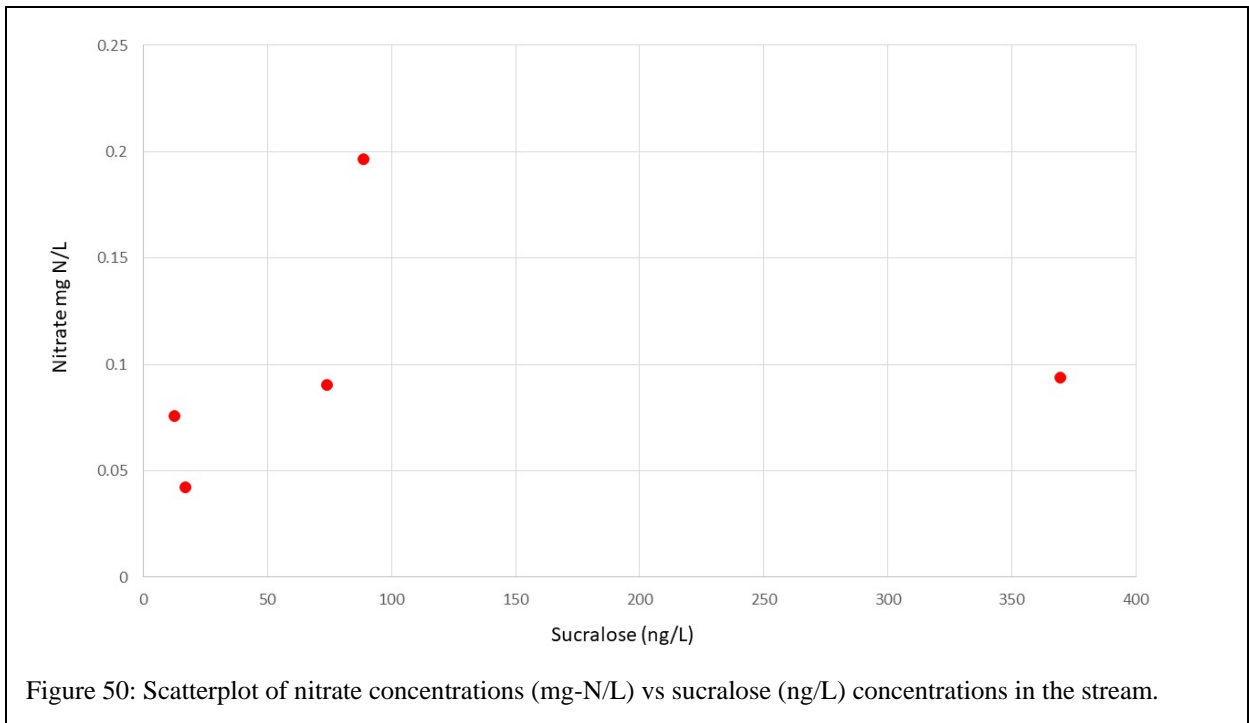
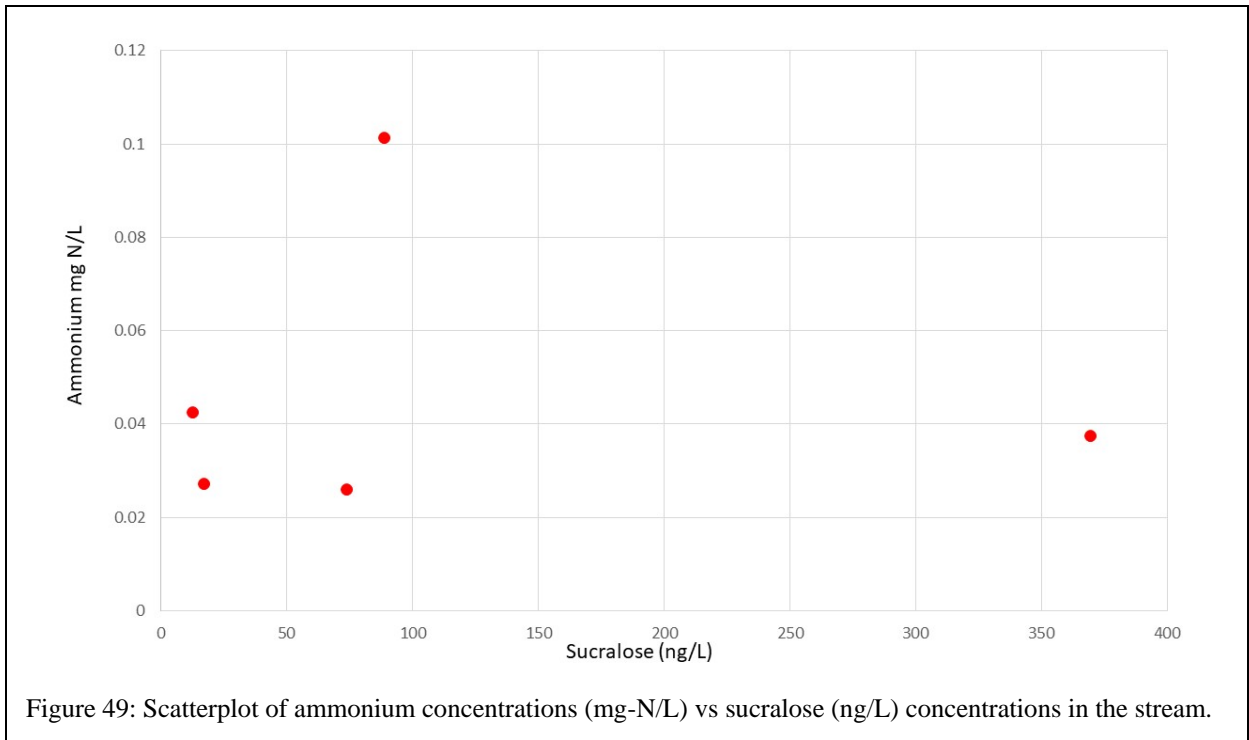
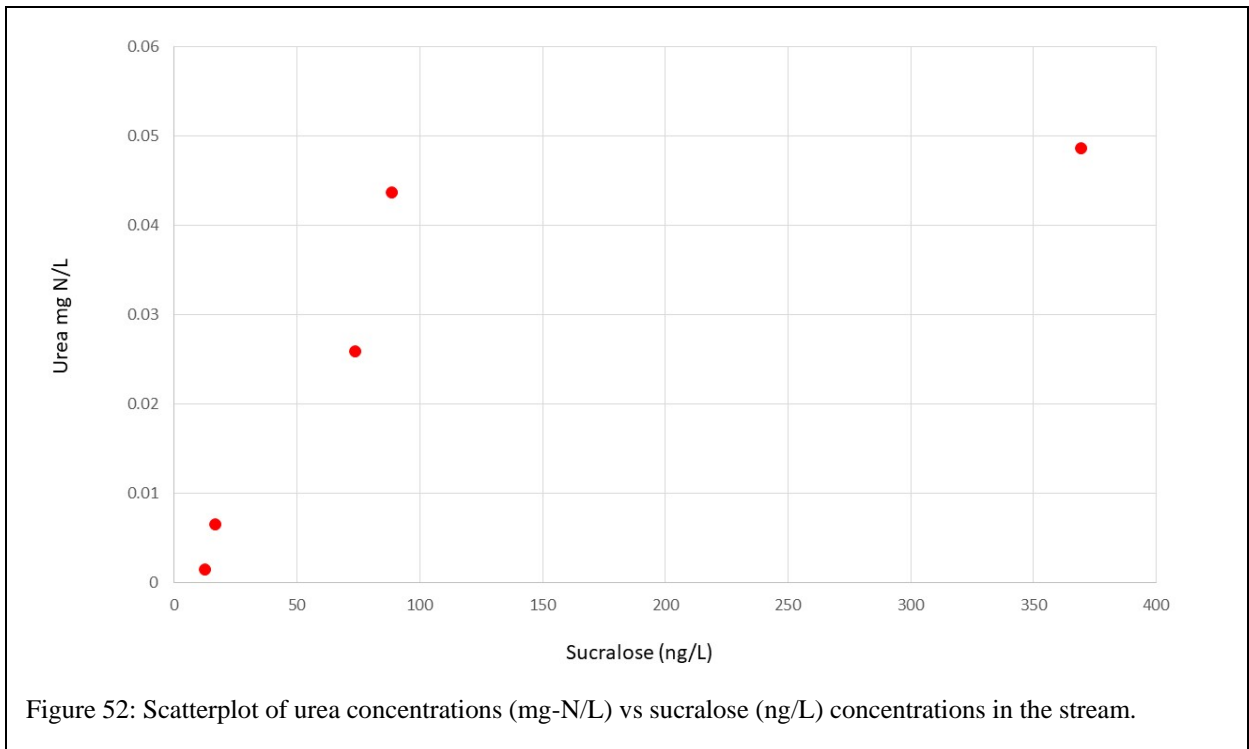
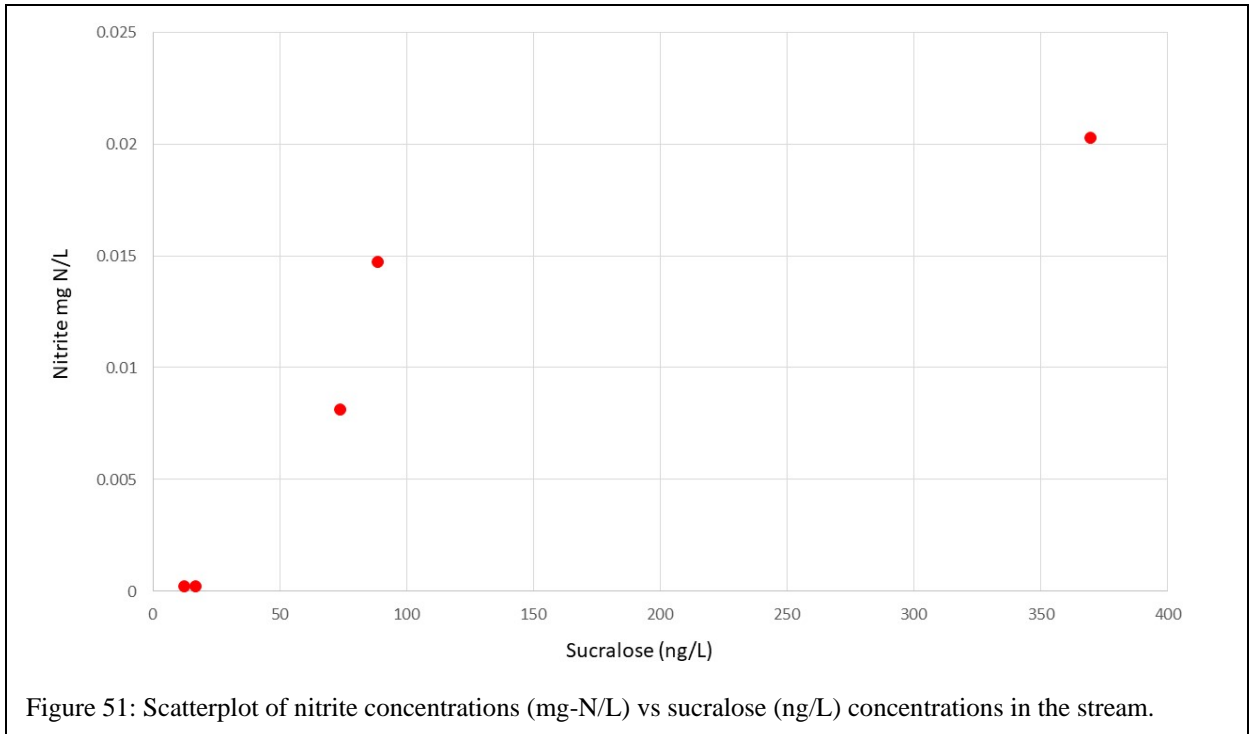


Figure 48: Time series of total nitrogen concentration (mg-N/L) for bottom samples at NB18.





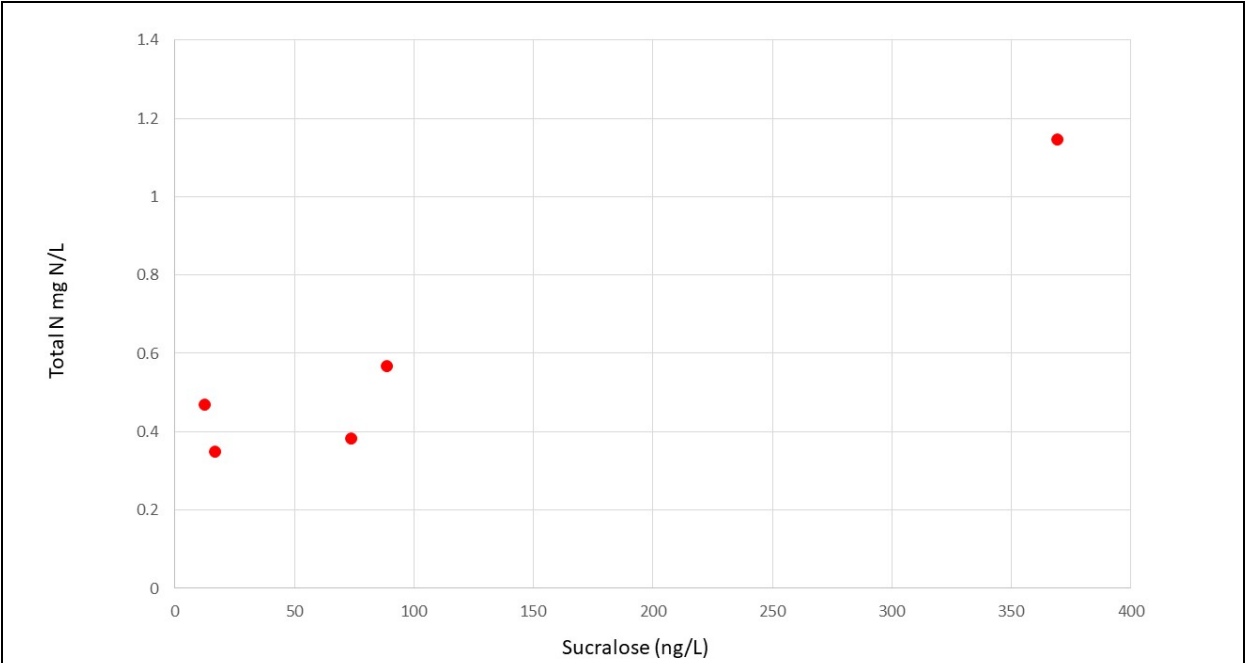


Figure 53: Scatterplot of total nitrogen concentrations (mg-N/L) vs sucralose (ng/L) concentrations in the stream.

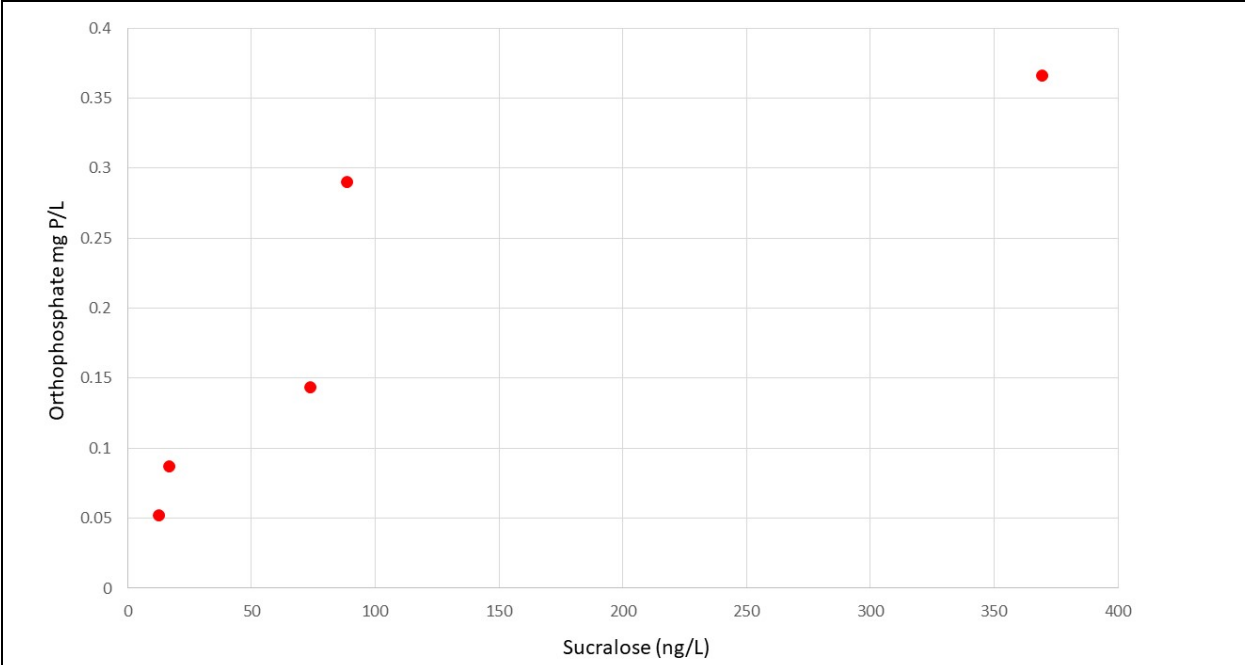
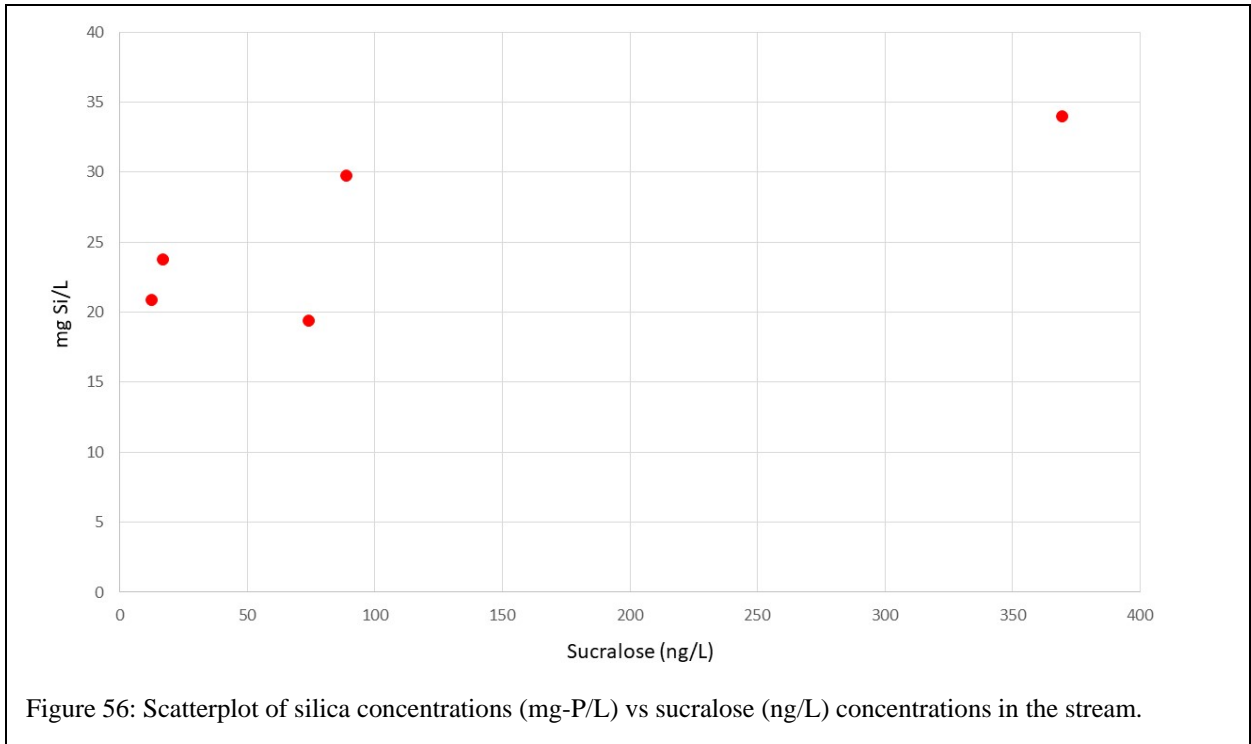
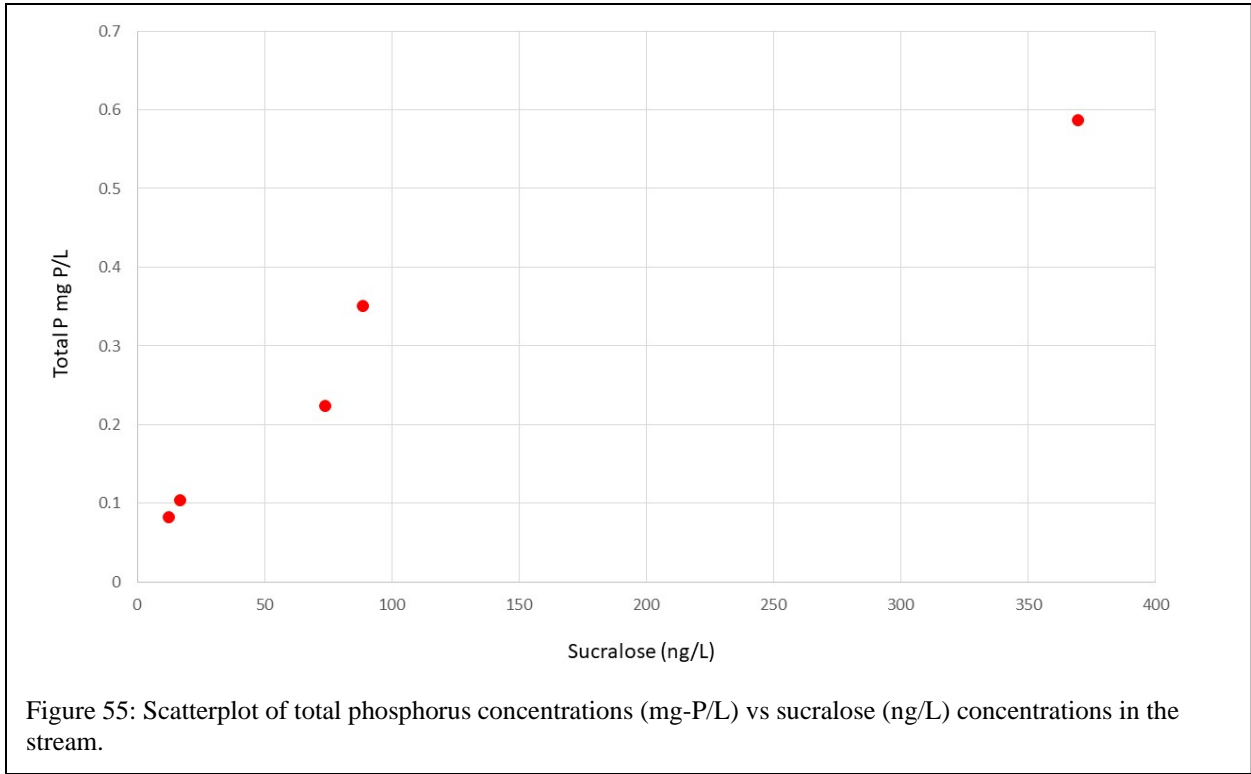
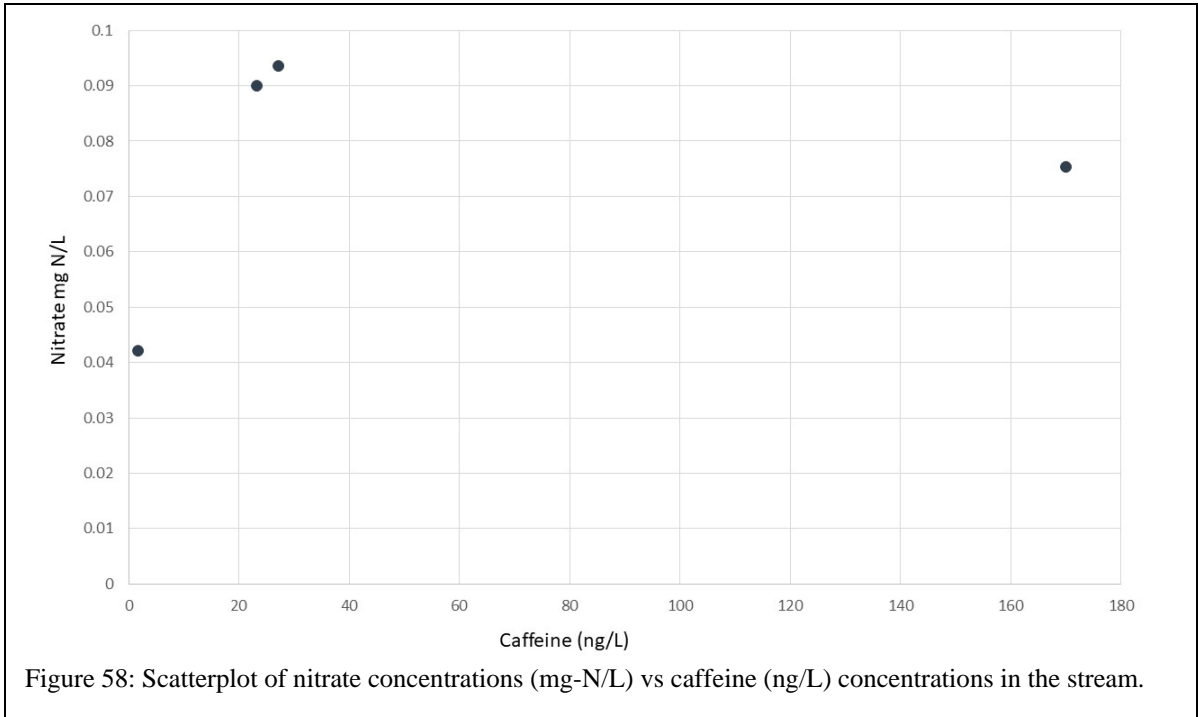
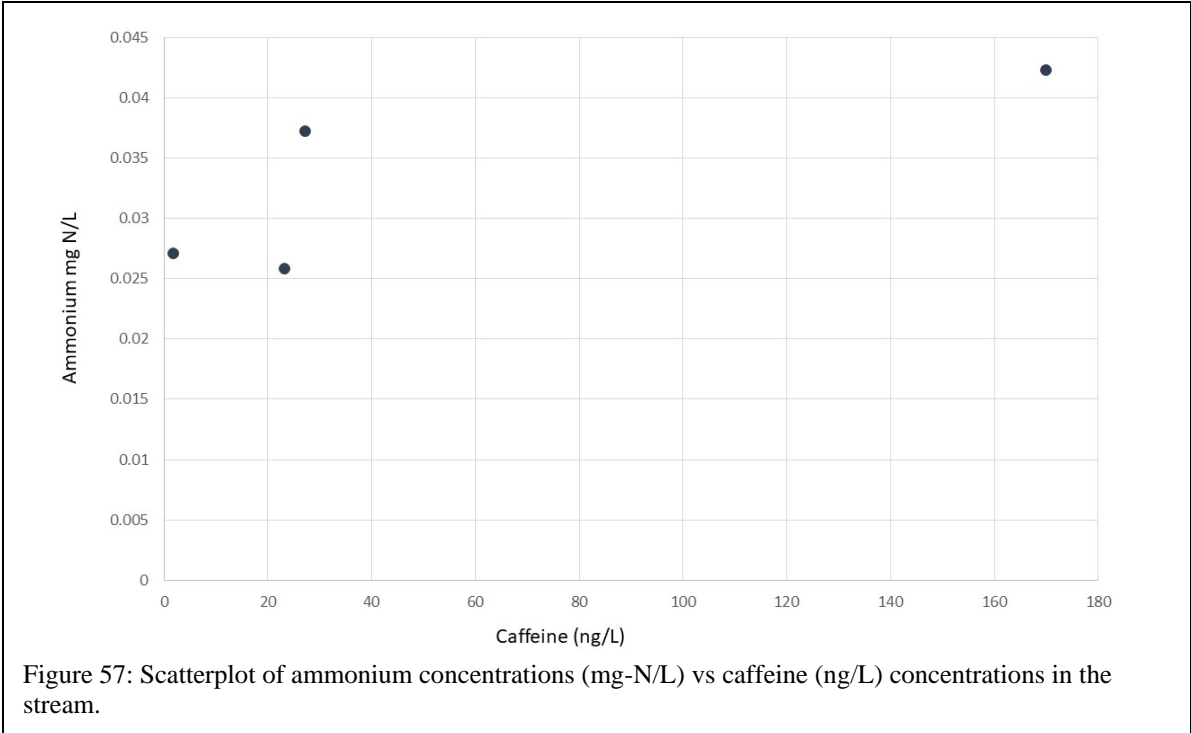


Figure 54: Scatterplot of orthophosphate concentrations (mg-P/L) vs sucralose (ng/L) concentrations in the stream.





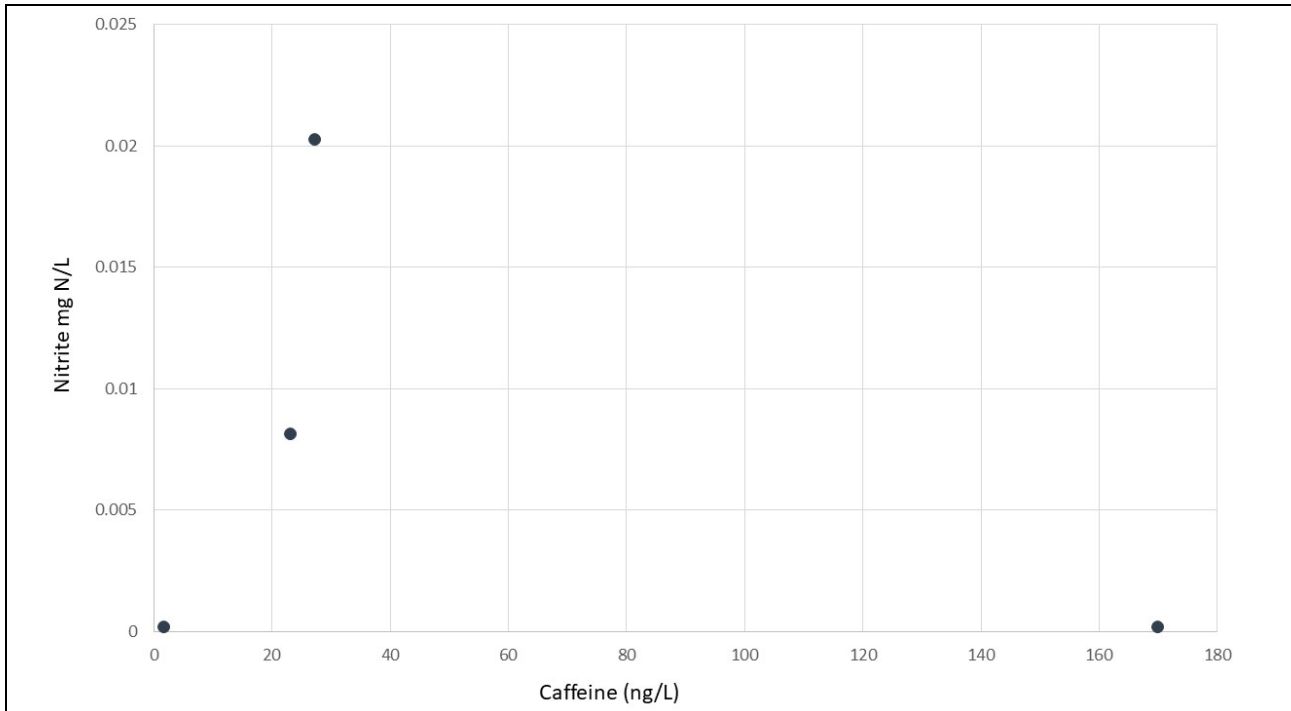


Figure 59: Scatterplot of nitrite concentrations (mg-N/L) vs caffeine (ng/L) concentrations in the stream.

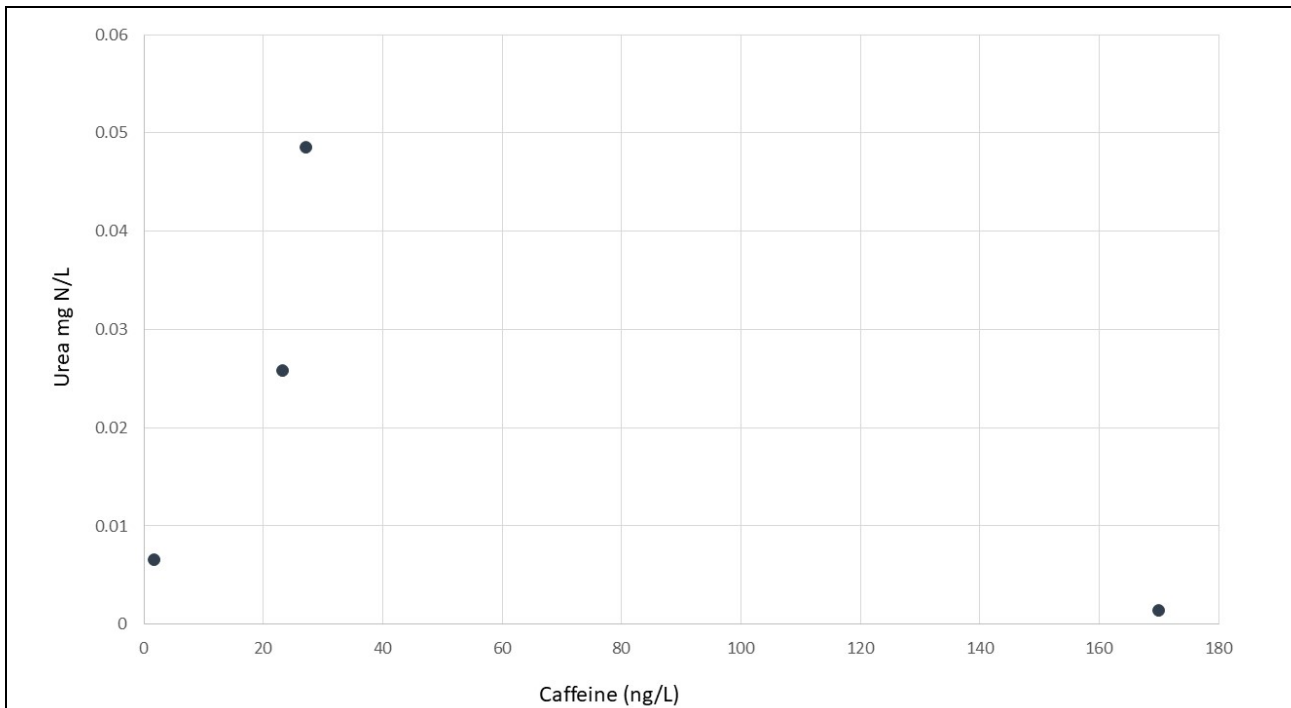
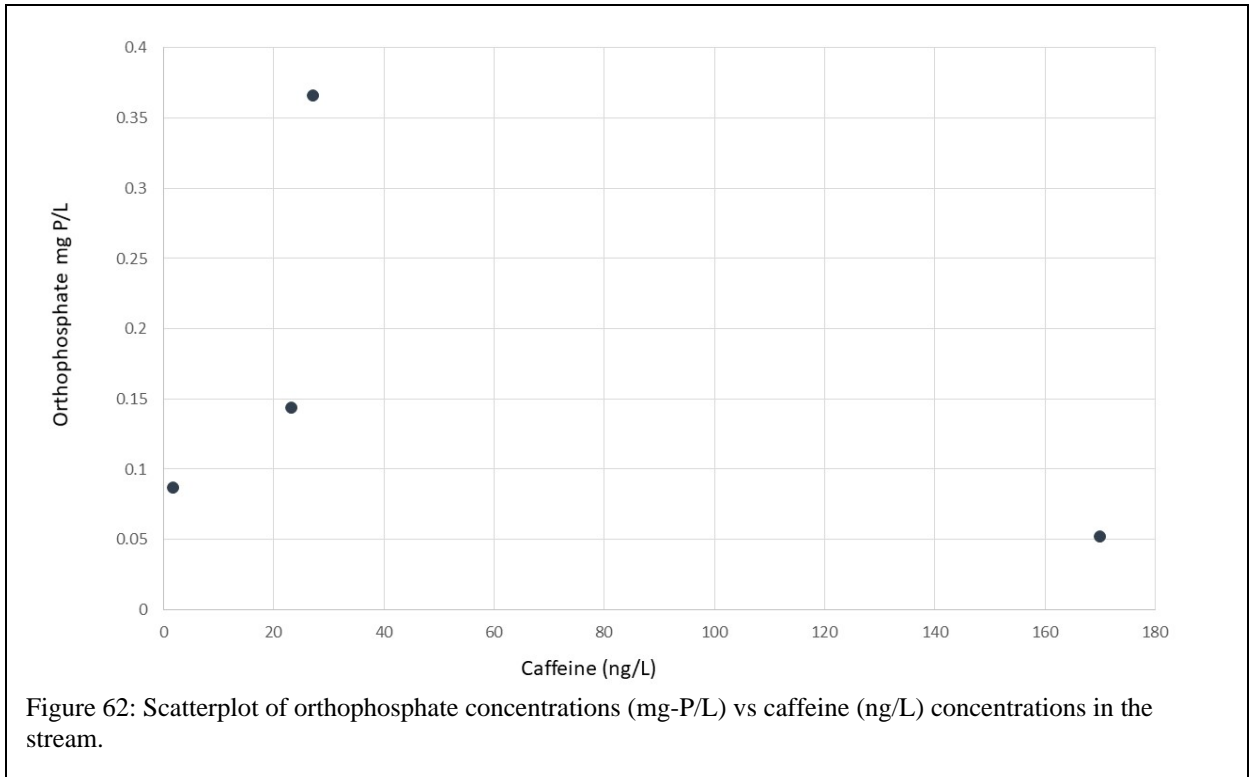
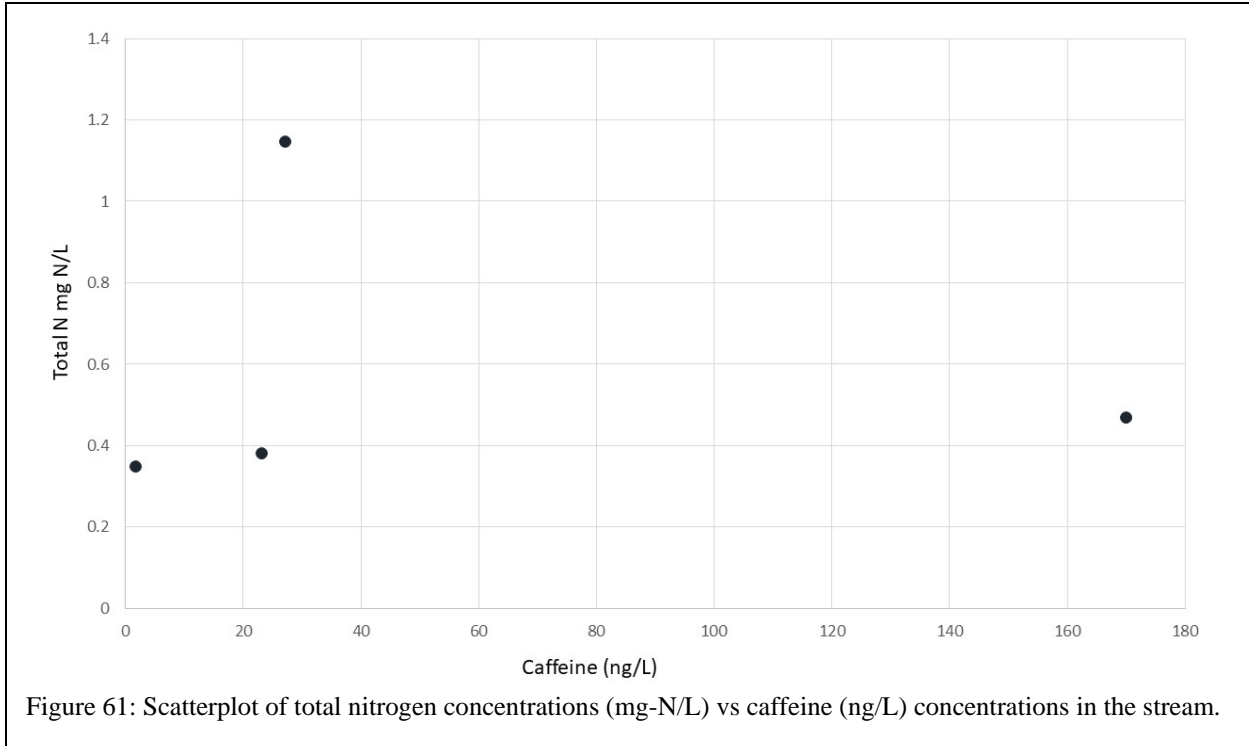


Figure 60: Scatterplot of urea concentrations (mg-N/L) vs caffeine (ng/L) concentrations in the stream.



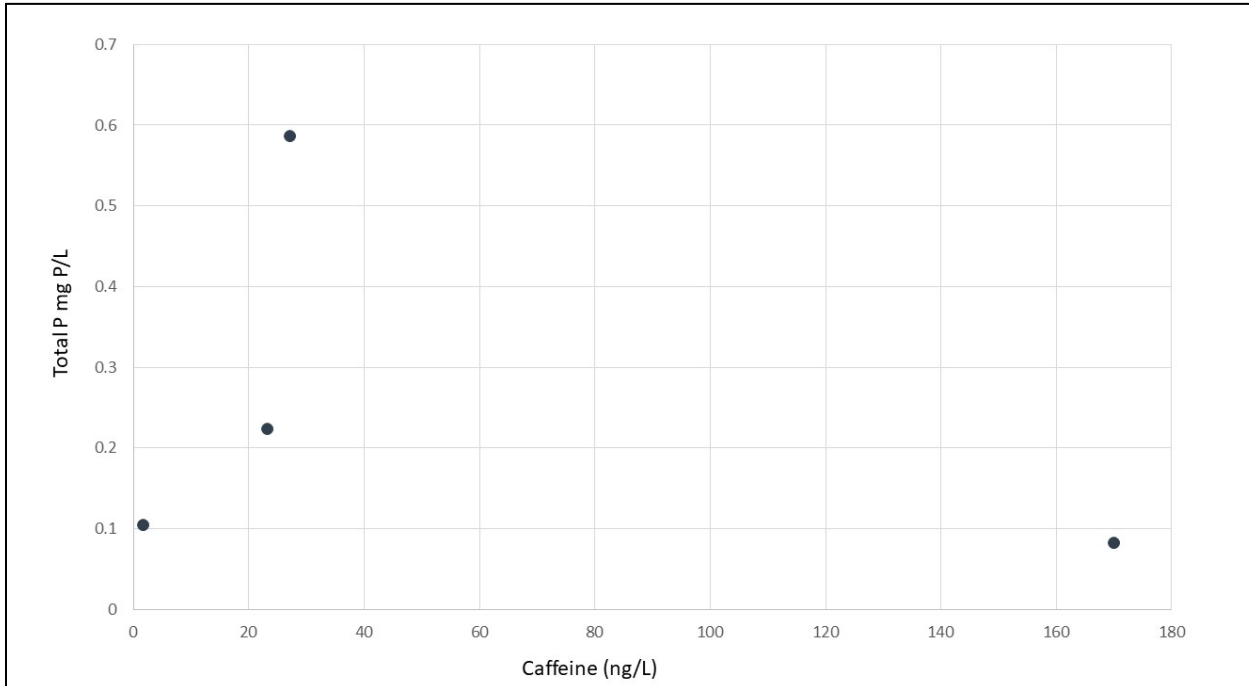


Figure 63: Scatterplot of total phosphorus concentrations (mg-P/L) vs caffeine (ng/L) concentrations in the stream.

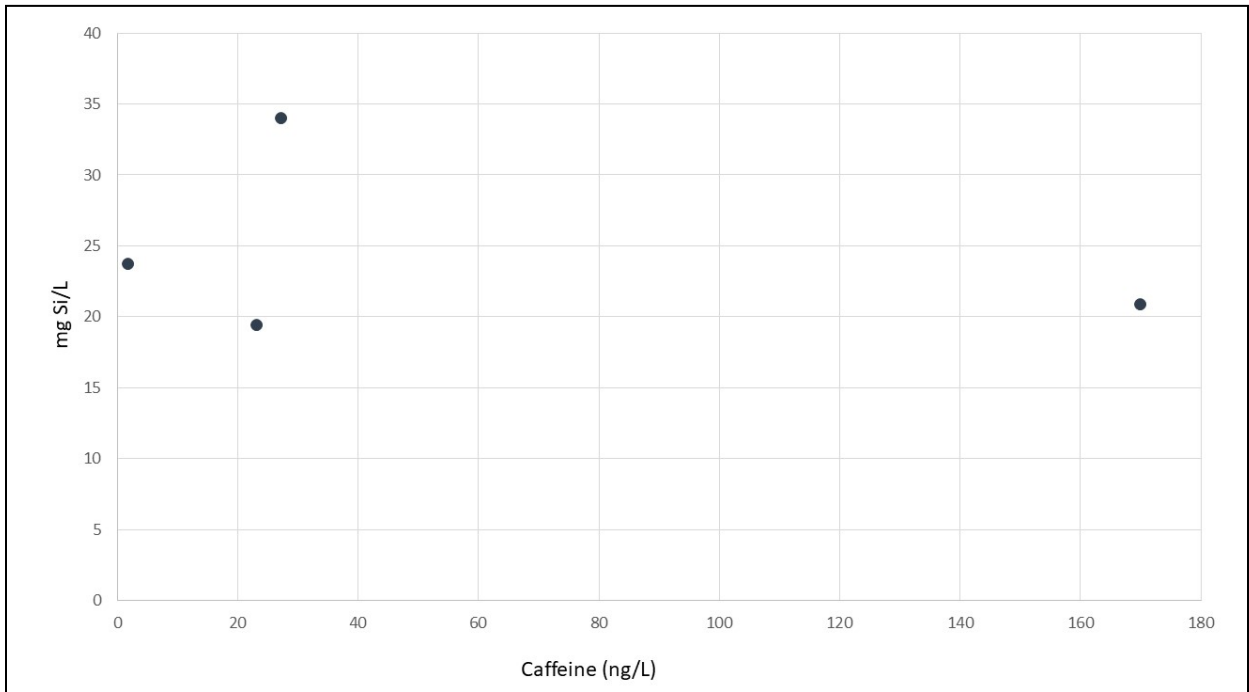


Figure 64: Figure 38: Scatterplot of silica concentrations (mg-P/L) vs caffeine (ng/L) concentrations in the stream.

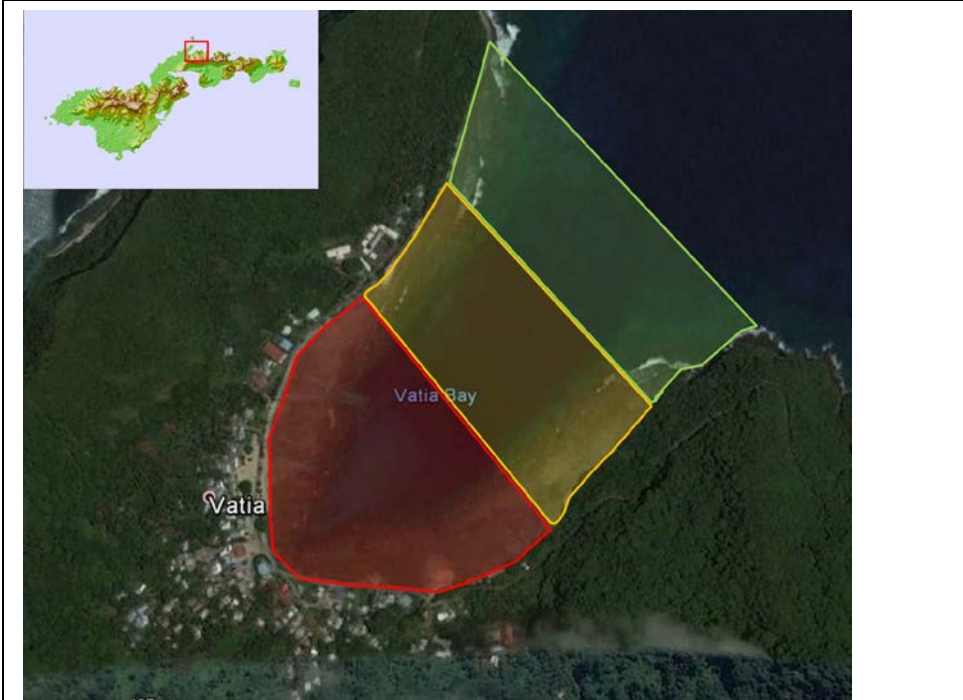


Figure 65: Zones of coral condition as delineated by Vargas-Angel and Schumacher 2018 based on benthic surveys. Green is “good”, yellow is “fair” and red is “impacted.”

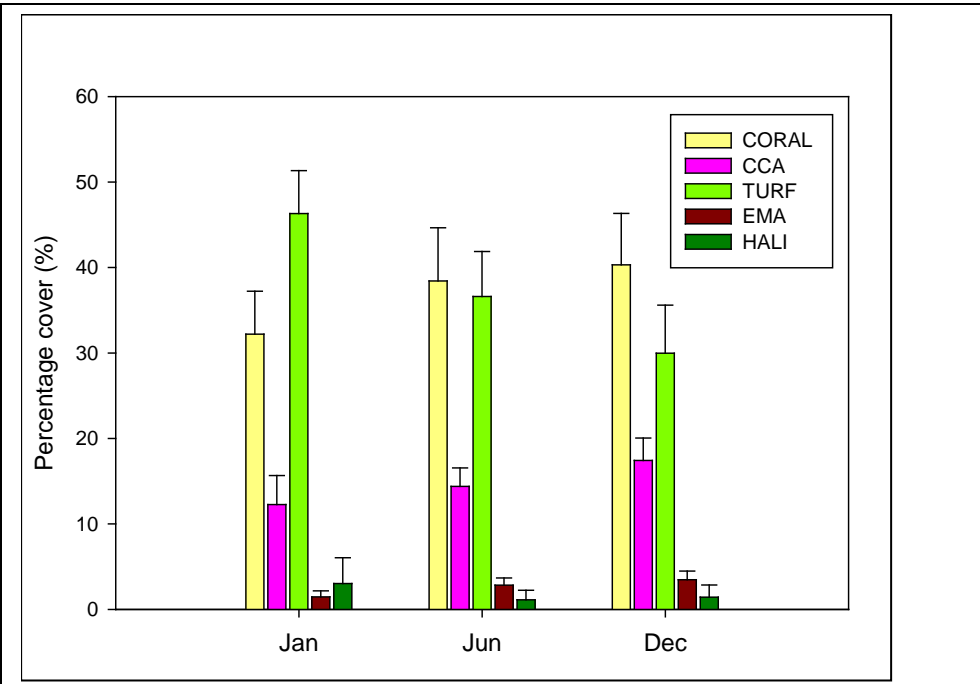


Figure 66: Mean percent cover at photo quadrat sites during 2016.

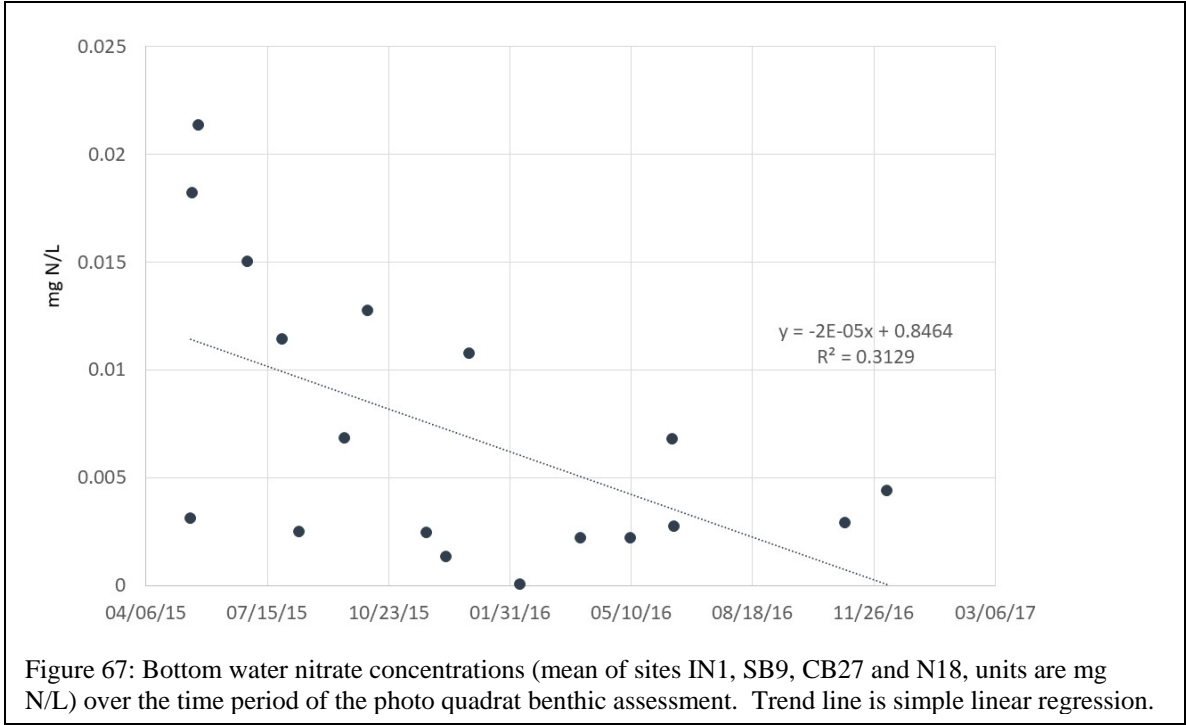


Figure 67: Bottom water nitrate concentrations (mean of sites IN1, SB9, CB27 and N18, units are mg N/L) over the time period of the photo quadrat benthic assessment. Trend line is simple linear regression.

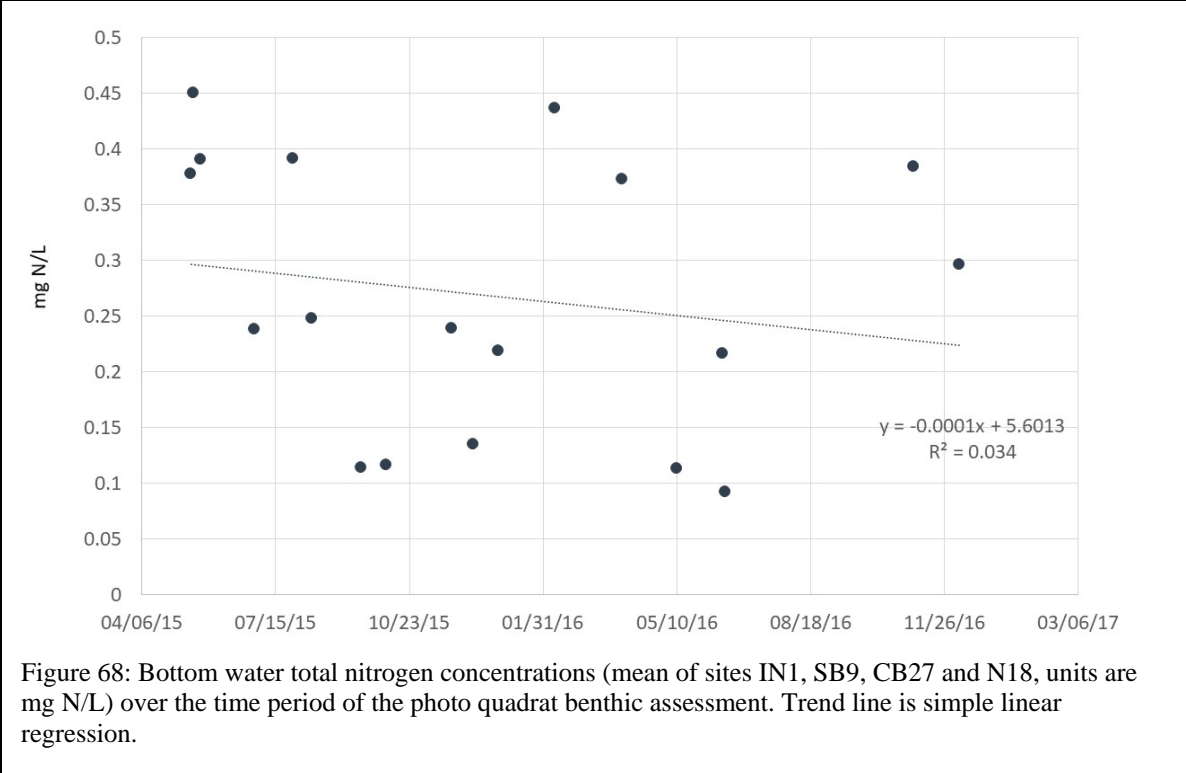


Figure 68: Bottom water total nitrogen concentrations (mean of sites IN1, SB9, CB27 and N18, units are mg N/L) over the time period of the photo quadrat benthic assessment. Trend line is simple linear regression.

